

IMPROVED TRANSMISSION LINE PROTECTION PERFORMANCE CONCERNING HIGH  
RESISTANCE FAULTS

A dissertation by

RHULANI DAPHNEY MATSHIDZA

A postgraduate thesis submitted to the Discipline of Electrical Engineering in partial fulfilment for  
the requirements for the degree of

MASTER OF SCIENCE IN POWER AND ENERGY

UNIVERSITY OF KWAZULU NATAL

Academic Supervisors: Prof N.M. Ijumba and Prof R. Zivanovic

Industrial Supervisor: Mr Adam Bartylak

December 2006

## ACKNOWLEDGEMENTS

I extend my sincere gratitude to my Lord and Saviour, Jesus Christ for giving me the opportunity, guidance, ability, intellect and strength to complete my research. Through him I can do all things.

I acknowledge with gratitude the help extended to me by my supervisors, Prof. R. Zivanovic (academic), Prof. N.M Ijumba (academic) and Mr Adam Bartylak (industrial), whose suggestions, guidance and encouragement was always valuable to me. And a specific thanks to Mr Adam Bartylak who discovered the potential in me, introduced me to this topic and helped me to network with the different experts in the field.

A special thanks to Paul Keller who helped me to collect all the data and information I needed on transmission high resistance faults. Thys Bower and Graeme Topham who initialised this project, formulated its scope and entrusted it to me. Gawie Pretorius and Alex Dierks for sharing their knowledge and expertise, which was helpful in doing this research. To all Engineers, Technologists and Technicians who assisted me.

My sincere thanks are due to Piet Jooste, who have always been my source of encouragement and continued support in the protection field.

I would like to apologise to my family and friends for neglecting them during the time it has taken me to do this research, in particular, my sunshine Dalton and my two angels Phathu and Rendi. Their support and patience over the previous three years will always be valued.

## DECLARATION

I, Rhulani Matshidza, declare that this research is my own work, and all sources that I have quoted have been acknowledged by means of a complete reference.

.....

R.D. Matshidza

December 2006

South Africa

## ABSTRACT

ESKOM has relied primarily on impedance-based measurement protection relays for the protection of transmission lines. One of the main disadvantages of distance relays is the limited fault resistance measurement capability. High-resistance faults are characterised by low fault currents, therefore the impedance calculated would be much bigger and so the fault will appear to be beyond the protected line.

The main aim of the study is to gain clear understanding of the capability of the existing relays used in Eskom Transmission network, to be able to give recommendations on the refinements to the transmission line protection philosophy required to improve future protection performance.

Omicron relay tests, showed that the dynamic characteristics of the three selected relays which were tested covers more fault resistance than that of the normal static impedance and also that the effect of DC offset is negligible with regards to fault resistance measurement capability. Normally the relays have built in algorithms which are able to filter nuisance signals.

Theoretical case study that compared the most used relays in Eskom Transmission was done and the results are documented. Settings recommendations to improve fault resistance coverage were deduced from the above study.

Fault investigation by using digital simulations (Matlab simulations) has proven the lack of capability to operate for some impedance relays in some fault conditions, as the fault resistance sometimes moves fault impedance beyond relay characteristic even when actual polarization of the relay is considered.

Analysis of the protection performance in transmission proved that high resistance faults accounts for at least half of protection equipment performance index (PEPI) incidents.

Finally the author made recommendations to improve the protection performance concerning high resistance faults.

## LIST OF ABBREVIATIONS

%	Percentage
$3I_0$	Residual current
$3U_0(3V_0)$	Residual voltage
ARPI	Auto Reclose Performance Index
CT	Current Transformer
COMTRADE	Common Format for Transient Data Exchange
Direc	Direction
DC	Direct Current
DFR	Digital Fault records
E/F	Earth Fault
EHV	Extra High Voltage
Forw	Forward direction
HV	High Voltage
$I_E$	Earth over current threshold
km	kilo metre
KPI	Key Performance Indicator
kV	kilo Volt
MV	Medium Voltage
NRS	National Regulatory Services
NSF	Non System Faults
O/C	Over Current
PEPI	Protection Equipment Performance Index
R	Resistance
Rx	Receive (T for siemens 7sa513 relay)
rms	Root mean square
SIR	Source Impedance Ratio
SPI	System Performance Index
T-DELAY	Time delay
TEF	Definite and inverse time delayed residual over current
Tx	Transmit (T for siemens 7SA513 relay)
$U_E$	Phase to earth Voltage
VT	Voltage Transformer
X	Reactance
Z3F	Zone 3 Forward
Z3R	Zone 3 Reverse

## TABLE OF CONTENTS

CHAPTER 1.....	1
1 INTRODUCTION.....	1
1.1 Background.....	1
1.2 Importance of the research.....	1
1.3 Aim of the research.....	2
1.4 Hypothesis .....	3
1.5 Research question .....	3
1.5.1 Subsidiary questions.....	3
1.6 Outline of subsequent chapters .....	3
CHAPTER 2.....	5
2 LITERATURE REVIEW.....	5
2.1 IMPEDANCE PROTECTION .....	5
2.1.1 Principles of comparator.....	5
2.1.2 Plain impedance characteristics.....	6
2.1.3 Mho Characteristics.....	7
2.1.4 Polarization.....	9
2.1.5 Self - polarized mho characteristics.....	10
2.1.6 Offset –mho relay characteristic.....	11
2.1.7 Memory polarization mho relay characteristic.....	12
2.1.8 Cross – polarised mho relay characteristic .....	13
2.2 Reactance characteristics .....	15
2.3 Quadrilateral characteristics .....	15
2.4 alternatives for Transmission line protection.....	16
2.4.1 Directional overcurrent.....	16
2.4.2 Differential protection .....	17
2.5 Eskom EHV feeder protection schemes .....	18
2.5.1 Principle of distance protection.....	21
2.5.1 YTG Relay [13].....	22
2.5.2 TLS RELAY [14].....	23
2.5.3 R3Z27 relay [15] .....	25
2.5.4 LZ32 relays [16].....	26
2.5.5 Type H relays [17].....	26
2.5.6 Slyp/slen relays [18].....	26
2.5.7 Micromho relays [19].....	27
2.5.8 Siemens 7SA513 relays [20] .....	27

2.5.9	SEL-321 relay [21] .....	30
2.5.10	ABB REL-531 relay [22] .....	32
2.6	Analysis of distance relay performance .....	36
2.7	Effect of fault resistance on the distance relay performance .....	43
2.8	Distance protection relay simulations .....	45
2.8.1	Differential Equation Based Algorithm.....	45
2.8.2	Discrete Fourier Transform. ....	47
2.8.3	Recursive Vs Non-recursive Filters.....	47
2.8.4	Inaccuracies expected from digital signal processing .....	48
2.9	Transmission protection performance.....	48
2.10	Quality of SUPPLY: NRS 048 Requirements on Voltage Dips .....	50
2.10.1	Voltage Dip parameters.....	50
2.10.2	Compatibility Levels.....	52
2.10.3	Power quality economics .....	53
2.10.4	Custom power .....	53
CHAPTER 3: .....		54
3	RESEARCH METHODOLOGY .....	54
3.1	Introduction.....	54
3.2	Intended purpose of the research .....	54
3.3	Process of the research.....	54
3.3.1	Obtain network high resistance fault statistics .....	54
3.3.2	Obtain and review manufacturer’s documentation.....	54
3.3.3	Testing methodology for relay characteristics using Matlab simulations; .....	55
3.3.4	Obtain and implement settings for each relay type .....	56
3.3.5	Test three protection relay type using an Omicron [29].....	56
3.4	Logic of the research.....	59
3.5	Outcome of the research .....	59
CHAPTER 4 RESULTS .....		60
4.1	High resistance fault statistics.....	60
4.2	Relay characteristics tests by simulations.....	61
4.2.1	Plotting the steady state and dynamic characteristics of a Mho relay .....	61
4.2.2	Matlab simulation exercise for fault analysis .....	61
4.3	OMICRON RELAY TEST.....	64
4.3.1	SEL 321 dynamic relay tests .....	64
4.3.2	GEC YTG Relay tests .....	66
4.3.3	Siemens R3Z27 Relay tests .....	68
4.3.4	Siemens R3Z27 relay tests – NON HOMOGENEOUS .....	74

4.4	Protection performance history.....	80
4.4.1	Protection performance – 2005 to 2006 .....	80
4.4.2	Protection performance – 2006 .....	82
4.5	Voltage dips.....	83
4.5.1	S type dips - 2005.....	83
4.5.2	Z type dips - 2005.....	85
4.5.3	S-type -2006 .....	86
4.5.4	Z-type – 2006 .....	86
CHAPTER 5: ANALYSIS AND DISCUSSION.....		87
5.1	Introduction.....	87
5.1.1	High Resistance fault statistics.....	87
5.1.2	Analysis of distance relay performance.....	87
5.1.3	Relay characteristics tests using Matlab simulations; .....	87
5.2	Omicron test results .....	88
5.3	Transmission protection performance analysis.....	90
5.4	Summary.....	92
5.5	Voltage dips performance.....	93
CHAPTER 6: RECOMMENDATIONS .....		94
6.1	YTG - R3Z27 protection scheme.....	94
6.2	YTG - LZ32 protection scheme.....	94
6.3	H-type - Mho protection scheme .....	94
6.4	TLS – TLS protection scheme .....	95
6.5	Micromho Micromho protection scheme.....	95
6.6	SLYP/SCLN – SLYP/SLCN protection scheme .....	95
6.7	REL 531 - REL 531 protection scheme.....	95
6.8	7SA513 – 7SA513 protection scheme .....	96
6.9	SEL 321- SEL 321 protection scheme.....	97
CHAPTER 7: CONCLUSIONS.....		98
7.1	fulfilment of the objectives .....	98
7.2	Highlights of the research .....	98
7.3	Further reserach .....	98
7.3.1	Creating models for all the relays to do the theoretical evaluation to improve fault investigation.....	98
7.3.2	Determining the optimum setting for the directional earth fault relays .....	98



## LIST OF TABLES AND FIGURES

FIGURE 2.1: REPRESENTATIVE OF AN IDEAL COMPARATOR.....	6
FIGURE 2.2: PLAIN IMPEDANCE RELAY CHARACTERISTIC .....	7
FIGURE 2.3: MHO RELAY CHARACTERISTIC .....	8
FIGURE 2.4: SCHEMATIC DIAGRAM OF A SINGLE-PHASE MHO RELAY.....	8
FIGURE 2.5: VECTOR DIAGRAMS OF DIFFERENT POLARISING SIGNALS.....	10
FIGURE 2.6: SELF POLARIZED MHO RELAY CHARACTERISTICS.....	11
FIGURE 2.7: OFFSET - MHO RELAY CHARACTERISTIC.....	12
FIGURE 2.8: MEMORY POLARIZED MHO RELAY CHARACTERISTIC .....	13
FIGURE 2.9: CROSS-POLARIZED MHO RELAY CHARACTERISTICS .....	14
FIGURE 2.10: CROSS-POLARISED MHO RELAY CHARACTERISTICS FOR A REVERSE FAULT.....	14
FIGURE 2.11: REACTANCE CHARACTERISTICS .....	15
FIGURE 2.12: QUADRILATERAL CHARACTERISTICS .....	16
TABLE 2.1: MOST USED DISTANCE RELAYS IN ESKOM TRANSMISSION.....	19
FIGURE 2.21: 7SA513 DIRECTIONAL CHARACTERISTICS [20].....	28
FIGURE 2.22: 7SA513 DIRECTIONAL CHARACTERISTIC WITH SOURCE IMPEDANCE, FORWARD FAULT [20] .....	28
FIGURE 2.23: 7SA513 CHARACTERISTIC WITH SOURCE IMPEDANCE, REVERSE FAULT [20] .....	29
FIGURE 2.24: 7SA513 DIRECTIONAL EARTH FAULT PROTECTION [20].....	30
FIGURE 2.25: SEL PHASE CHARACTERISTICS [21] .....	31
FIGURE 2.26: SEL EARTH FAULT CHARACTERISTIC [21].....	31
FIGURE 2.27: ABB REL 531 TYPICAL CHARACTERISTIC FOR PHASE LOOP [22].....	32
FIGURE 2.28: ABB REL 531 TYPICAL CHARACTERISTICS FOR PHASE TO EARTH LOOP [22] .....	33
FIGURE 2.29: SIMPLIFIED LOGIC DIAGRAM FOR REL531 TEF [22] .....	35
FIGURE 2.30: SINGLE LINE DIAGRAM.....	36
FIGURE 2.32: DIFFERENT RELAY CHARACTERISTICS (R3Z27, LZ32 AND TYPE H RELAYS) .....	41
FIGURE 2.33: DIFFERENT RELAY CHARACTERISTICS (YTG AND MICROMHO RELAYS).....	41
FIGURE 2.34: DYNAMIC CHARACTERISTICS OF A TLS RELAY.....	42
FIGURE 2.35: EFFECT OF LOAD FLOW ON FAULT RESISTANCE.....	44
FIGURE 2.36 – DEFINITION OF VOLTAGE DIP PARAMETERS: DURATION AND MAGNITUDE.....	50
FIGURE 2.37 – NRS DIP CHARACTERISTICS PARADIGM FOR DIP MAGNITUDES .....	51
TABLE 2.2 – CLASSIFICATION OF VOLTAGE DIPS [27].....	52
TABLE 2.3: NRS-048 95% DIP “COMPATIBILITY” LEVELS .....	53
FIGURE 3.1: MHO CHARACTERISTIC SHOWING THE REACH TEST.....	57
FIGURE 3.2: MHO CHARACTERISTIC SHOWING THE REACH TEST.....	58
FIGURE 4.2: WHITE PHASE VOLTAGE AND CURRENT SIGNALS FOR A HIGH RESISTANCE FAULT .....	62
FIGURE 4.3: IMPEDANCE PLANE FOR FAULT IMPEDANCE LOCUS .....	62
FIGURE 4.4: DYNAMIC IMPEDANCE PLOT .....	63
TABLE 4.1: SEL321 LONG LINE HOMOGENEOUS TEST POINTS.....	64
TABLE 4.2: SEL LONG LINE NON-HOMOGENEOUS TEST POINTS.....	64

TABLE 4.3: SEL321 SHORT LINE HOMOGENEOUS TEST POINT .....	65
TABLE 4.4: SEL321 SHORT LINE NON- HOMOGENEOUS TEST POINT .....	65
FIGURE 4.6: SEL321 SHORT LINE CHARACTERISTICS .....	66
TABLE 4.5: YTG LONG HOMOGENEOUS TEST POINTS.....	66
FIGURE 4.7: YTG LONG LINE CHARACTERISTICS .....	67
TABLE 4.7: YTG SHORT LINE HOMOGENEOUS TEST POINTS .....	67
TABLE 4.8: YTG SHORT LINE NON HOMOGENEOUS TEST POINT .....	67
FIGURE 4.8 YTG SHORT LINE CHARACTERISTICS.....	68
TABLE 4.9: R3Z27 LONG LINE HOMOGENEOUS TEST POINTS – PLAIN IMPEDANCE .....	68
FIGURE 4.9: R3Z27 LONG LINE HOMOGENEOUS CHARACTERISTICS, PLAIN IMPEDANCE.....	69
TABLE 4.10: R3Z27 LONG LINE HOMOGENEOUS TEST POINTS, K=1.05 .....	69
FIGURE 4.10: R3Z27 LONG LINE HOMOGENEOUS CHARACTERISTICS, K=1.05.....	70
TABLE 4.11: R3Z27 LONG LINE HOMOGENEOUS TEST POINTS, K=2.1 .....	70
FIGURE 4.11: R3Z27 LONG LINE HOMOGENEOUS CHARACTERISTICS, K = 2.1 .....	71
TABLE 4.12: R3Z27 SHORT LINE HOMOGENEOUS TEST POINTS – PLAIN IMPEDANCE.....	71
FIGURE 4.12: R3Z27 SHORT LINE HOMOGENEOUS CHARACTERISTICS, PLAIN IMPEDANCE .....	72
TABLE 4.13: R3Z27 SHORT LINE HOMOGENEOUS TEST POINTS, K=1.05 .....	72
FIGURE 4.13: R3Z27 SHORT LINE HOMOGENEOUS CHARACTERISTICS, K=1.05 .....	73
TABLE 4.14: R3Z27 SHORT LINE HOMOGENEOUS TEST POINTS, K=2.1 .....	73
FIGURE 4.14: R3Z27 SHORT LINE HOMOGENEOUS CHARACTERISTICS, K = 2.1 .....	74
FIGURE 4.15: R3Z27 LONG LINE NON-HOMOGENEOUS CHARACTERISTICS, PLAIN IMPEDANCE.....	75
TABLE 4.16: R3Z27 LONG LINE NON-HOMOGENEOUS TEST POINTS, K =1.05.....	75
FIGURE 4.16: R3Z27 LONG LINE NON-HOMOGENEOUS CHARACTERISTICS, K =1.05.....	75
TABLE 4.17: R3Z27 LONG LINE NON-HOMOGENEOUS TEST POINTS, K =2.1 .....	76
FIGURE 4.17: R3Z27 LONG LINE NON-HOMOGENEOUS CHARACTERISTICS, K =2.1 .....	76
TABLE 4.18: R3Z27 SHORT LINE NON-HOMOGENEOUS TEST POINTS, PLAIN IMPEDANCE.....	76
FIGURE 4.18: R3Z27 SHORT LINE NON-HOMOGENEOUS CHARACTERISTIC, PLAIN IMPEDANCE .....	77
TABLE 4.19: R3Z27SHORT LINE NON-HOMOGENEOUS TEST POINTS, K = 1.05 .....	77
FIGURE 4.19: R3Z27 SHORT LINE NON-HOMOGENEOUS CHARACTERISTICS, K = 1.05 .....	78
TABLE 4.20: R3Z27 SHORT LINE NON-HOMOGENEOUS TEST POINTS, K = 2.1 .....	78
FIGURE 4.20: R3Z27 SHORT LINE NON-HOMOGENEOUS CHARACTERISTICS, K = 2.1 .....	79
TABLE 4.21: 2005 PROTECTION PERFORMANCES .....	80
TABLE 4.23: DIPS RELATED TO APOLLO ESSELEN FAULT 31/05/05 .....	83
TABLE 4.24: DIPS RELATED TO ARNOT MERENSKY FAULT 27/07/05.....	83
TABLE 4.25: DIPS RELATED TO GLOCKNER LETHABO FAULT 21/08/05 .....	83
TABLE 4.27: DIPS RELATED TO ACORNHOEK MARATHON FAULT 25/09/05.....	84
TABLE 4.28: DIPS RELATED TO APOLLO ESSELEN FAULT, 10/10/05 .....	84
TABLE 4.29: DIPS RELATED TO HERA WATERSHED FAULT, 19/11/05.....	84
TABLE 4.30: DIPS RELATED TO NORMANDIE UNFOLOZI FAULT, 05/12/06.....	84
TABLE 4.31: DIPS RELATED TO BACCHUS DROERIVIER FAULT, 06/03/06.....	85

TABLE 4.32: Z-DIPS RELATED TO KOMATIPOORT INFULENI FAULT 18/10/05 .....	85
TABLE 4.34: Z-DIPS RELATED TO AURORA JUNO FAULT 19/02/06 .....	85
4.35: Z-DIPS RELATED TO BACCHUS DROERIVIER FAULT 28/02/06.....	85
TABLE 4.36: DIPS RELATED TO CAMDEN NORMANDIE FAULT 14/06/06 .....	86
TABLE 4.37: DIPS RELATED TO PLUTO WATERSHED FAULT 26/06/06 .....	86
TABLE 4.38: DIPS RELATED TO MARATHON PRAIRE FAULT 24/07/06 .....	86
TABLE 4.39: DIPS RELATED TO INVUBU UMFOLOZI FAULT 09/10/06.....	86
TABLE 5.1: OMICRON RESULTS FOR LONG LINE.....	88
TABLE 5.2: OMICRON RESULTS FOR A SHORT LINE .....	89
FIGURE 5.1: RELAY TYPES IN ESKOM TRANSMISSION .....	90
FIGURE 5.2: PROTECTION PERFORMANCE FOR 2005 .....	91
FIGURE 5.3: PROTECTION PERFORMANCE FOR 2006 .....	92
TABLE 5.3 : NUMBER OF DIPS PER YEAR FOR EACH CATEGORY OF DIP WINDOW.....	93

# 1 CHAPTER 1 INTRODUCTION

## 1.1 BACKGROUND

Eskom is South Africa's electricity utility, and is a vertically integrated organisation that generates, transmits and distributes electricity to industrial, mining, commercial, agricultural and residential customers as well as redistributors. Eskom is Africa's largest energy utility, and ranks as one of the top five energy utilities in the world. Eskom generates over half the electricity produced in the whole of Africa [1].

The transmission network in Eskom consists of 160 substations interconnected via 27 000km of 220 - 765kV lines. Eskom's transmission network is exposed to large numbers of primary faults that can be classified in four major groups in terms of their origin [2]:

- Bird pollution (30%)
- Fires (27%)
- Lightning (25%), and
- Other (18%)

It can be seen that fires under the lines cause over a quarter of all faults on the Eskom transmission network. The dynamic characteristics of arc burning in the air often results in significant changes in arc length and resultant resistance during the fault. The heat dissipated on the entry point of arc to ground sometimes results in melting of sand on the surface, which can also substantially change the resistance of the fault. In Eskom's transmission system, about 16% of all the recorded faults are high resistance faults [2].

## 1.2 IMPORTANCE OF THE RESEARCH

Extended fault clearance times for high resistance faults in certain parts of the network have occurred for some power system disturbances. Slow clearances of faults have a negative impact on power quality. Long fault durations have a negative impact on power quality. Both electric utilities and end users of electrical power are becoming increasingly concerned about the quality of electric power. The major reasons for the growing concern include the following [3]:

- Load equipment is more sensitive to power quality variations than equipment applied in the past. Many new load devices contain microprocessor-based controls and power electronic devices that are sensitive to many types of disturbances;
- Increased awareness of power quality issues by the end user. Utility customers are becoming better informed about such issues as interruptions, sags, and switching transients and are challenging the utilities to improve the quality of power delivered;

- Many things are now interconnected in a network. Integrated processes mean that the failure of any component has much more important consequences.

Eskom has relied primarily on impedance-based measurement protection relays also known as distance protection relays for the protection of EHV transmission lines. The basic measurement principle of distance protection is that the relay calculates the ratio of the voltage and current at the relay location when a fault occurs. It, therefore, measures the impedance of the line from the bus bars to the point of the fault. If the measured fault impedance is smaller than the line impedance it means that the fault is somewhere on the line. If it is bigger, then the fault is beyond the remote substation.

High-resistance faults are characterised by low fault currents. Therefore the impedance calculated would be much bigger and so the fault will appear to be beyond the protected line. This scenario makes it very difficult for impedance protection to function correctly in case of high resistance faults. The consequences of high resistance faults is that faults are not cleared or long duration of faults on lines that use impedance-based measurement protection relays.

The suitability of the applied protection equipment per specific application has been questioned. Consequently, a study is being proposed to address these challenges. The main objective of this study is to gain a clear understanding of the measurement capability of the different EHV transmission line protection relays used, the impact on the transmission network performance and finally to give recommendations on the refinements to the EHV transmission line protection philosophy required to improve future protection performance.

### **1.3 AIM OF THE RESEARCH**

The scope of the research project is to study the fault resistance measurement capability of the relays by means of digital simulations and Omicron relay tests, and to determine the impact of high resistance faults on the transmission protection performance

The researcher's intention in conducting this research is to gain clear understanding of the capability of the existing relays used in Eskom Transmission network and to give recommendations on the refinements to the EHV transmission line protection philosophy required to improve future protection performance.

## **1.4 HYPOTHESIS**

Impedance-based measurement protection relays for the protection of EHV transmission lines alone are not sufficient to handle high resistance faults which are the main cause of long fault durations

## **1.5 RESEARCH QUESTION**

Main research question:

“What refinements to the EHV transmission line protection philosophy are required to improve future protection performance?”

### **1.5.1 Subsidiary questions**

The author has to answer further subsidiary research questions in order to answer the main research question:

- What is the pattern of the type of faults over the past 4 years, with regard to fault resistance?
- What is the capability, of existing transmission line protection devices used by Eskom, to detect high resistance faults?
- What is the impact of high-resistance faults on protection relay performance?
- What improvements are to be implemented in Eskom transmission line protection philosophy to improve the capability of protection performance concerning high resistance faults?

## **1.6 OUTLINE OF SUBSEQUENT CHAPTERS**

Chapter 1 is an introduction to the research content. It provides the background of the transmission system in which the research is carried out. It is demonstrated how important the general area of research is to Eskom transmission system, and how this research fits into the existing research project initialised by Eskom research division. The aim of the research is also given in this chapter to give the reader an idea of what the researcher aims to achieve by conducting this research.

Chapter 2 reviews the literature related to the research. It provides information necessary for the analysis and interpretation of the results, as well as the drawing of recommendations.

The research methodology is covered in Chapter 3, it describes the method and the techniques used to test the hypothesis and analyse data and validity of the study.

Chapter 4 and chapter 5 describe data analysis and discussion of results. The results will be presented and evaluated. The results of the hypothesis will be analysed. The theory from the literature review carried out is compared with the results of the study.

Recommendations are given in chapter 6 and conclusions Chapter 7, which compares the results to the original objectives, and presents the recommendations.

## 2 CHAPTER 2 LITERATURE REVIEW

### 2.1 IMPEDANCE PROTECTION

The basic measurement principle of distance protection is that the relay calculates the ratio of the voltage and current at the relay location when a fault occurs. It therefore measures the impedance of the line from the busbars to the point of the fault. If the measured fault impedance is smaller than the line impedance it means that the fault is somewhere on the line. If it is bigger, then the fault is beyond the remote substation.

The simplest impedance based protection relays use only a single-phase current and a single-phase voltage for the measurement of single-phase to earth faults. As the design improved other currents and voltages have been added to the relay operating quantities.

As a result of changes in protection technology over the last few decades a great variety of protection relays are in operation on the Eskom Transmission system from electromechanical (48%), through electronic (32%), digital (17%) to highly sophisticated programmable Intelligent Electronic Devices (3%) [2].

High-resistance faults are characterized by low fault current therefore impedance calculated would be much bigger and therefore the fault will appear to be beyond the protected line. This scenario makes it very difficult for impedance protection to function correctly in case of high resistance faults.

A composition of different type of characteristics applied on Eskom's network is as follows: reactance (0%), mho, and quadrilateral characteristics.

#### 2.1.1 Principles of comparator

Comparators are basically divided into two groups according to whether a comparison is done by comparing amplitudes of two inputs or of the phase angle between them. That is where they derive their name of amplitude comparator or phase comparator. See figure 2.1 below for an ideal comparator.



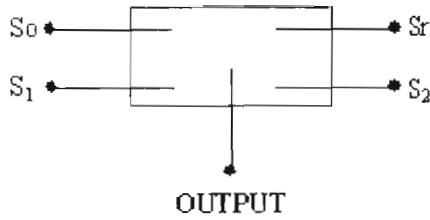


Figure 2.1: Representative of an ideal comparator.

$S_o$  (operating input) and  $S_r$  (restraining input) are designated inputs of the amplitude comparator while  $S_1$  and  $S_2$  are the inputs for phase comparators. For amplitude comparators  $S_o > S_r$  for an output  $> 0$ . For a phase comparator  $90^\circ < \theta < 270^\circ$  for an output  $> 0$ . The angle  $\theta$  is the phase angle between  $S_1$  and  $S_2$  and is also known as the characteristic angle. In general distance relays use phase angle comparators to perform the measuring function.

Considering the following example:

$I$  is the line current and  $Z_R$  is the relay reach.  $I Z_R$  is the operating input and  $V$  is derived from the line voltage and is the restraining input. The sum and the difference of these input quantities are fed to the phase comparator to compare the angles between them [4].

$$S_1 = S_r - S_o = V - I Z_{R1}$$

$$S_2 = S_o + S_r = V + I Z_{R2}$$

The generalized phase comparator inputs can be written as:

$$S_1 = K_1 V - K_2 I Z_{R1} \quad \text{[Equation 2.1]}$$

$$S_2 = K_3 V + K_4 I Z_{R2} \quad \text{[Equation 2.2]}$$

Where  $K_1$  to  $K_4$  are real numbers.  $Z_{R1}$  is assumed to have argument  $\theta_1$  and  $Z_{R2}$  an argument  $\theta_2$  [4]. By modifying the constants  $K_1$  to  $K_4$  into the phase comparator different distance relay characteristics are obtained

### 2.1.2 Plain impedance characteristics

This is the relay that responds to the magnitude of the impedance given by the applied voltage and current and is independent of the phase angle between these quantities. With  $K_1$  to  $K_4$  equal one in equations 2.1 and 2.2,  $Z_{R1}$  and  $Z_{R2}$  the same and equal to the relay reach  $Z_R$ , then

$$S_1 = V - I Z_R \quad \text{Boundary is } I Z_R = V \text{ or } Z = Z_R$$

and

$$S_2 = V + I Z_R \quad \text{Boundary is } I Z_R = -V \text{ or } Z = -Z_R$$

The Figure 2.2 below shows the characteristic plotted on the R/X diagram.

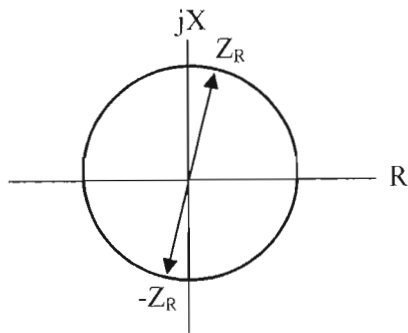


Figure 2.2: Plain impedance relay characteristic

The disadvantages of plain impedance relays are:

- It is non-directional.
- Highly sensitive to power swings due to large area covered by the impedance circle [4]

In order to improve the directional measurement capability, a directional relay is added on top of the impedance relay. Mho relay can be used which will be discussed on the next section. However, a mho relay covers less resistance area.

### 2.1.3 Mho Characteristics

The typical means of obtaining a mho characteristic is to use the cosine-phase comparator. This comparator measures the phase angle between the operating and polarizing signals. The logic used to measure the phase angle is called phase angle comparator. Other relays design employs three or more inputs to the logic and will be covered later. These additional inputs greatly improve the performance of the relay, but they bring more complexity on the understanding of the relay performance and require more complex setup to insure that all of the inputs have the proper phase relationship.

Figure 2.3 below shows mho characteristic plotted on the voltage plane ( $IR/IX$ ) diagram. Instead of the impedance plane ( $R/X$  diagram) the voltage plane is used to explain different types of relay characteristics which relate to the inputs of the comparator.

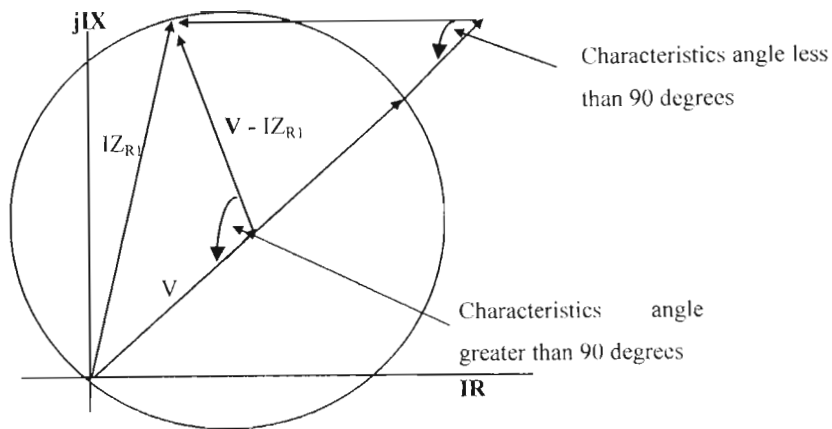


Figure 2.3: Mho relay characteristic

Consider a single-phase relay to explain the mho characteristics. The following diagram represents a single-phase relay input circuit connection:

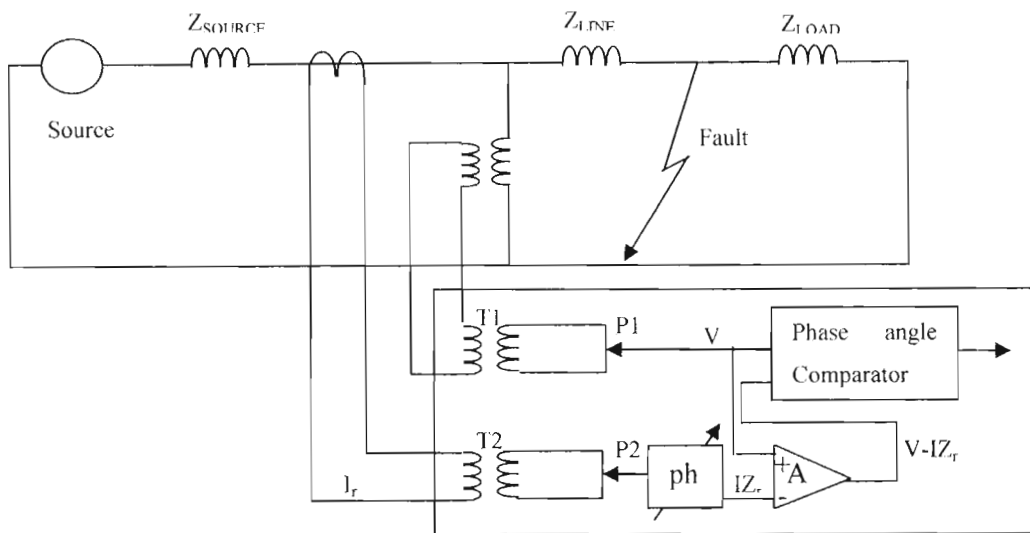


Figure 2.4: Schematic diagram of a single-phase mho relay

The phase voltage is isolated and stepped down by transformer  $T_1$ , the output of which can be attenuated by a potentiometer  $P_1$  giving voltage  $V$ . A transformer  $T_2$  attenuated by potentiometer  $P_2$  and phase shifted by a circuit  $Ph$ , giving a voltage signal  $I Z_r$  that isolates the phase current.

Amplifier  $A$  produces a signal  $V - I Z_r$  and at this point the phase angle between  $V - I Z_r$  and  $V$  is examined, the phase angle mentioned above can also be referred as the characteristic angle. If the characteristic angle is less than  $270$  degrees the fault lies outside the mho circle and if it is greater than  $90$  degrees the fault lies inside the circle.

#### 2.1.4 Polarization

The primary requirement for the polarising voltage is that the pre-fault phase angle of the polarising signal be the same as that of the restraint voltage used in the operating signal. The main reasons for different polarising quantities are [5]:

- Ensure operation for zero voltage single phase to earth faults
- Directional integrity
- Fault resistance impedance improved performance
- Correct phase selection in single phase tripping schemes

A mho distance relay function may be developed using a variety of voltages as the polarizing signal as mentioned before. For a self-polarised relay, the faulted phase is used as the polarising voltage, the characteristic remains unchanged under changing system and fault conditions. “However distance relays polarised by potential other than the faulted voltage have a family of circles for different fault conditions and hence their characteristics are more difficult to show on an impedance diagram” [5]. These characteristics are explained below GE [6]:

- Dynamic characteristic

It is the initial characteristic of time varying impedance characteristic. The variation with time is due to memory action

- Variable characteristic

This is due to the use of some form of healthy phase polarisation. The characteristic varies as a function of the relay design, the power system, and the fault type. The variable characteristic does not vary with time.

- Steady state characteristic

It is the classical mho characteristic that passes through the origin on the R-X diagram. This is the characteristic that is typical plotted during routine relay testing.

Some relays utilize part of or all of the unsaluted phase voltages in the polarizing signal, these phenomena is called ‘Cross polarisation’ or a healthy phase polarisation’.

- Polarising signals

There is a wide variety of polarising voltages that can be used. Consider a three-phase power system with phase A, B and C. Typical signals for a phase A function are [7]:

- $(V_{A-G}) M$ , that is faulted phase voltage with memory
- $(V_{BC} < 90^\circ) M$ , which is healthy phase voltage rotated 90 degrees with memory.
- $(V_{AM}) M$ , which faulted phase to the midpoint of  $V_{BC}$  with memory.
- $(V_{AG1}) M$ , Positive sequence voltage referenced to phase A with memory

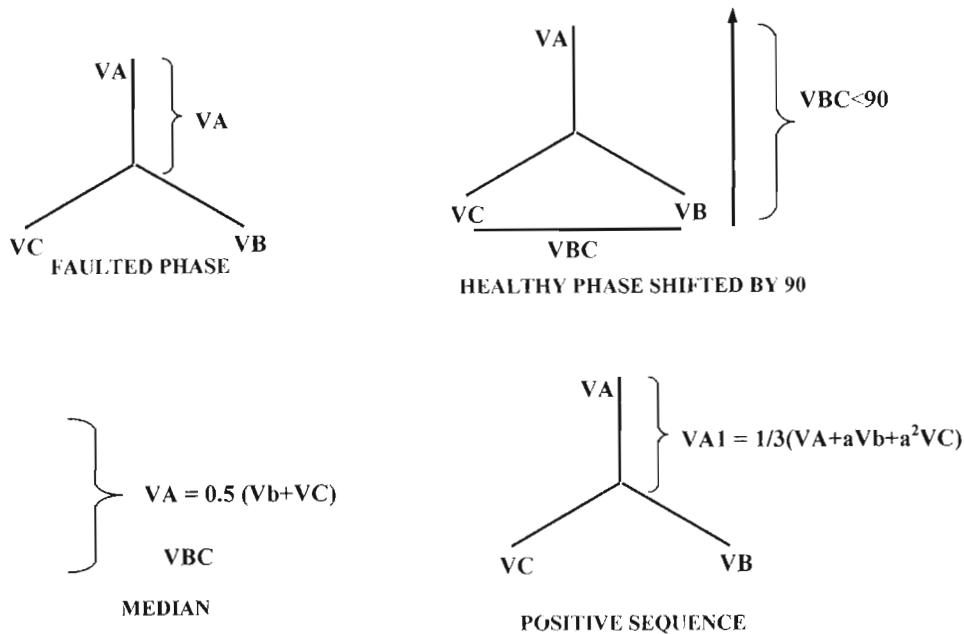


Figure 2.5: Vector diagrams of different polarising signals

### 2.1.5 Self - polarized mho characteristics

This type of characteristic is dependent on both magnitude and phase angle of voltage and current for its operation. The relay uses the voltage on the faulted phase for its polarizing voltage. Setting  $K_1, K_2, K_3$  equals to 1 and  $K_4$  equal to 0 in equations 2.1 and 2.2, gives a mho relay.

$$S_1 = V - IZ_R$$

$$\text{Boundary is } IZ_R = V \text{ or } Z = Z_R$$

and

$$S_2 = V$$

$$\text{Boundary is } V = 0 \text{ or } Z = 0$$

Figure 2.6 below shows the self-polarized mho relay with faults at different points of the characteristics plotted on the voltage plane (jIX/IR diagram)

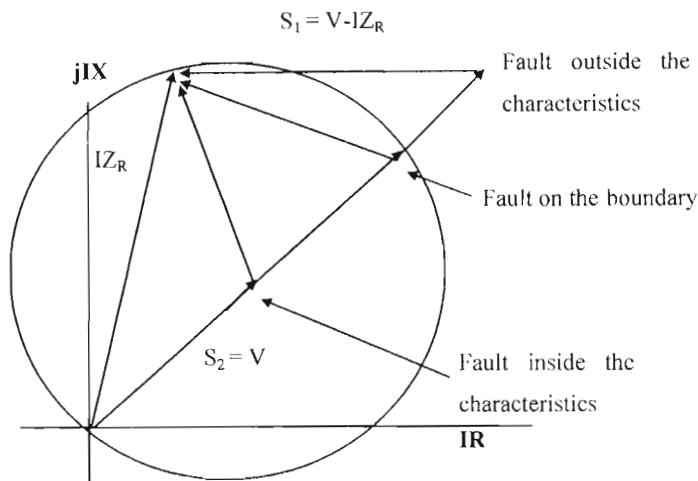


Figure 2.6: Self polarized mho relay characteristics

#### Disadvantages

- This type of a relay has less resistance coverage than the plain impedance characteristic.
- The relay may fail to operate for a close up fault because the polarizing voltage falls to zero or near zero [7].

#### Solution

Offset Mho relay, cross polarization and memory polarization are able to operate for close up faults.

#### 2.1.6 Offset –mho relay characteristic

Offset mho impedance relay is derived by making  $K_1, K_2, K_3$  equals to one and  $K_4 = K$  in equations 2.1 and 2.2, where  $K$  determines the degree of offset.  $Z_{R1}$  and  $Z_{R2}$  are the same and equal the relay reach  $Z_R$

$$S_1 = V - IZ_R$$

$$\text{Boundary is } IZ_R = V \text{ or } Z = Z_R$$

and

$$S_2 = V + K IZ_R$$

$$\text{Boundary is } K IZ_R = -V \text{ or } Z = -K Z_R$$

The offset mho relay has an advantage of being able to operate for a close up faults, both in forward and reverse direction. Offset -mho characteristic is shown on figure 2.7 below:

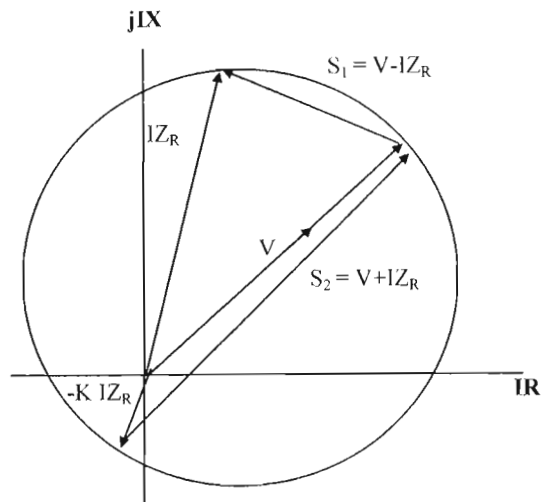


Figure 2.7: Offset - mho relay characteristic

### 2.1.7 Memory polarization mho relay characteristic

Refer to the schematic diagram of a two input phase angle comparator in figure 2.4. In series with the polarizing voltage ( $V$ ) the memory circuit is added, which in the case of a fault remembers the pre-fault voltage for some few cycles, and this voltage will be used as a polarizing voltage until the memory circuit decays and thereafter the voltage of the faulted phase will be used as a polarizing voltage. Referring to the memory polarized mho relay characteristics figure 2.8, when the fault occurs at time  $T_0$  the initial expanded characteristic is represented by the outside circle. After a certain time  $T_1$  the polarising signal ( $I Z_{R2}$ ) becomes smaller and the result is the dotted characteristic in the middle. After time  $T_2$  elapses, there relay becomes self polarised and the resultant is the steady state characteristics. The memory action will cause an expanded characteristic, which is a transient condition that changes as the memory decays. The duration of the expanded characteristics is determined by the design constants of the relay. This expanded characteristic gives a better coverage of high resistance faults than the normal steady state characteristics [7]. The relay uses the pre-fault voltage, which closely resembles the source voltage for its polarizing signal, therefore the expansion of the mho circuit depends on the source impedance.

Eskom's old relays (Electromechanical and Electronic) have a polarization circuit that utilizes a tuned circuit [8]. Most of the new relays (Digital and highly sophisticated programmable Intelligent Electronic Devices) use a digital synchronous polarizing circuit, which gives a

better performance than the tuned circuits, used by old relays. Digital filters have the time constant of four cycles, and provide very strong polarization for over 20 cycles [8]. The figure below shows the characteristics of the memory relay.

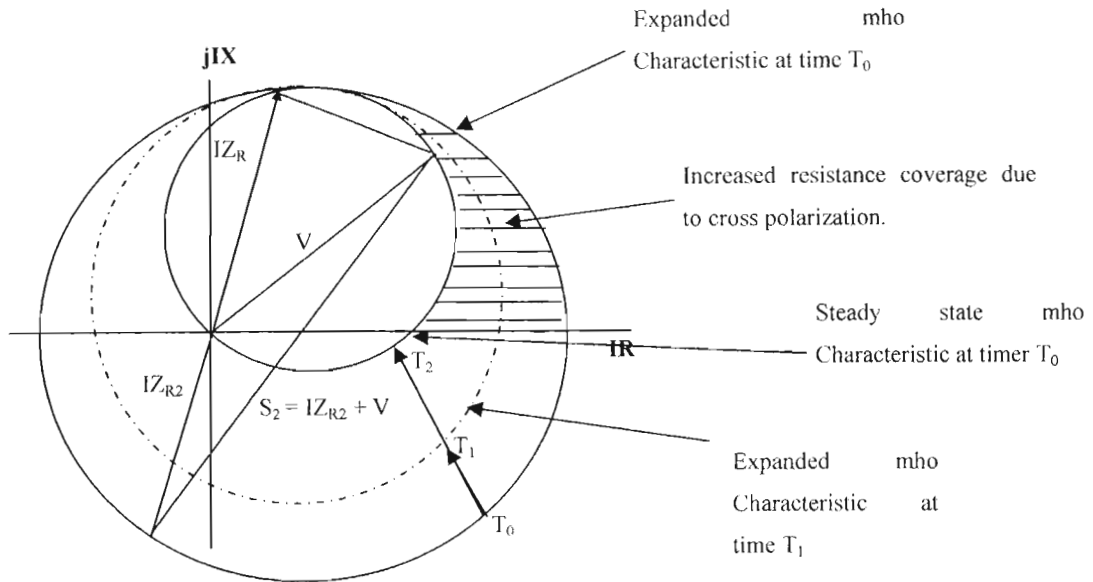


Figure 2.8: Memory polarized mho relay characteristic

### 2.1.8 Cross – polarised mho relay characteristic

The polarizing voltage is derived from a healthy phase voltage or a combination of healthy and faulted phase voltage. The characteristic is derived by making  $K_1$  and  $K_2 = 1$ ,  $K_4 = K$  and  $K_3 = 1$  in equations 2.1 and 2.2. Where  $Z_{R1}$  is the impedance setting on the relay  $Z_R$ , and  $Z_{R2}$  a function of the source impedance.  $K_1 Z_{R2}$  is a certain amount of cross-polarized voltage

$$S_1 = V - IZ_{R1} = Z - Z_{R1}$$

$$S_2 = V + K_1 Z_{R2} = Z + KZ_{R2}$$

Cross polarization will cause an expanded variable characteristic as can be seen in figure 2.9 below in which the expanded characteristic is due to some of the healthy phase voltage.



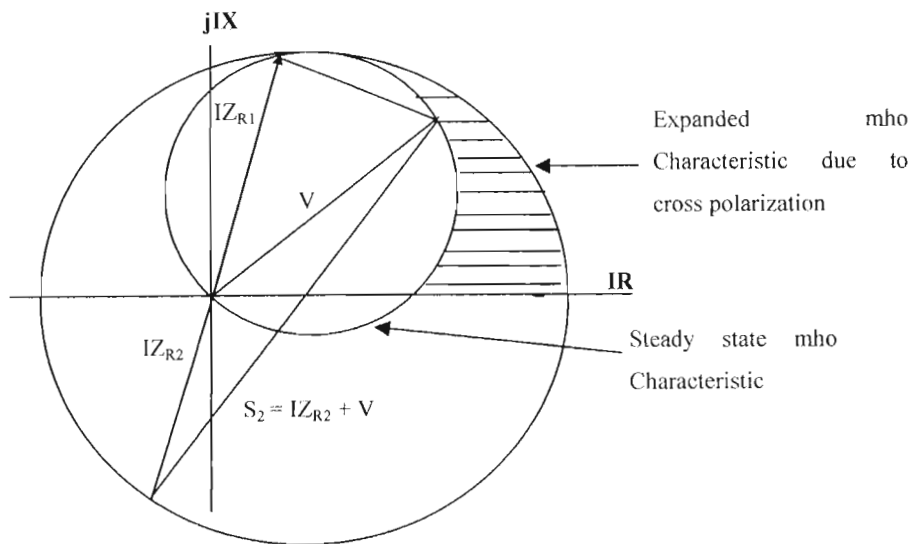


Figure 2.9: Cross-polarized mho relay characteristics

$Z_{R1}$  is the impedance setting on the relay and  $Z_{R2}$  a function of the source impedance.  $K_1 Z_{R2}$  is a certain amount of cross-polarized voltage. The expansion depends on the source impedance, the higher the source impedance behind the relay, the more the expansion of the normal mho characteristic [7]. When the source impedance is nil, there is no expansion.

For reverse faults, the fault current viewed by the relay is negative therefore:

$$S_1 = V + IZ_{R1} = Z + Z_{R1}$$

$$S_2 = V + IZ_{R2} = Z + Z_{R2}$$

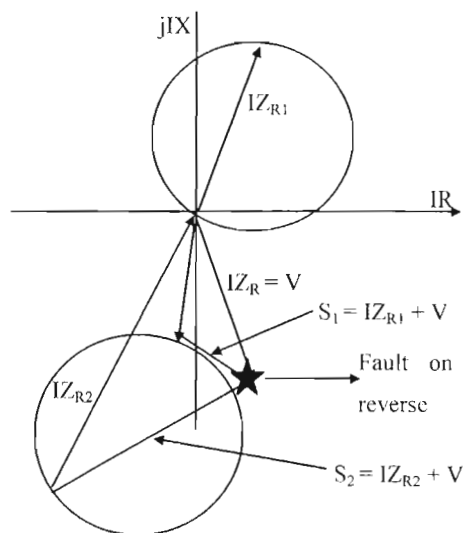


Figure 2.10: Cross-polarised mho relay characteristics for a reverse fault.

It can be seen that the relay will not operate for reverse faults. A disadvantage of a fully cross-polarized relay is that the relay installed on a healthy phase can operate for a fault due to the expansion [9]. Therefore fully cross-polarized relays are used only when the same relay is used for different types of faults or for a switched impedance protection. For full schemes where separate measurement elements are used, partially cross polarization type characteristics are used.

## 2.2 REACTANCE CHARACTERISTICS

To improve arc resistance coverage a reactance characteristic with a starter of a Mho characteristic could be used. These types of characteristics measure the reactance and ignore the resistance. Directional supervision is used with this characteristic, because faults are seen in all directions. The reactance relay achieves the directionality from the Mho relay as the Mho relay is inherently directional.

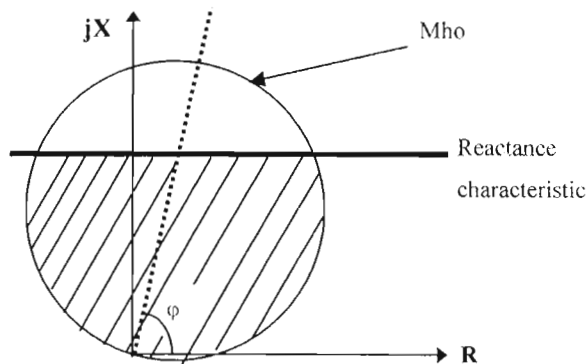


Figure 2.11: Reactance characteristics

## 2.3 QUADRILATERAL CHARACTERISTICS

The quadrilateral characteristic is often used to cater for high resistance fault i.e. for short lines for which the fault impedance is relatively high and for which no load encroachment is expected [10]. A quadrilateral ground distance characteristic consists of four boundary settings. Each side of the quadrilateral characteristic shown in Figure 2.12 represents a different settings: the reactance boundaries (top line), positive and negative resistance boundaries (right and left sides, respectively), and the directional (bottom line). A quadrilateral distance characteristic operates if the measured impedance is inside the box defined by the four boundaries mentioned above.

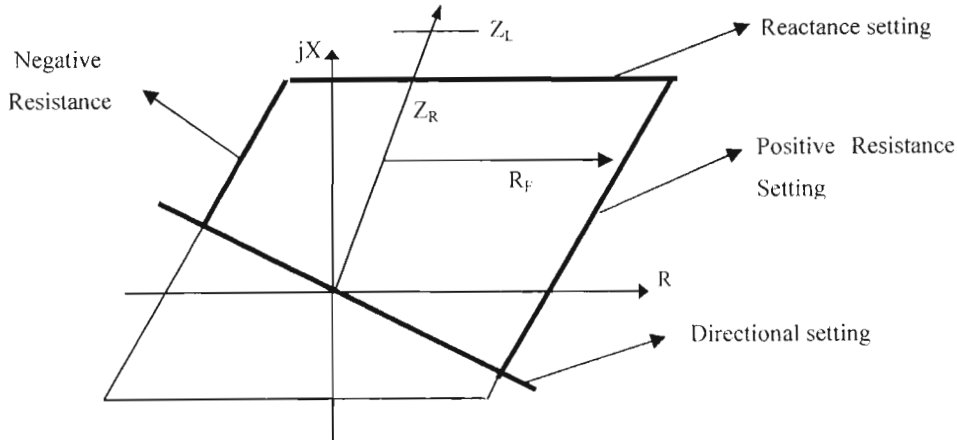


Figure 2.12: Quadrilateral characteristics

## 2.4 ALTERNATIVES FOR TRANSMISSION LINE PROTECTION

### 2.4.1 Directional overcurrent

Directional overcurrent relays are used to detect phase or ground faults in a particular direction on a power system and to initiate isolation of these faults [9]. They require a polarizing quantity as a reference. The directional overcurrent relay is widely used for earth fault protection [10]. All sequence-quantities are available for faults involving ground. The positive-sequence quantities are adversely affected by load and therefore should be avoided when considering earth fault protection [10], leaving only zero- and negative sequence quantities as possible inputs to a ground directional element. The polarization method used is specified as part of the relay type. Methods available are:

- Zero sequence voltage polarisation

A zero-sequence overcurrent relay simply measures the sum of the three phase currents as in the equation below:

$$I_r = 3I_0 = I_a + I_b + I_c$$

These residual elements should never be set more sensitive than the normal system unbalance. System unbalances can be caused by conditions such as loading conditions and untransposed transmission lines. A zero-sequence voltage polarized ground directional element uses  $V_0$  or  $3V_0$  as the polarizing reference.

$$3V_0 = V_a + V_b + V_c$$

Equation below represents the torque for a zero-sequence voltage polarized directional element:

$$Torque = |3V_0| * |3I_0| * \cos([\angle -3V_0 - (\angle 3I_0 + \angle ZL_0)])$$

The sign of the torque is positive for forward faults and negative for reverse faults. If the polarizing voltage magnitude becomes too small, its angle becomes unreliable.

The main problem with this zero sequence voltage polarisation is that if the zero-sequence voltage magnitude presented to the relay for a remote fault is too low, the torque produced by the zero-sequence voltage directional element may be too low to cross its minimum torque threshold [10]. The solution to low polarizing voltage magnitude applications is to use a current polarized directional element.

- Zero sequence current

A zero-sequence current polarized ground directional element measures the phase angle difference between the line residual current ( $3I_0$ ) and an external polarizing source current ( $I_{POL}$ ).

- Dual polarized

A dual polarized zero-sequence directional element is the combination of a zero-sequence voltage polarized directional element and a zero-sequence current polarized directional element. This element provides more flexibility than a single method of zero-sequence polarization [10].

- Negative sequence voltage

It is also effective as an earth fault protection. Negative-sequence polarized directional elements have the following advantage when compared to zero-sequence voltage polarized directional elements:

Negative-sequence directional elements are insensitive to zero-sequence mutual coupling associated with parallel transmission line applications [10].

- Positive sequence voltage

This type is usually applied as a phase relay with a directional unit polarized by the healthy phase to phase voltage.

#### **2.4.2 Differential protection**

Differential relays are used to detect faults by comparing electrical quantities at all the terminals of a system element. Current differential relaying is the most common principle used for transmission line protection. The current differential schemes can only be applied on short lines, for long lines (distances above 100km) the use of communication channel has the disadvantage of being costly and reliability of the channels becomes a problem.

## 2.5 Eskom EHV feeder protection schemes

The Transmission EHV feeders are protected by two equivalent protection systems – main 1 and main 2 which back each other up. For longer feeders (above 20km) two distance relays are usually installed. The distance relays were preferably from different manufacturers; this was the practice on Eskom old schemes. The practice, however, since the introduction of Digital technology, is to install relays from the same manufacturer. The rationale behind this practice is to select the most suitable product in terms of both performance and economic life cycle efficiency. Shorter feeders (below 20km) should be equipped with a combination of distance and differential relays to improve performance for high resistance faults. On very short feeders (below 5km) installation of differential relays for both main 1 and main 2 is considered on condition that adequate remote back-up for busbar faults is also provided. The installation of differential relays is limited to the availability of adequate communication channels.

According to transmission protection design standard, the main 1 and main 2 protection systems are fully segregated in secondary circuits [11]:

- Main 1 and main 2 are supplied from different cores of the instrument transformers (CTs and VTs).
- Protection panels are powered from two independent DC supplies.
- Main 1 and main 2 use two different telecommunication media or at least different channels.
- Tripping is provided to independent circuit-breaker tripping coils.
- For reliability, cross tripping between main 1 and main 2 relays is provided.

Usually an additional back up earth-fault function is incorporated in the main protection relays or installed separately to improve possible deficiencies of distance relays in the detection of low fault current, high resistance faults. However back up earth fault relay has the disadvantage of being non-directional, so it can not be set to operate instantaneously. Back up earth fault relay will trip more slowly for high resistance faults due to low fault currents [11].

Currently there is a great variety of protection relays that are in operation on the Eskom transmission system from electromechanical (48%), through electronic (32%), digital (17%) to highly sophisticated programmable Intelligent Electronic Devices (3%) [2]. both main 1 and main 2 are expected to clear a fault in 100ms All faults that are cleared after 100ms are considered poor performance on protection equipment.

There are currently more than 20 relay types applied as line protection on the Eskom's transmission network with the most common types of characteristic being Mho characteristic and polygonal characteristics [12]. Most used relays are listed in the Table 2.1 below.

Table 2.1: Most used distance relays in Eskom Transmission

Relay Type	Manufacturer	Generation
Type -H	Reyrolle	Phase 1
P10/P40	Alstom	Phase 1
LZ32	ABB	Phase 1
THR	Reyrolle	Phase 1
R3Z27	Siemens	Phase 1
YTG	Alstom	Phase 1
SlypSlcn	GE	Phase 2
Micromho	Alstom	Phase 2
SLS	GE	Phase 2
TLS	GE	Phase 2
PXLN	Alstom	Phase 3
7SD512	Siemens	Phase 3
7SA513	Siemens	Phase 3
REL 561	ABB	Phase 4
REL 531	ABB	Phase 4

Eskom's different naming of protection schemes has always been based on the type of technology used. Below are the definitions of Eskom's protection schemes [12]

- Phase 1, Electromechanical relays and very early discrete electronic relays
- Phase 2, Electronic relays
- Phase 3, Digital relays
- Phase 4, Programmable Intelligent Electronic Devices

Most common schemes used in Eskom are listed below (Main 1 and Main 2)

Phase 1 scheme:

- YTG - R3Z27
- YTG - LZ32
- H-type and back up Mho

Phase 2 schemes

- TLS - TLS
- Micromho Micromho
- SLYP/SCLN – SLYP/SLCN

Phase 3, 4 and 5 schemes

- REL 531 - REL 531
- 7SA513 – 7SA513
- SEL 321- SEL 321

### 2.5.1 Principle of distance protection

Eskom distance protection relays typically consists of three stages, with mho, quadrilateral and or reactance characteristics. The distance protection relay caters for phase faults and earth faults. The three stages are: zone 1 protection which typically covers 80% of the line, zone 2 which typically covers 120 % of the line, zone 3 reverse reach which covers typically 20% of the line on the reverse direction and zone 3 forward which covers typically 150% of the line [11].  $Z_L$  is the line impedance. The zones of protection of this relay can be shown on the  $jIX$ ,  $IR$  diagrams below.

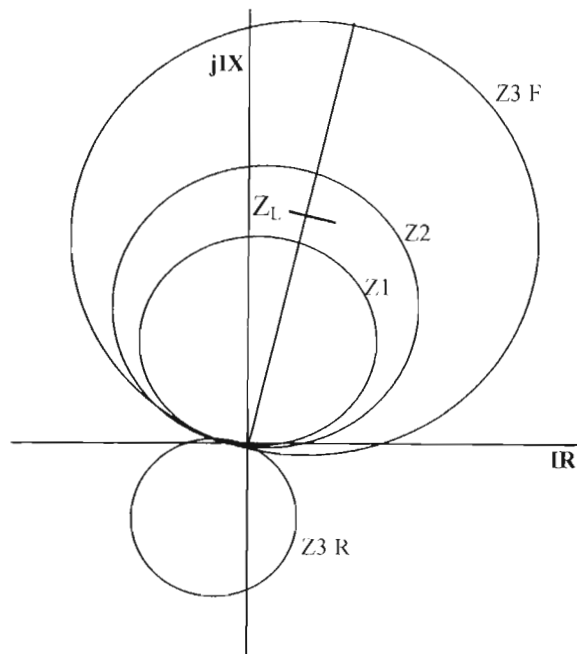


Figure 2.13: Three zones of protection for a mho or reactance characteristic relay

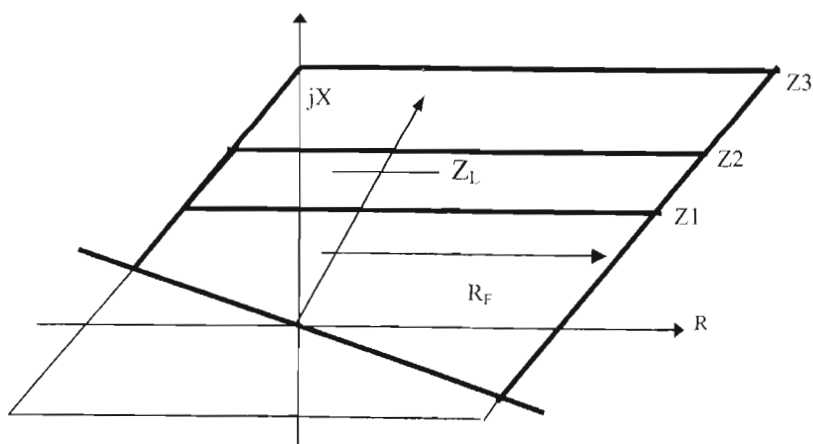


Figure 2.14: Three zones of protection for a Quadrilateral characteristic relay



Zone 1 is to trip instantaneously as it is assumed that it covers the fault inside the line only. Zone 2 is to ensure that the remaining part of the line, which not covered by zone 1, is protected and zone 2 covers the remote busbars also. Zone 2 is normally delayed, typically set to trip after 400ms. Zone 3 has the forward reach and the reverse reach. The zone 3 reverse reach is to provide a back up for local busbar faults taking into account 20% measuring errors, infeed and high fault resistance. The zone 3 reverse reach must not overreach adjacent transformers taking into account 20% measuring errors and infeed. The zone 3 forward reach is the overreaching element is to provide a back up for the remote stations, but should not overreach zone 2 of shortest line adjacent to the remote end. Zone 3 is normally delayed by 1 second.

### 2.5.1 YTG Relay [13]

YTG relay is an impedance based type of protection and it is three stages, three phase relay with a mho characteristic. The YTG relay caters for phase faults and earth faults. Eskom transmission network currently has about 140 YTG relays installed for the protection of EHV lines. The zones of protection of this relay can be shown on the IX, IR diagram below.

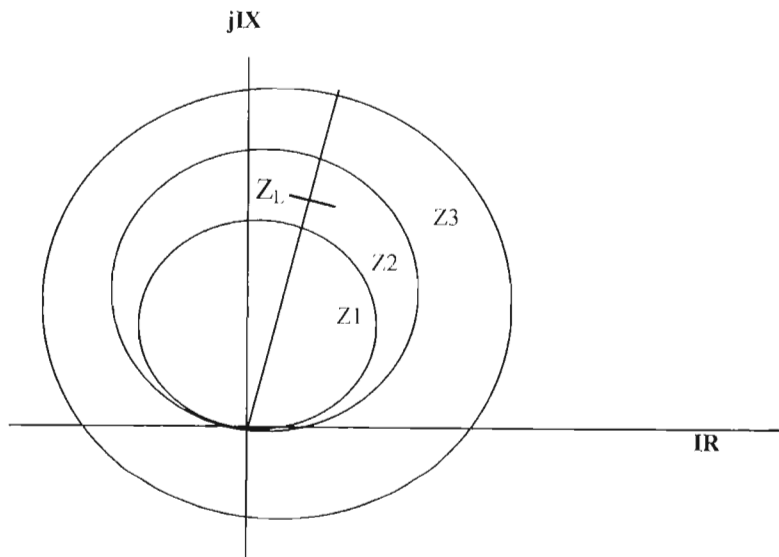


Figure 2.15: Three zones of protection for a YTG relay

- Polarising technique

Due to a lack of operation for zero voltage unbalanced faults, a YTG relay utilises a polarising voltage that is equal to 2% of the healthy phase voltage plus the faulted phase voltage for zone 1 and zone 2 faults [13]. The technique is also known as partial cross-polarisation of the mho characteristic. For zone 3 an offset mho characteristic relay is used.

Cross polarisation has the effect of increasing the steady state mho characteristic in such that it covers for better resistance coverage [7]. For the YTG relay the effect of polarising is very small as only 2% of healthy voltage is utilised.

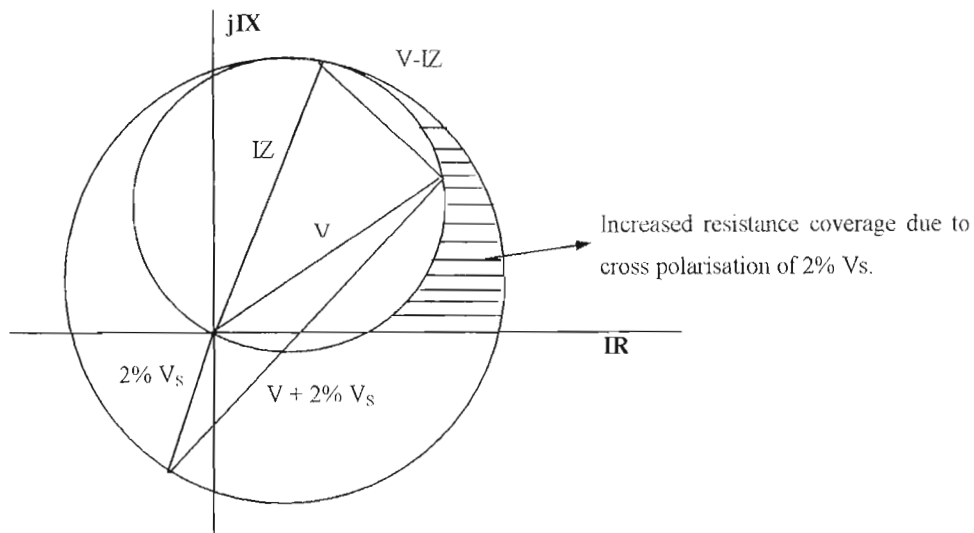


Figure 2.16: IR-IX diagram with an effect of polarisation on a YTG relay

- Relay Characteristic angle setting

The relay characteristic angle of the relay can increase the fault resistance coverage if it is set lower than the line impedance angle. The setting ranges from  $45^\circ$  to  $75^\circ$ . In Eskom transmission, relay characteristic angle is set below the line angle to allow for better fault resistance coverage. Consider the following mho characteristic diagram for the explanation

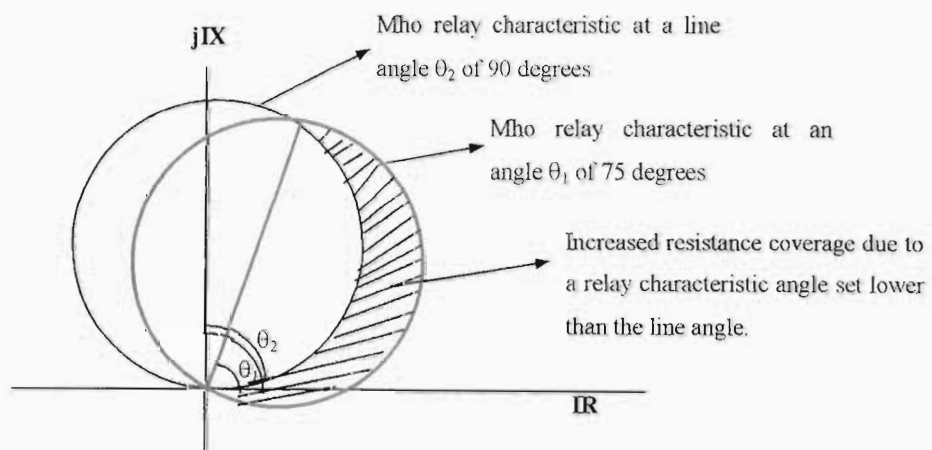


Figure 2.17: Effect of relay characteristic angle

### 2.5.2 TLS RELAY [14]

TLS relays use multi input phase angle comparators to derive a variable mho type characteristic with self-polarization and memory action [14]. The distance function of the

TLS relay uses a positive, negative and zero sequence voltage as the polarizing quantity for earth faults. The TLS relay has the following characteristics: Variable  $mho$  characteristic, Reactance characteristic, and Directional characteristics.

- Fault resistance coverage capability

TLS relays have the following additional features to improve resistance coverage.

- Characteristic timer angle adjustment:

This feature allows the shape of the characteristic to be set in three ways: normal circle if  $\theta = 90$  degrees, Lens  $\theta > 90$  and tomato  $\theta < 90$ . Tomato shape provides better resistance coverage.

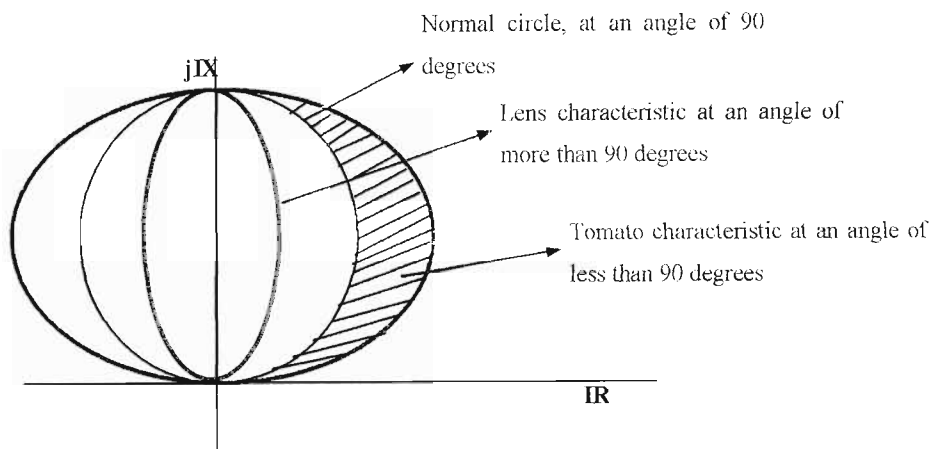


Figure 2.18: Effect of characteristic timer angle

- Lens

For long lines with bigger characteristics a TLS impedance protection may trip due to load encroachment, as the relay can not differentiate between load conditions and fault conditions. The Lens characteristics on the TLS relay helps improve stability of the function by allowing the relay characteristic to be moved away from load area as demonstrated in figure 2.18 above.

- Tomato

For short lines, the amount of fault resistance covered is very small and may result in the relay not tripping for high resistance faults on the line. The tomato characteristics allow the TLS relay shape to be adjusted to cover for more resistance as demonstrated in figure 2.18 above.

- Adjustable phase shift.

The polarizing voltage is phase shifted by 20 degrees in the leading direction.

- Reactance relay.

This type characteristic measures only the reactive component of the line irrespective of the resistance value. If utilised this characteristic improves the TLS relay capability to measure high resistance faults.

### 2.5.3 R3Z27 relay [15]

The R3Z27 impedance protection relay has measuring elements for each phase. The R3Z27 has the following three methods for distance measurements: R3Z27 relay has an electrically separated contact associated with each phase for distance and direction measurement.

#### 2.5.3.1 Plain impedance. Normally used on Long lines (Line impedance greater than 25ohms )

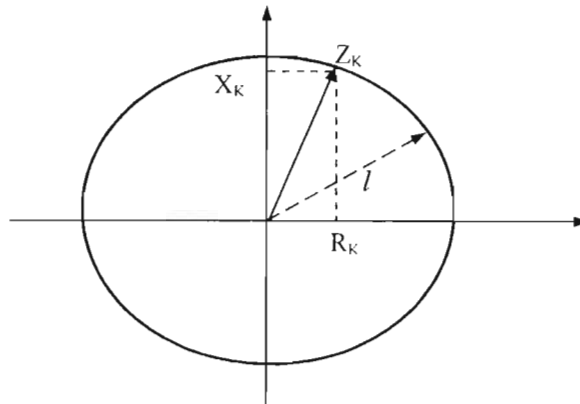


Figure 2.19: Plain impedance circle of an R3Z37 relay,  $l = Z$  (radius).

#### 2.5.3.2 Modified impedance with normal tolerance to arc resistance that covers at least 66% of X.

This relay allows for the characteristic to be shifted along the R-axis by 66% of X to be able to give better resistive coverage without changing the X-reach along the line. Normally used for medium Line Length (Line impedance between 10 and 25 ohms)

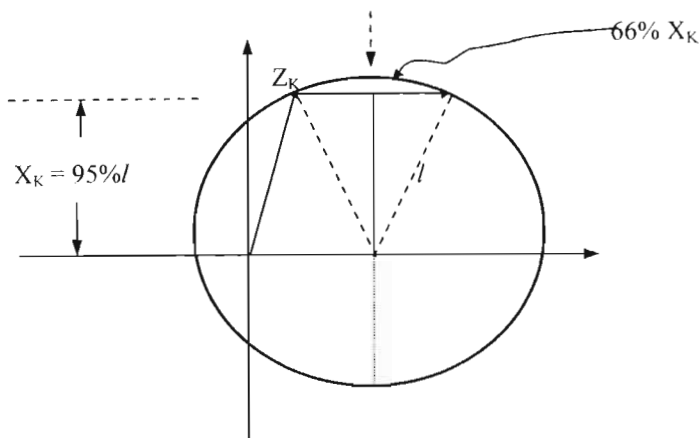


Figure 2.20: Plain impedance circle of an R3Z37 relay,  $l = Z$  (radius).

### 2.5.3.3 Modified impedance with an increased tolerance to arc that covers 132% of X. Normally used for short lines (Line impedance less than 10ohms )

### 2.5.4 LZ32 relays [16]

The basic measuring element used in the LZ32 relay protection is the phase angle comparator. LZ32 uses fully cross-polarized Mho characteristics. For three phase faults, the measured impedance is shifted by 30 degrees to give a better fault coverage. For single phase to earth faults, the polarizing voltage is phase shifted by 12 degrees in the leading direction.

### 2.5.5 Type H relays [17]

The basic measuring element used in type-H protection is the rectifier-bridge current-comparator or amplitude comparator. The phase angle comparator of a Type H relay is derived from the rectifier bridge current-comparator. Type-H distance relays use a cross-polarized Mho with a memory action for zone 1 and zone 2. For zone 3 an offset mho characteristic is used. The polarizing voltage is derived from the faulty phase voltage and the small amount of the healthy phase voltage. For close up three-phase faults a back up offset Mho characteristic is used.

### 2.5.6 SLYP/slcN relays [18]

The SLYP/SLCN relays are more complex relays designed specifically for those lines with series capacitors. SLYP/SLCN use multi input phase angle comparators to derive different type's characteristics. SLYP/SLCN has the following mho characteristics: Self polarized mho relay with memory action, lenticular characteristics, Offset-mho characteristics and directional characteristics. SLYP/SLCN relays can also be set as a reactance relay.

### 2.5.7 Micromho relays [19]

Micromho relays use multi input phase angle comparators to derive a variable mho type characteristic. Micromho has the following mho characteristics:

- 16% cross - polarized mho characteristic
- Offset Mho characteristic
- Lenticular or lens Mho characteristic.

The sound phase cross-polarised voltage is converted to a square wave before combining with 16% of it with a sine wave self-polarizing voltage to give maximum fault coverage [25].

### 2.5.8 Siemens 7SA513 relays [20]

Siemens 7SA513 is a numeric distance protection relay with a polygon characteristic. The relay is microprocessor based with digital processing. The relay provides five measured current inputs and seven measured voltages. Three current inputs are intended for inputs of the phase currents of the protected line and the remaining for earth current. One voltage input is available for each of the line-to-earth and line-line voltages.

Earth fault detection is achieved by comparing the zero sequence current and the negative sequence current.  $3I_0$  is measured and the value is compared with the negative phase sequence current for stability purposes ( $3I_0$  should be at least 0.3 times the negative phase sequence current).

The relay utilises cross polarisation method with the healthy phase voltage rotated 90 degrees. For directional determination, sound phase and stored reference or polarising voltages are used. Theoretical directional line is shown in the figure 2.20 below. The position is dependent on source impedance as well as the load current carried by the line immediately before the fault.

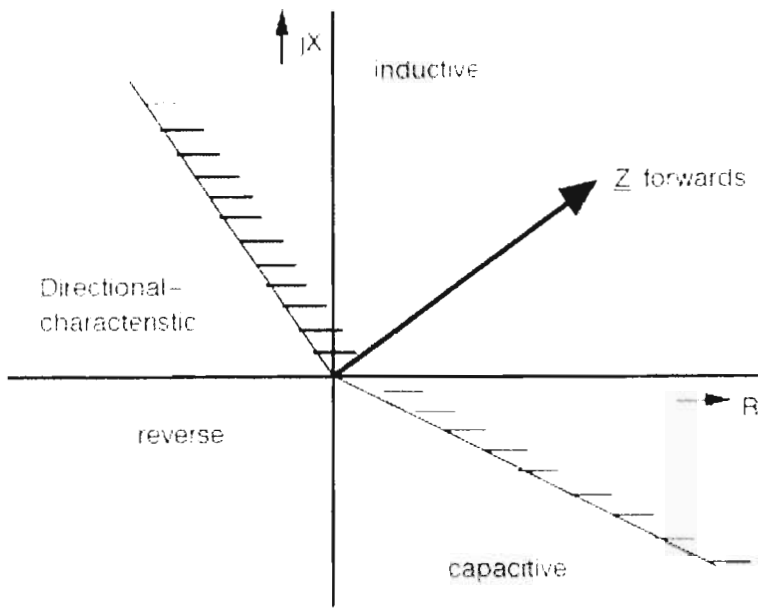


Figure 2.21: 7SA513 directional characteristics [20]

Consider the following diagram for the directionality when the source impedance is considered for a forward fault.

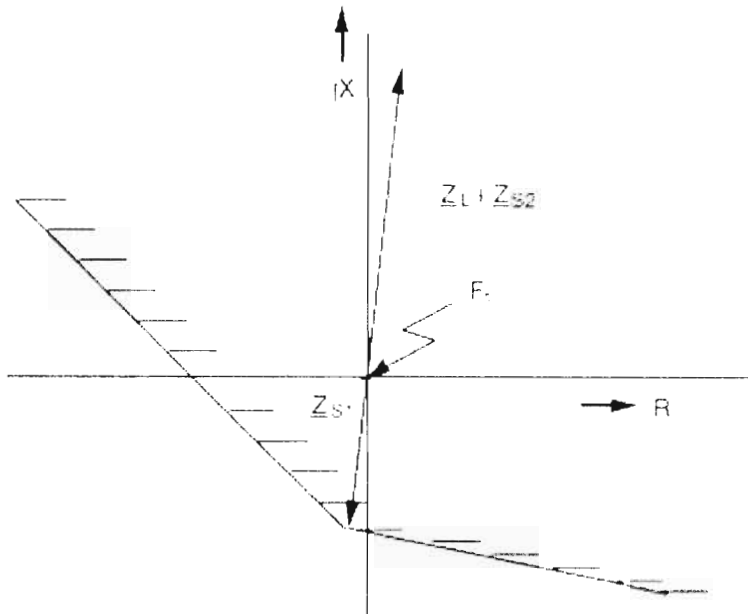


Figure 2.22: 7SA513 directional characteristic with source impedance, forward fault [20]

Consider the following diagram for the directionality when the source impedance is considered for a reverse fault.

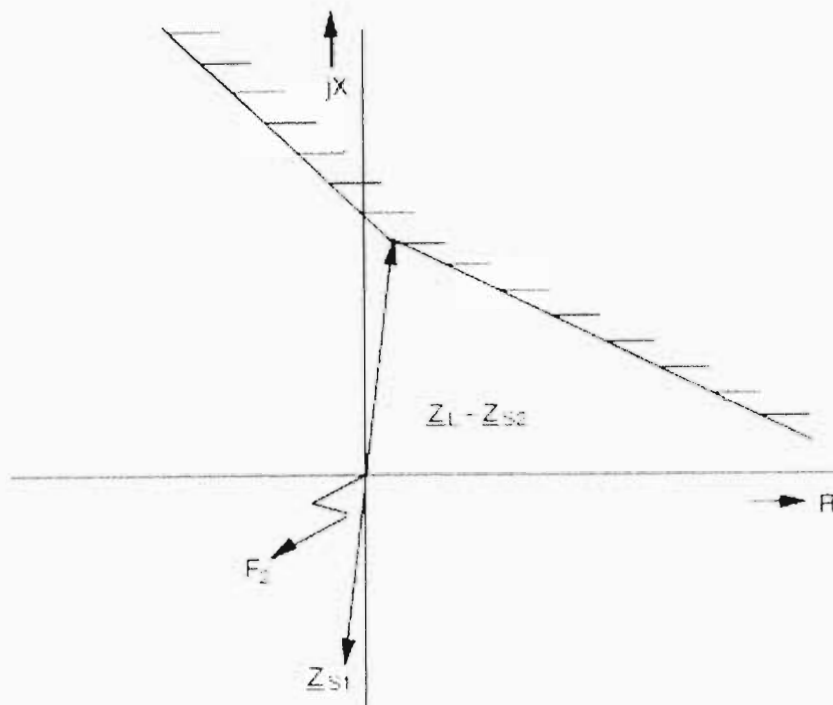


Figure 2.23: 7SA513 characteristic with source impedance, reverse fault [20]

$Z_L$  – Line impedance

$Z_{S1}$  – Source impedance at source 1

$F_1$  – Fault on the forward direction

$F_2$  – Fault on the reverse direction

$Z_{S2}$  – Source impedance at source 2

It can be clearly seen from figure above that the relay is stable for reverse faults.

### 2.5.8.1 High-resistance earth fault protection

For directional determination, the following polarisation methods are available

- Zero sequence voltage polarisation
- Zero sequence voltage polarisation
- Dual polarisation (with both current and voltage)

The following features are optionally available for high resistance fault protection

- Directional earth fault with non directional back up

Directional earth fault can be used as a definite time or inverse time over current protection.

Definite time provides adjustable pick up stage and adjustable time delay. For inverse time an over current value and a time multiplier can be set.



- Directional inverse time zero sequence voltage

This function operates with an inverse time characteristics whose trip time is dependent on the magnitude of the zero sequence voltage

- Directional comparison earth fault comparison

It is a directional protection function that has been extended to form a directional comparison. This can be achieved with the aid of telecommunication systems. Carrier channel is essential for each direction, which transmits signals of the directional earth fault protection to the other end of the line. Tripping is only allowed if the relay has picked up and the signal was received from the other end. This function has an advantage that it can be used as a primary protection, allows for accelerated tripping. Logic diagram is shown on the figure below:

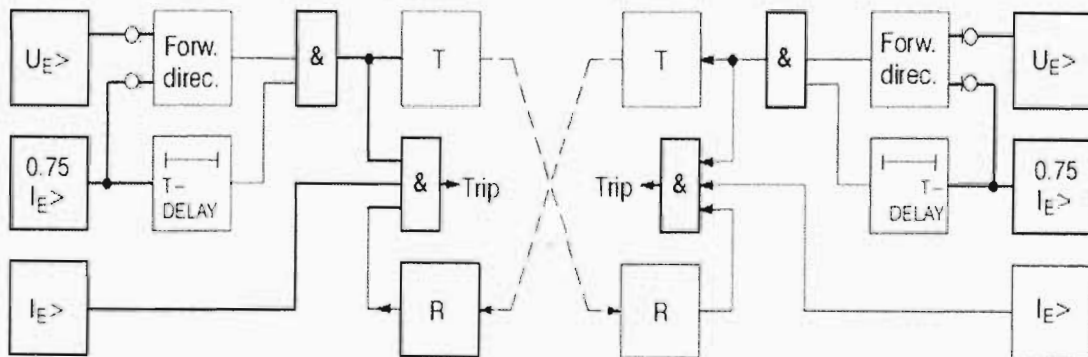


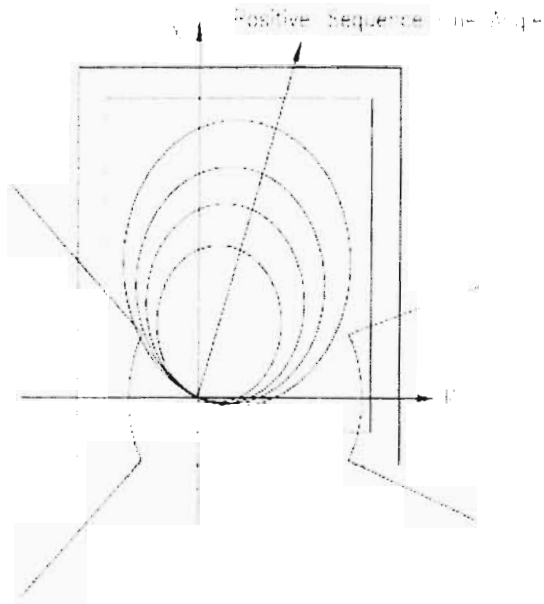
Figure 2.24: 7SA513 directional earth fault protection [20]

- Instantaneous earth fault stage before auto reclosure and or switch on to fault stage

If the line with a fault is switched on to a live bus, it is imperative that tripping should happen immediately; this function is referred to as switch on to fault protection. The same principle can be achieved when the earth fault is detected; the current is above the setting pick up level and additional directional discrimination is achieved.

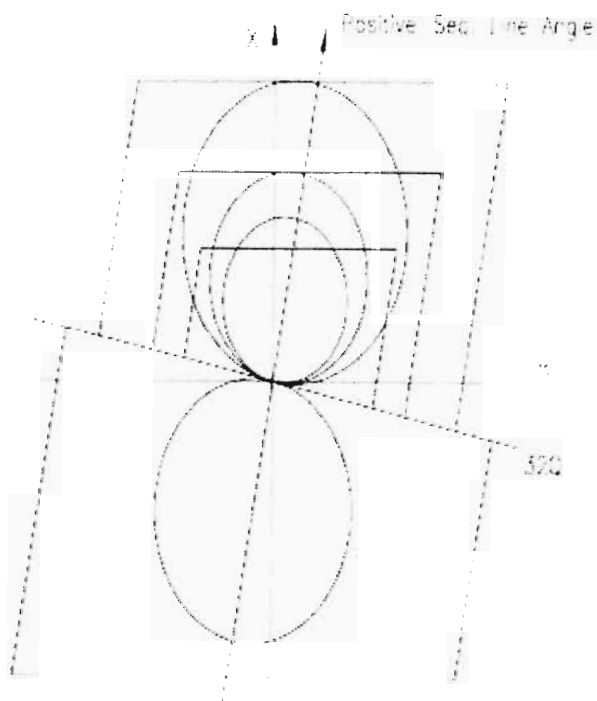
### 2.5.9 SEL-321 relay [21]

SEL-321 is a numeric distance protection relay with a Mho characteristic for phase faults, and quadrilateral characteristic for earth faults.



- Four mho zones
- Two quadrilateral zones for OOS
- Two load zones
- Set only characteristics you need
- All zones reversible

Figure 2.25: SEL phase characteristics [21]



- Four mho zones
- Four quadrilateral zones
- User quadrilateral, mho, none, or both

Figure 2.26: SEL earth fault characteristic [21]

### 2.5.10 ABB REL-531 relay [22]

ABB REL 531 is a numeric distance protection relay with a polygonal characteristic. The REL 531 allows for setting of line resistance, reactance and fault resistance for positive and zero sequence independently. The main purpose of the REL 531 terminal is the protection; control and monitoring of overhead lines and cables in solidly earthed networks with high requirements for fast operating times (less than one cycle).

Typical characteristic can be shown on the figure below

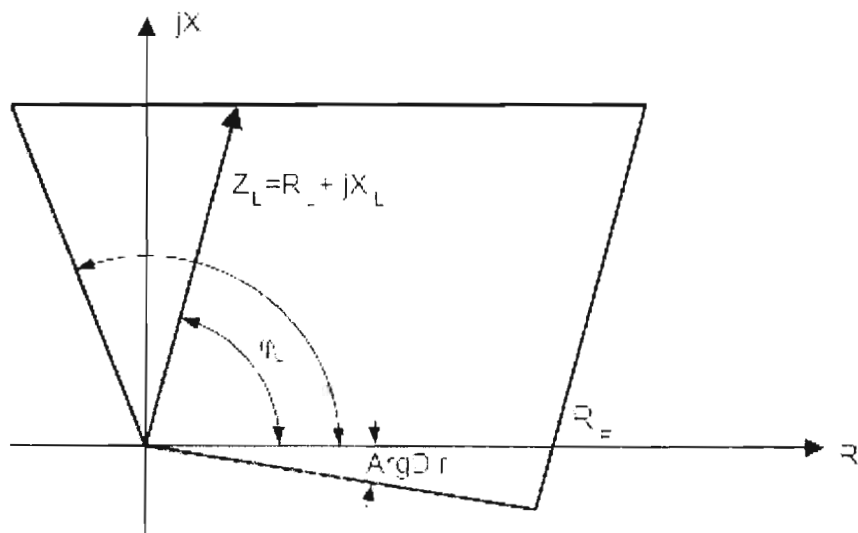


Figure 2.27: ABB REL 531 typical characteristic for phase loop [22]

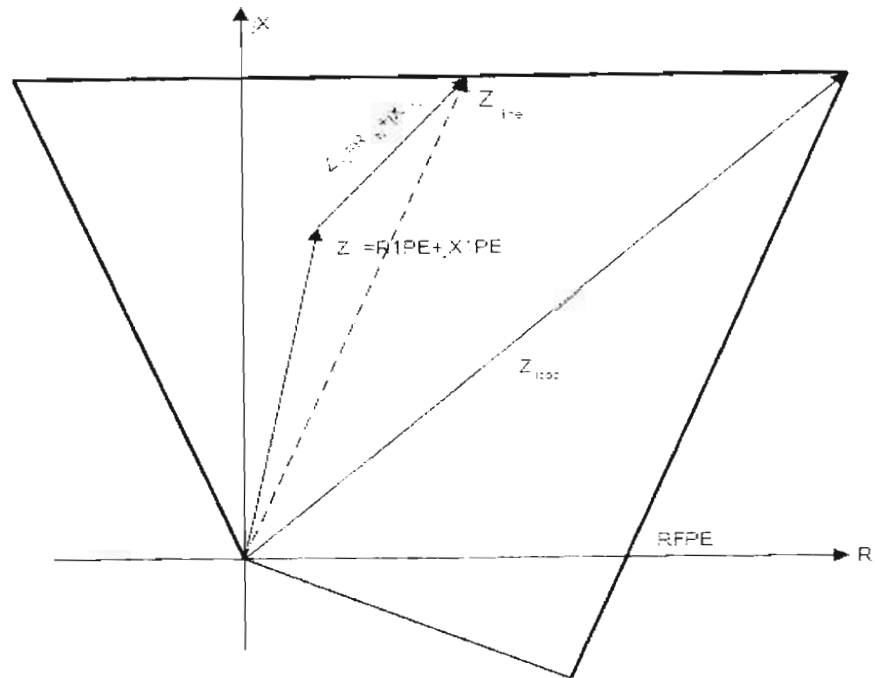


Figure 2.28: ABB REL 531 typical characteristics for phase to earth loop [22]

$Z_N$  is earth return impedance

RFPE - Phase to earth fault resistance.

X<sub>1PE</sub> - Zone 1 reactance setting for phase to earth loop

R<sub>1PE</sub> - Zone 1 resistive setting for phase to earth loop

### 2.5.10.1 High resistance earth fault protection

As mentioned before that the distance protection cannot detect very high-resistive earth faults, because the load impedance and load transfer limit its reach. For faults with resistance higher than those that can be detected by the impedance measurement, an optional earth-fault over current protection can be included in the REL 531 terminals.

The resistive reach is restricted by the setting of the reactive reach and the load impedance.

$$RFPE < 0.8 (2 \cdot X_{1PE} + X_{OPE})$$

$$RFPE < 0.8 (Z_{LOAD MIN})$$

### 2.5.10.2 The following features are optionally available for high resistance fault protection

- Instantaneous over current

The instantaneous residual over current function is suitable as back-up protection for phase to earth faults close to the terminal. This enables a short back-up fault clearance time for the phase to earth faults with high fault current. The instantaneous, non-directional, earth-fault over current protection (IOC), which can operate in 15 ms (50 Hz nominal system frequency) for faults characterized by very high currents, is included in some of the REL 531 terminals

- Time delay over current protection

The time delayed residual over current protection (TOC) which is an earth-fault protection, serves as a built-in local back-up function to the distance protection function. The time delay makes it possible to set the relay to detect high resistance faults and still perform selective trip.

- Definite and inverse time delayed residual over current protection (TEF)

Earth-faults with high fault resistances can be detected by measuring the residual current ( $3I_0$ ). Directional earth-fault protection is obtained by measuring the residual current and the angle between this current and the zero-sequence voltage ( $3V_0$ ).

The earth-fault over current protection is provided with second harmonic restraint, which blocks the operation if the residual current ( $3I_0$ ) contains 20% or more of the second harmonic component to avoid tripping for inrush current.

It is not possible to measure the distance to the fault by using the zero-sequence components of the current and voltage, because the zero-sequence voltage is a product of the zero-sequence components of current and source impedance. It is possible to obtain selectivity by the use of a directional comparison scheme, which uses communication between the line ends.

- Directional comparison

In the directional comparison scheme, information of the fault current direction is transmitted to the other line end. A short operate time enables auto-reclosing after the fault. During a single-phase reclosing cycle, the auto-reclosing device must block the directional comparison earth-fault scheme.

The logic diagram is shown on the figure below:

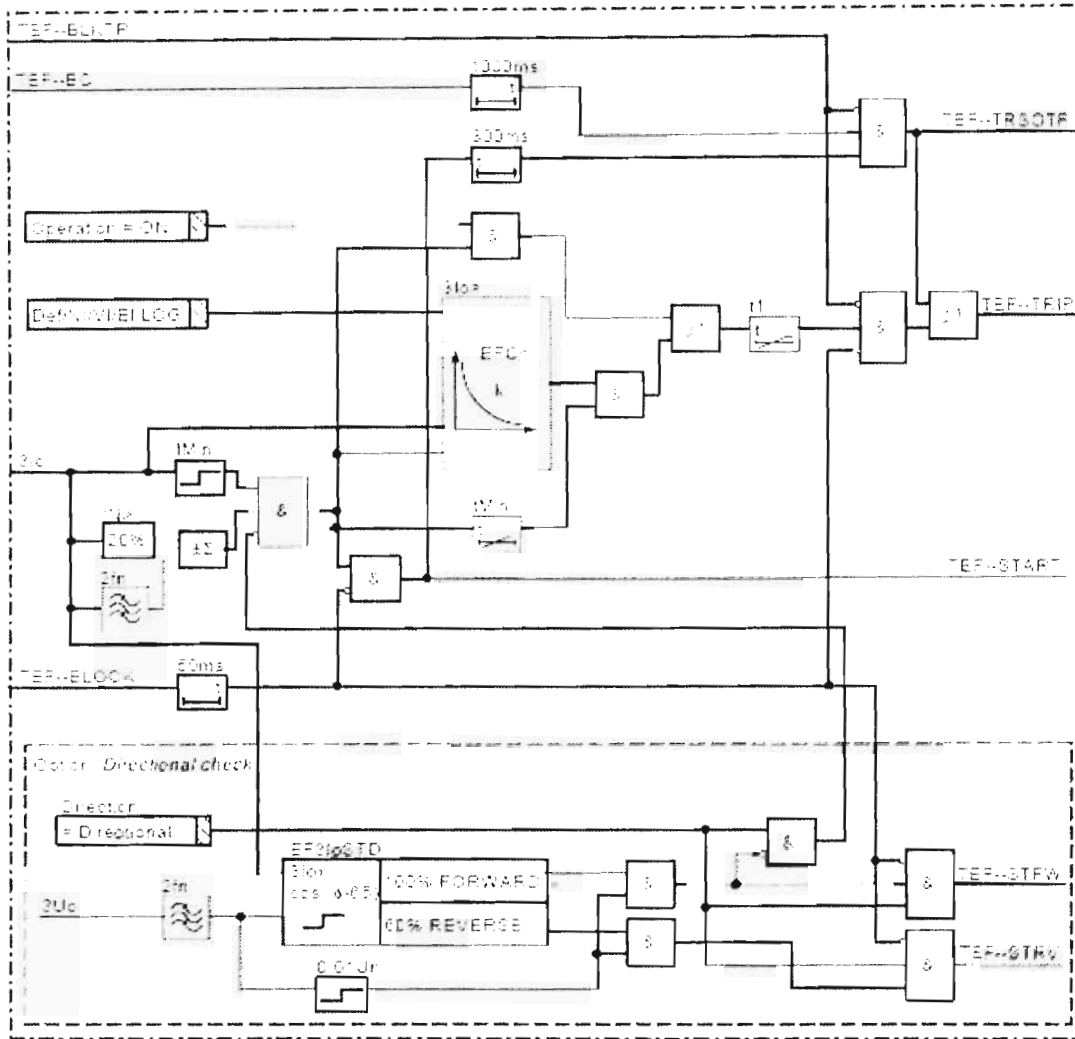


Figure 2.29: Simplified logic diagram for REL531 TEF [22]

## 2.6 ANALYSIS OF DISTANCE RELAY PERFORMANCE

A simple radial feeder on the figure 2.30 below will be used as a case study to determine the capability of the most widely used impedance relays in the transmission system. In order to understand the theory of polarization and relay measurement principles, a fault calculation study for a single phase to earth fault is done below. Single-phase to earth fault will be used as they are regarded as faults with high resistances. Only a zone 1 element will be looked at. It has to be noted that the following exercise was based on the theoretical information collected from the relay manufactures manuals

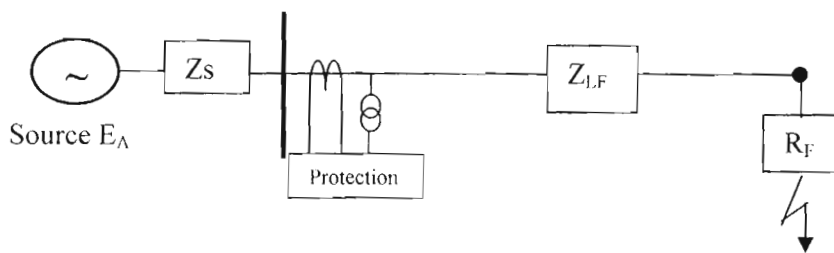


Figure 2.30: Single line diagram

$Z_{L1} = 10\angle 85^\circ$ , Positive sequence line impedance,

$Z_{S1} = 8\angle 85^\circ$ , Positive sequence source impedance

$Z_{S2} = 8\angle 85^\circ$ , Negative sequence source impedance

$Z_{S0} = 8\angle 85^\circ$ , Zero sequence source impedance.

$Z_{LF} = 8\angle 85^\circ$ , Impedance of the line to the point of the fault

$R_F = 10\angle 0^\circ$ , Fault resistance

$E_A = 63.5\angle 0^\circ$ , Source voltage

$Z_{R1} = 8\angle 85^\circ$ , Zone 1 relay setting, 80% of the line

Figure below is the sequence network diagram:

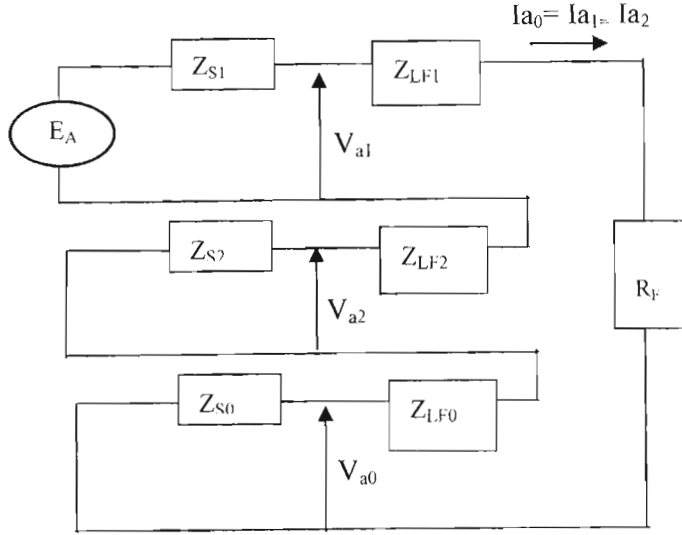


Figure 2.31: Sequence network diagram

Current flowing in the loop can be calculated as follows:

$$I_0 = \frac{E_a}{2(Z_{S1} + Z_{LF1}) + Z_{S0} + Z_{LF0} + 3R_F} \quad \text{[Equation 2.3]}$$

$$I_0 = \frac{63.5 \angle 0^\circ V}{80.38 \angle 63^\circ \Omega} = 0.79 \angle -63^\circ A$$

Then sequence voltages at the relay point are:

$$V_{a1} = E_a - I_0 Z_{S1} = 57.7 \angle -2.3^\circ V \quad \text{[Equation 2.4]}$$

$$V_{a2} = -I_0 Z_{S2} = 6.32 \angle -158^\circ V \quad \text{[Equation 2.5]}$$

$$V_{a0} = -I_0 Z_{S0} = 6.32 \angle -158^\circ V \quad \text{[Equation 2.6]}$$

The faulted phase voltage can be derived below:

$$V_a = E_a - I_0 (2Z_{S1} + Z_{S0})$$

$$V_a = 46.5 \angle -8.7^\circ V$$

For the fault loop seen by the relay the following voltage equation is obtained

$$V_{a1} - I_0 Z_{LF1} + V_{a0} - I_0 Z_{LF0} + V_{a2} - I_0 Z_{LF2} = I_0 3R_F \quad \text{[Equation 2.7]}$$

$$V_{a1} + V_{a0} + V_{a2} = I_0 3R_F + I_0 Z_{LF1} + I_0 Z_{LF2} + I_0 Z_{LF0} \quad V_{a1} + V_{a0} + V_{a2} = V_a$$

$$V_a = Z_{F1} \left( I_0 \frac{3R_F}{Z_{LF1}} + I_0 + I_0 + I_0 \frac{Z_{F0}}{Z_{LF1}} \right)$$



$$K_0 = \frac{1}{3} \left( \frac{Z_{LF0}}{Z_{LF1}} - 1 \right) \quad \text{[Equation 2.8]}$$

$$V_a = Z_{F1} \left( I_0 \frac{3R_F}{Z_{LF1}} + I_0 + I_0 + I_0(3K_0 + 1) \right)$$

$$V_a = Z_{F1} \left( I_0 \frac{3R_F}{Z_{LF1}} + I_0 + I_0 + I_0 3K_0 + I_0 \right)$$

$$I_a = 3I_0 \quad \text{[Equation 2.8]}$$

$$V_a = Z_{LF1} \left( I_0 \frac{3R_F}{Z_{LF1}} + I_a + I_0 3K_0 \right)$$

$$Z_{LF1} = \frac{V_a}{I_a + 3I_0 \left( K_0 + \frac{R_F}{Z_{LF1}} \right)} \quad \text{[Equation 2.9]}$$

$$Z_{LF1} = \frac{46.5 \angle -8.7^\circ}{2.37 \angle -63^\circ + 3.95 \angle -111^\circ} = 8 \angle 84.9^\circ \Omega$$

The impedance measured is exactly the same as the positive sequence impedance of the fault. Impedance relays use the formula below measure the impedance for a single phase to earth fault.  $Z_M$  Is the fault impedance seen by the relay.

$$Z_M = \frac{V_a}{I_A + 3I_0 K_0} \quad \text{[Equation 2.10]}$$

$$Z_M = \frac{46.5 \angle -8.7^\circ V}{2.37 \angle -63^\circ A + 2.37 \angle -63^\circ A} = 9.81 \angle 54.3^\circ \Omega$$

It can be seen that a fault resistance ( $R_F$ ) of zero in equation 2.9 makes equation 2.9 equals equation 2.10. The relay does not compensate for fault resistance as it varies; some faults have zero fault resistance, while some faults have high fault resistance. That is the reason faults with high resistance sometimes appear to be out of the characteristics for most relays used. If relays were designed to use equation 2.9 to measure the impedance to the point of the fault, therefore first calculate the amount of fault resistance and adjust the formula accordingly, the problem of high fault resistance could have been catered for.

For this specific example, a self-polarized relay will measure the inputs to the phase angle comparator as:

$$S_1 = Z - Z_R = Z_{F1} - Z_{R1} \quad [\text{Equation 2.11}]$$

$$S_2 = Z = Z_{F1} \quad [\text{Equation 2.12}]$$

For memory polarization, the inputs will be as follows:

$$S_1 = Z - Z_R = Z_{F1} - Z_{R1} \quad [\text{Equation 2.13}]$$

$$S_2 = Z + KZ_{R2} = Z_{F1} + Z_{R2} \quad [\text{Equation 2.14}]$$

For cross polarization

$$S_1 = Z - Z_{R1} = Z_{F1} - Z_{R1} \quad [\text{Equation 2.15}]$$

Take as a polarizing voltage the healthy  $V_b$  voltage, rotated to coincide with the fault voltage  $V_a$ .

$$V_b = V_{b1} + V_{b2} + V_{b0}$$

$$V_b = a^2 V_{a1} + a V_{a2} + V_{a0}$$

$$V_B = a^2 E_a - I_0 (a^2 Z_{S1} + a Z_{S1} + Z_{S0})$$

$$S_2 = V_{POL} = a V_b = E_a - I_0 (Z_{S1} + a^2 Z_{S1} + Z_{S0})$$

Dividing the polarizing voltage by the current gives the equation below:

$$S'_2 = \frac{E_a - I_0 (Z_{S1} + a^2 Z_{S1} + Z_{S0})}{3I_0 + 3I_0 K_0} \quad [\text{Equation 2.16}]$$

Replacing  $E_a$  by  $V_a + I_0(2Z_{S1} + Z_{S0})$  gives the following equation

$$S'_2 = \frac{V_a + I_0(2Z_{S1} + Z_{S0}) - I_0(Z_{S1} + a^2 Z_{S1} + Z_{S0})}{3I_0 + 3I_0 K_0} \quad [\text{Equation 2.17}]$$

$$S_2 = Z_{F1} + Z_{S1} \left[ \frac{(1-a^2)}{3+3K_0} + (1-a) \frac{\frac{Z_{S0}}{Z_{S1}}}{3+3K_0} \right]$$

$$S_2 = Z_{F1} + Z_{S1} \frac{\sqrt{3}}{3 + 3K_0} \left( 1 \angle 30^\circ + 1 \angle -30^\circ * \frac{Z_{SO}}{Z_{S1}} \right)$$

$$\text{Let } Z_{S1} \frac{\sqrt{3}}{3 + 3K_0} \left( 1 \angle 30^\circ + 1 \angle -30^\circ * \frac{Z_{SO}}{Z_{S1}} \right) = Z_{R2}$$

$$S_2 = Z_{LF1} + Z_{R2}$$

For fully cross polarized relay  $Z_{R2} = 4 \angle 85^\circ$

For partially cross-polarized

$$Z_{R2} = \frac{pZ_{R2}}{1 + p} \quad \text{[Equation 2.18]}$$

Where p is the ratio of cross-polarized voltage to self-voltage measured under healthy line conditions.

For 2% partially polarized  $Z_{R2} = 2.667 \angle 85^\circ$

For 16% partially polarized  $Z_{R2} = 3.76 \angle 85^\circ$

$Z_{R1}$  Is the relay setting.

Figure 2.32, 2.33 and 2.34 below represent the dynamic and steady state relay characteristics plotted in one R/X diagram. For the specific case study used with a 10 ohm fault resistance at different location of the relay reach, point A, B and C. Point A is for a fault at 80 percent of the line with the measured impedance of

$$Z_M = 9.81 \angle 54.3^\circ, \text{ This was calculated above}$$

Point B and C fault calculations are not shown in this study because the calculation method used is the same as used for calculating point A. Point B is for a fault at 40% of the line and the measured impedance of:

$$Z_M = 6.67 \angle 37^\circ$$

Point C is for a fault at 10% of the line and the measured impedance of:

$$Z_M = 5.18 \angle 11^\circ$$

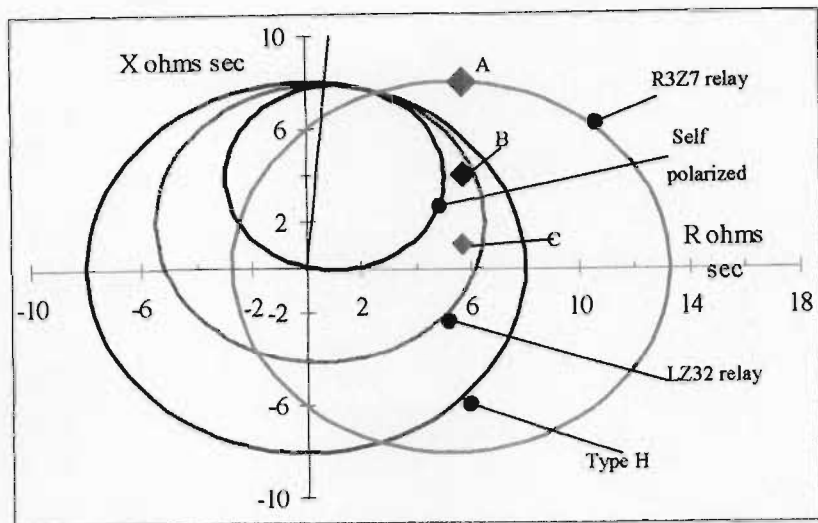


Figure 2.32: Different relay characteristics (R3Z27, LZ32 and type H relays)

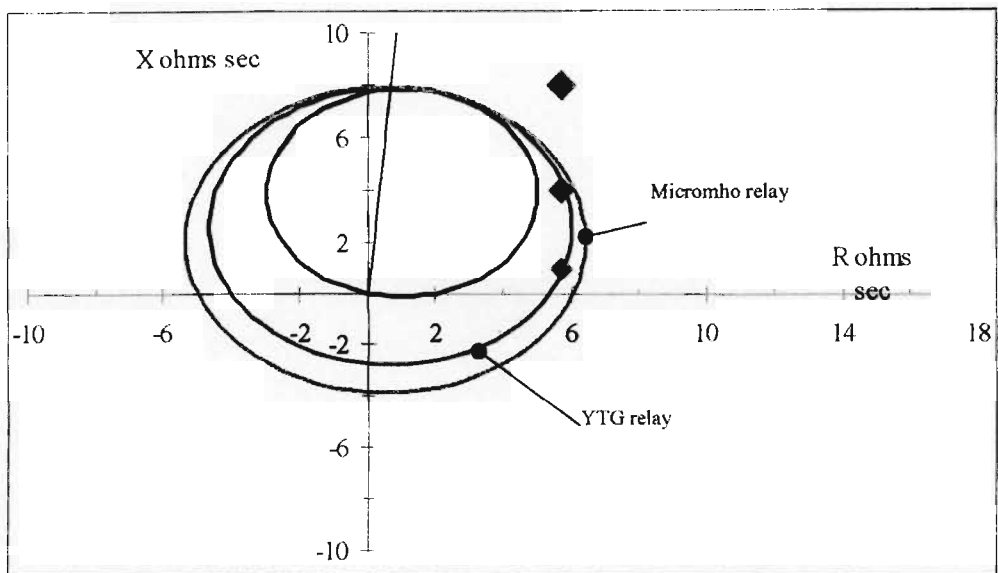


Figure 2.33: Different relay characteristics (YTG and Micromho relays)

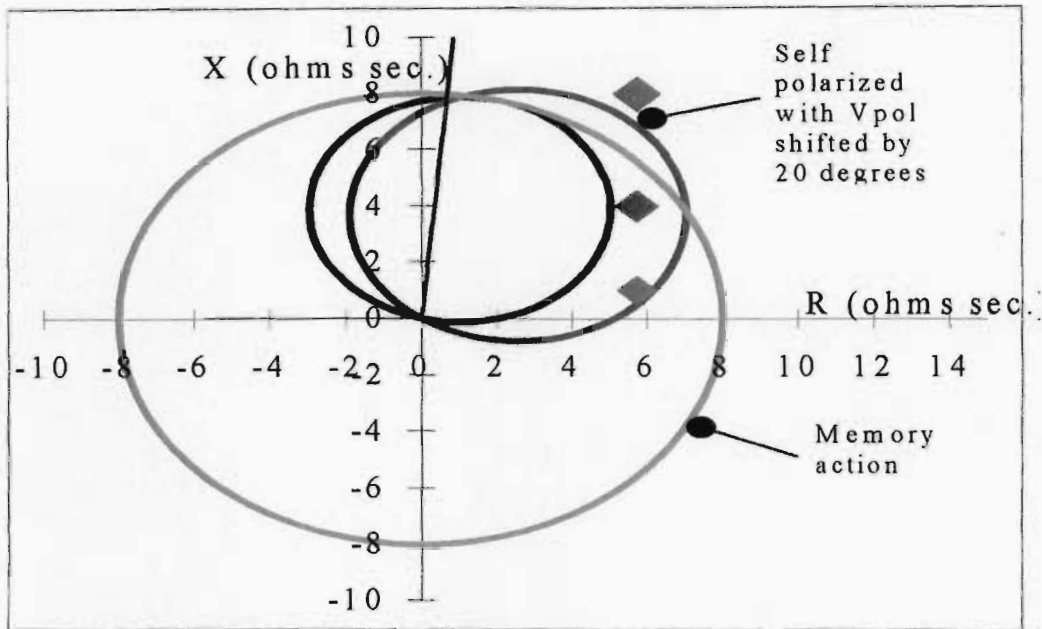


Figure 2.34: Dynamic characteristics of a TLS relay

## 2.7 EFFECT OF FAULT RESISTANCE ON THE DISTANCE RELAY PERFORMANCE

For faults not involving ground, the resistance is made up of the arc products alone and it is maintained across the arc [10].

In faults involving ground there is a linear component of resistance in addition to the non-linear arc component. This linear component can be introduced by tower footing resistance, ground wire resistance, arc resistance, tower resistance and ground return path. These faults can involve trees growing into the line, in which case fault resistance can reach hundreds of ohms [23]. A contributing factor in South African environment is very dry winter in most of the country resulting in difficulties in maintaining tower footing resistance within required limits and additional fault resistance on entry point of fault arc to the ground [2].

It must be noted that the amount of resistive fault coverage by any relay is influenced by a number of factors [10]:

- Distance element reach

Distance protection measurement is not capable of providing unlimited coverage of fault resistance. Maximum load transfer capability limits the possible resistance coverage settable in all types of impedance relays. High resistance faults in the load area can never be cleared by impedance relays as the relay cannot differentiate between the load conditions and the fault condition. Faults of this nature will be cleared by back up earth faults or can only be cleared if the fault develops to a phase to phase and the resistance is reduced.

- Remote infeed and, thus, the source impedance behind the relay location

The effect of infeed is to cause the voltage to be magnified in value so that the resistance can appear much bigger than it actually is [10]. In this case, the resistance may appear too large for the fault to be cleared by any distance function.

- Line length

For long lines with bigger characteristics protection may trip due to load encroachment, as the relay can not differentiate between load conditions and fault conditions. For short lines, the amount of fault resistance covered is very small and may results in the relay not tripping for high resistance faults on the line.

- Normal system unbalance

On a looped system, current can be supplied from two or more sources. The effect of the infeed currents from the opposite end is to make the actual resistance of the fault to appear to be larger as seen by the relay. Multiple sources supplying current into a high-resistance fault magnify the actual fault resistance as seen by the relay at both ends. The relay at the weaker source sees a bigger magnification

A system is non-homogeneous when the source and line impedance angles are not the same. In a non-homogeneous system, the angle of the total current in the fault is different than the angle of current measured at the relay. For a bolted fault (a condition that assumes no resistance in the fault), a difference between the fault current angle and the current angle measured at the relay is not a problem. However, if there is fault resistance, the difference between the fault and relay current angles can cause a ground distance relay to severely underreach or overreach [10].

- Load flow (in some distance relay designs)

Consider the following illustration for an explanation:

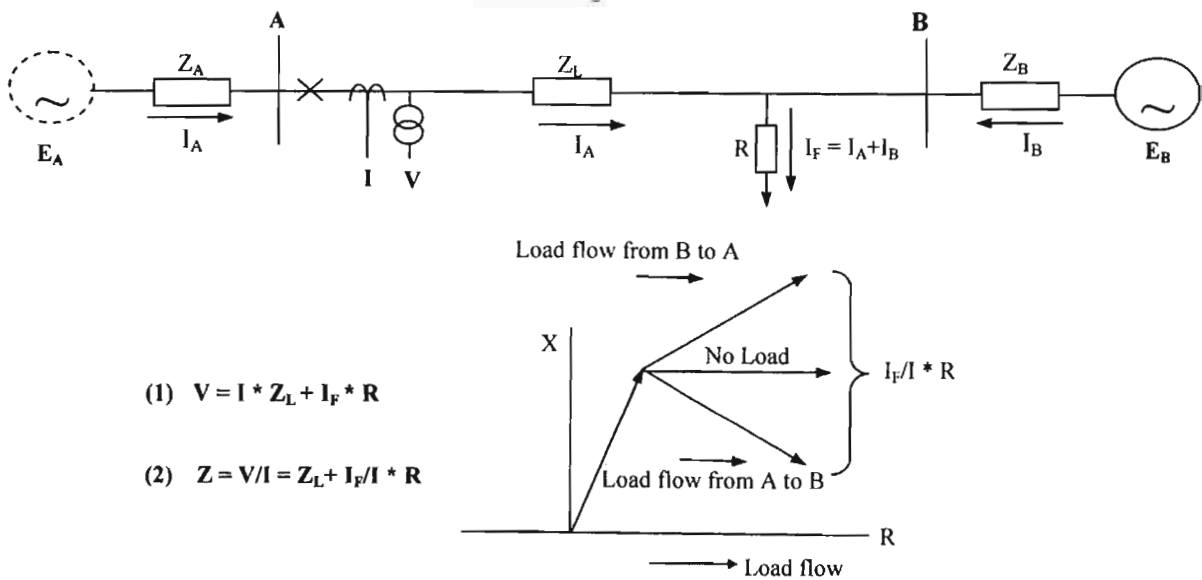


Figure 2.35: Effect of load flow on fault resistance

The effect of load is to shift the resistance so that it appears to have a reactive component. The direction of the shift and the amount of shift depend on the direction and magnitude of the load flow [10].

## 2.8 DISTANCE PROTECTION RELAY SIMULATIONS

The use of digital protection relays has gained popularity over the years. The protection field has been transformed by this technology. Basic understanding of numeric relay simulation should become very important for field Technicians, Protection Engineers and top management. One of the most important factors in protection performance is the correct application of the appropriate relays that satisfies the functional and user requirements. This section aims to give a background of basic simulation of distance protection algorithms, different types of polarising methods and methods to test distance characteristics for high resistance fault coverage by the means of impedance plots. Impedance plots are very useful when investigating line impedance protection relay operations since they display what the relay “saw” during the incident. Analysis of all high resistance faults needs an impedance plot.

### 2.8.1 Differential Equation Based Algorithm

In this approach no special assumption is made with regard to the existing components of current and voltage waveforms recorded during fault conditions. This technique is based on the fact that protected equipment can be modelled by using a number of differential equations of first order [24].

This algorithm assumes that the current and voltage waveforms contain a DC component but are otherwise free from high-frequency oscillations. The high-frequency components are filtered out using low pass filtering. Therefore voltage and current are related by

$$v = Ri + L \frac{di}{dt} \quad \text{[Equation 2.19]}$$

To determine the values of  $R$  and  $L$  using this equation, it is basically required to have at least three sets of voltage and current samples. Using sample notation and approximating  $\frac{di}{dt}$

using  $\frac{i_{k+1} - i_{k-1}}{2T_s}$  ( $T_s$  is the sampling interval), the above differential equation becomes

$$v_k = Ri_k + L \frac{i_{k+1} - i_{k-1}}{2T_s} \quad \text{[Equation 2.20]}$$

$$v_{k+1} = Ri_{k+1} + L \frac{i_{k+2} - i_k}{2T_s} .$$

In matrix form, the above two equations can be combined to give



$$\begin{bmatrix} i_k & \frac{i_{k+1} - i_{k-1}}{2T_s} \\ i_{k+1} & \frac{i_{k+2} - i_k}{2T_s} \end{bmatrix} \begin{bmatrix} R \\ L \end{bmatrix} = \begin{bmatrix} v_k \\ v_{k+1} \end{bmatrix} \quad [\text{Equation 2.21}]$$

Or in the short form

$$\mathbf{A}\mathbf{p} = \mathbf{v} \quad [\text{Equation 2.22}]$$

$$\text{Where } \mathbf{A} = \begin{bmatrix} i_k & \frac{i_{k+1} - i_{k-1}}{2T_s} \\ i_{k+1} & \frac{i_{k+2} - i_k}{2T_s} \end{bmatrix} \quad [\text{Equation 2.23}]$$

$$\mathbf{p} = \begin{bmatrix} R \\ L \end{bmatrix}, \quad \mathbf{v} = \begin{bmatrix} v_k \\ v_{k+1} \end{bmatrix} \quad [\text{Equation 2.24}]$$

The Least Squares technique can be used to solve the matrix equation

$$\hat{\mathbf{p}} = (\mathbf{A}^T \mathbf{A})^{-1} \mathbf{A}^T \mathbf{v} \quad [\text{Equation 2.25}]$$

The closed-form LS solution produces two formulas for estimating  $R, L$  from current and voltage samples:

$$R = \frac{v_k(i_{k+2} - i_k) - v_{k+1}(i_{k+1} - i_{k-1})}{i_k(i_{k+2} - i_k) - i_{k+1}(i_{k+1} - i_{k-1})} \quad [\text{Equation 2.26}]$$

and

$$L = 2T_s \frac{i_k v_{k+1} - i_{k+1} v_k}{i_k(i_{k+2} - i_k) - i_{k+1}(i_{k+1} - i_{k-1})} \quad [\text{Equation 2.27}]$$

This algorithm produces a succession of estimates as the sampled data is acquired. These estimates can be compared for convergence to the correct fault value [24].

### 2.8.2 Discrete Fourier Transform.

The basic approach used in this algorithm is to extract the fundamental frequency component of a waveform by correlating one cycle (or half cycle) of the waveform with stored reference sine and cosine waves. The full-cycle Fourier transform based algorithm can completely reject a DC signal (constant DC offset different from a DC decay), and harmonics of the fundamental frequency (signals at the frequencies of multiples of the fundamental). However, signals with continuous spectrum such as that generated in DC decay, or signals that are not harmonics of the fundamental can not be rejected satisfactorily as a result of the limited length of data window.

### 2.8.3 Recursive Vs Non-recursive Filters

There are two types of DFT, recursive and non-recursive. Non recursive means that the sine and cosine factors are recalculated and re-summed every sample. For recursive, only the sine and cosine factors for the present sample are calculated, then the oldest sample's sine and cosine terms are removed from the sum and the newest terms are added in to the sum. This reduces the amount of calculations performed. The non-recursive method, on the other hand, requires more time and/or computing speed to complete.

Discrete Fourier Transform Calculation of the fundamental components can be defined by the following equations.

$$V_{real} = \frac{2}{N} \sum_{k=1}^N y_k * \sin\left(\frac{2 * \pi * k}{N}\right) = Y_s \quad \text{[Equation 2.28]}$$

$$V_{imag} = \frac{2}{N} \sum_{k=1}^N y_k * \cos\left(\frac{2 * \pi * k}{N}\right) = Y_c \quad \text{[Equation 2.29]}$$

$$\bar{Y} = \frac{2}{N} \sum_{k=1}^N y_k \exp(-j\theta_v) = Y_c - jY_s \quad \text{[Equation 2.30]}$$

The magnitude of the voltage phasor can be calculated by the following equation.

$$V_{mag} = \frac{1}{\sqrt{2}} \sqrt{Y_c^2 + Y_s^2} \quad \text{[Equation 2.31]}$$

$$V_{mag} = \sqrt{[V_{peak}]^2 + [\cos^2(\phi_v) + \sin^2(\phi_v)]^2} \quad \text{[Equation 2.32]}$$

#### 2.8.4 Inaccuracies expected from digital signal processing

While analysing digital signals certain precautions have to be considered in order to ensure precise results. Some of the problems are indicated below:

##### **Decaying DC offset.**

The full-cycle Fourier transform based algorithm can completely reject a DC signal; however decaying DC signals can not be rejected satisfactorily as a result of the limited length of data window [24].

##### **Inter -harmonics**

DFT can completely reject harmonics of the fundamental frequency but harmonics which are not multiples of fundamental frequency can not be rejected [24].

##### **Frequency deviations**

In the case of faults where the system frequency is not the same as the fundamental frequency, some small errors will be introduced due to these frequency deviations. In order to avoid these errors some relays use frequency following techniques to ensure that the protection algorithm is synchronous with actual system frequency.

##### **Transition period**

In the transition period when the window of the Fourier filter includes samples from pre-fault and fault conditions, the resultant phasors do not have theoretical representation, as different models are required to describe these two different conditions. As a result, a step change in measuring quantity will be reflected as slow transition over a period of the window length.

### 2.9 TRANSMISSION PROTECTION PERFORMANCE

All protection operations are investigated and classified according to the indicators which are predefined in Eskom transmission division. A database of performance was created which includes all the calculations of the relevant indicators. Below are some of the indicators that are used in Eskom Transmission protection performance

SPI – System Performance Index

SPI indicates the reliability of a protection system. When there is a fault on the system the breakers that are supposed to clear a primary fault must operate [25]. Should any breaker operate thereafter, the operation is considered to be incorrect.

$$SPI = \frac{P - I}{P} * 100\% \quad \text{[Equation 2.33]}$$

Where: P, is the total number of primary system faults

I, is the total number of system faults incorrectly cleared

NSF – Non System Faults

NSF indicates the number of circuit breaker operations without any primary fault, when it was not required for the breaker to operate [25].

NSF = Total number of circuit breaker operations due to non-system faults.

PEPI – Protection Equipment Performance Index

PEPI- indicates the performance of main 1 and main 2 protection relays according to the protection philosophy. PEPI indicator will be classified as incorrect if the operation is not according to philosophy that may include reasons such as:

- Lack of operation for high resistance faults
- Slow operation > 100 milliseconds
- Application or design error, etc.....

$$PEPI = \frac{T - INC}{T} * 100\% \quad \text{[Equation 2.34]}$$

T – Total number of protection operations, being correct, incorrect or failures

INC – Number of incorrect protection operations and failures of protection to operate for system and non-system faults

High resistance faults are included in SPI, PEPI and some instances auto reclude performance index (ARPI).

## 2.10 QUALITY OF SUPPLY: NRS 048 REQUIREMENTS ON VOLTAGE DIPS

Since 1996, the South African National Electricity Regulator (NER) has regulated utility power quality performance through application of the NRS-048 standard.

### 2.10.1 Voltage Dip parameters

Voltage dips describe events associated with a sudden reduction in the voltage for a short time (typically less than 3 seconds) [26]. The magnitude of the dip is defined as the maximum depth of the deviation from the declared voltage. The duration can be defined as the time when the voltage drops below the threshold until when the voltage recovers. NRS048 defines 0.9p.u of the declared voltage for HV and MV systems.

Voltage dips are characterised by the measurement of dip duration below the dip threshold, and by the dip magnitude, as illustrated in Figure 2.36 below:

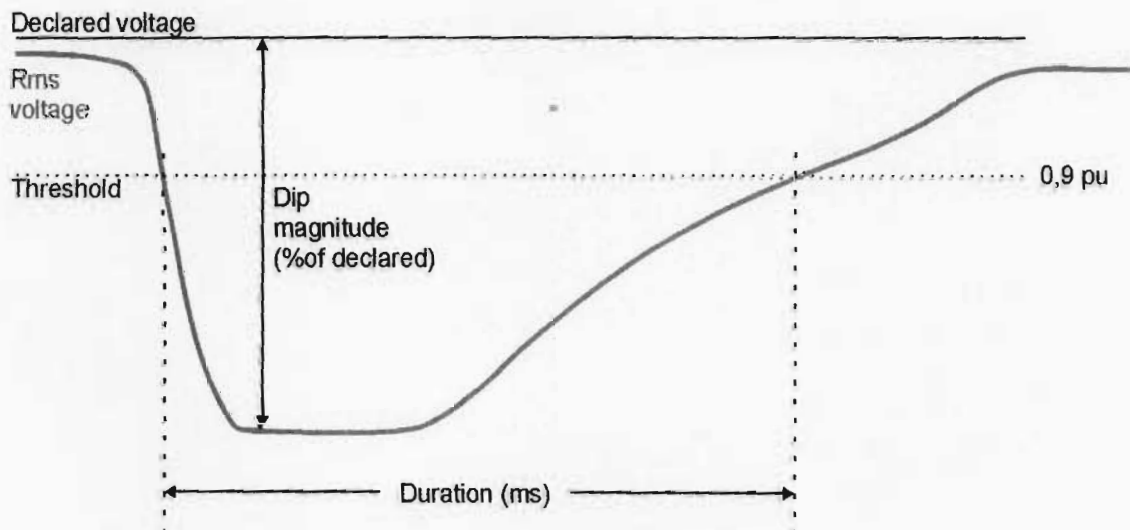


Figure 2.36 – Definition of voltage dip parameters: duration and magnitude  
Source: NRS 048-2 (1996:9)

Voltage dips can be represented graphically, in terms of duration and magnitude, on a graph known as a voltage dip window illustrated by Figure 2.37 below.

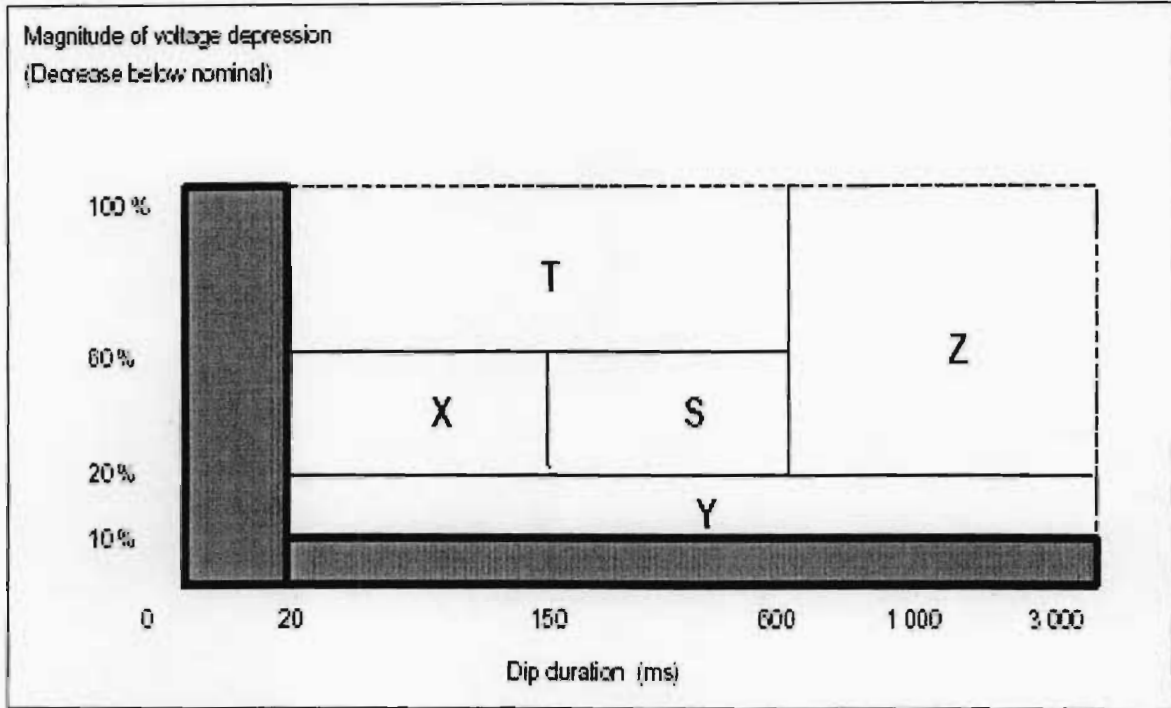


Figure 2.37 – NRS dip characteristics paradigm for dip magnitudes  
Source: NRS 048-2 (1996:9)

The philosophy on which dips are categorised is based on the following [27]

- Protection performance time must be managed by the utilities
- Utilities must manage number of faults close to customers
- Customers shall specify the dip sensitivity of their process equipment to ensure that the number of utility fault events that actually affect the plant is limited.

The table 2.2 below summarises the basis for these definitions

Table 2.2 – Classification of Voltage Dips [27]

Class of Dip	Magnitude of Dip	Duration	Description
Y	10% - 20%	20 ms – 3 sec	Dip definition (20ms to 3s)
X	20% - 60%	20 ms – 150 ms	Typically Zone 1 clearance. Generally do not impact on customer plant operations.
S	20% - 60%	150 ms – 600 ms	Typically Zone 2 and accelerated clearance Faults with a delay in network recovery. Most drives trips due to this faults
T	60% - 100%	20 ms – 600 ms	Zone 1 and Zone 2 clearance times Voltage dips produced by utility close faults.
Z	20% - 100%	600 ms – 3 sec	Back up and thermal protection clearance Major system disturbance with delayed network recovery.

### 2.10.2 Compatibility Levels

The compatibility levels for voltage dips are given in the form of a maximum number of dips per year for defined ranges of voltage dip duration and magnitude, designated as dip window categories ‘Z’, ‘T’, ‘S’ and ‘X’. The compatibility levels are given in Table 2.3 below. The development of compatibility levels was based on the actual network performance.

Table 2.3: NRS-048 95% dip “compatibility” levels

Network voltage range	Number of voltage dips per year				
	Dip window category				
	Z	T	S	X	Y
6,6kV to ≤ 44kV	20	30	30	100	150
6,6kV to ≤ 44kV rural	49	54	69	215	314
> 44kV to ≤ 132kV	16	25	25	80	120
220kV to ≤ 765kV	5	6	11	45	88

Source: NRS 048-2 (1996:9)

### 2.10.3 Power quality economics

The costs related to poor power quality can be significant to some industries. Voltage dips and interruption were found to be the primary problems that South African industry faced as far as power quality is concerned [27]. Mining industry only worries about interruptions whereas most industry worries about dips. Dips are industries biggest problem than interruptions, due to their frequency of occurrence.

The effects of interruptions and dips on consumers depend on the use being made of electricity. Both the frequency and duration of outages affect different consumers in different ways. Transient outages are acceptable to some consumers, but are disruptive to others. Frequent switching to clear faults increases the maintenance needed on the system, and line outages and forced maintenance require the deployment of skilled staff.

### 2.10.4 Custom power

Custom power is a means by which utilities can provide a customer with high levels of power quality, usually at a price. The approach entails installation of mitigation equipment within the customer facility and the establishment of a separate agreement with the customer.

Eskom has branded its custom power programs as “premium power”. In most cases a customer pays a monthly charge and is guaranteed a certain level of performance. Should the contracted performance not be met, the customer does not pay the monthly charge of the month that the performance is not met.



## **3 CHAPTER 3: RESEARCH METHODOLOGY**

### **3.1 INTRODUCTION**

This chapter details the research methodology used for the study. The data that the researcher collected is described along with where the data was collected and how it was analysed.

The scope of the research project is to study the capability of existing distance protection relays by means of theoretical analysis from manufacturer's documentation, digital simulations, testing the fault resistance measurement capability of three relay types by means of Omicron test set and to determine the impact of high resistance faults on the transmission protection performance.

### **3.2 INTENDED PURPOSE OF THE RESEARCH**

The researcher's intention in conducting this research is to gain clear understanding of the capability of the existing relays and to give recommendations on the refinements to the EHV transmission line protection philosophy required to improve future protection performance.

### **3.3 PROCESS OF THE RESEARCH**

The process of the research refers to the way in which data is collected and analysed and it is described as follows:

The researcher collected the following data:

- Obtain high resistance fault statistics;
- Data from the relay manufacturer's documentation;
- Relay characteristics tests using Matlab simulations;
- Relay tests from Omicron;
- Protection Performance history

#### **3.3.1 Obtain network high resistance fault statistics**

Actual fault resistances experienced on the network, as calculated from P531 disturbance records, were obtained so as to obtain a range of the possible and typical fault resistances that are likely to be experienced.

#### **3.3.2 Obtain and review manufacturer's documentation**

All the technical manuals are available within the Eskom transmission libraries. The necessary technical manuals and related documentation for each relay device was located and

obtained. A review of the measurement principle of each device was undertaken, and a summary of the operation principles were made and analysed through chapter 2.

### **3.3.3 Testing methodology for relay characteristics using Matlab simulations;**

To evaluate protection performance during transmission incidents, digital fault record (DFR) information is used to extract voltage and current phasors and use them to plot on the X/R impedance plain both fault impedance locus and dynamic, relay characteristic. OSCOP software is used to download the record from the DFRs. A record is then imported to a normal Common Format for Transient Data Exchange (COMTRADE) file. A COMTRADE file stores samples of the analogue signals in a digital format, which effectively means that the values stored are purely magnitudes with associated time. Conversion of these digital records must be done to extract the frequency and phasor components that are then used to compute power system quantities such as phasors of voltages, currents and impedances. Discrete Fourier analysis technique (DFT) is used to extract the harmonically related phasor magnitudes and angles from the recorded analogue signals.

A COMTRADE file of an actual recorded fault was simulated on the Matlab m-file. The full detained of the Matlab file is shown in detail in Appendix 1. The basic steps that were used to do the simulations with Matlab are listed below in the point form:

- Load a COMTRADE file of the recorded fault in to an m-file.
- Apply DFT at all voltages and currents to be able to get the phasors values.
- It is not easy, if not impossible, to get the information of the type of filtering used in the relay from different manufactures. Signals recorded during disturbances in an electrical network are sometimes corrupted with nuisance components and noise. It was then decided to use DFT algorithm as it is less sensitive to noise compared to differential equation based algorithm.
- Information of the relay is gathered to do the correct modelling.
- Compute fault impedance and polarizing quantities.
- Plot a steady state characteristic using an impedance of a line and relay settings. Calculate the polarizing quantities and plot the dynamic characteristics.
- Plots of measured fault impedance; steady state and dynamic relay characteristics during fault development are done.

### **3.3.4 Obtain and implement settings for each relay type**

To make the tests realistic, settings as currently calculated (i.e. according to the current practices applied in Transmissions) were applied to the relays to be tested. The influence of ground resistivity was not considered.

### **3.3.5 Test three protection relay type using an Omicron [29]**

In accordance with the testing methodology developed, three relay types were selected to be tested and the results analysed and documented. The testing methodology including the approach, the constraints and the necessary parameters was developed. Omicron test equipment available in Eskom Transmission was used. Both the steady state and dynamic characteristics were tested.

The following distance relays were tested:

1. SEL 321
2. GEC YTG
3. Siemens R3Z27

#### **3.3.5.1 Steady state testing methodology**

Each of the relays was tested with the following benchmark set of settings applied

- Zone 1 reach =  $25\Omega$  ( representing the long line) and Zone 1 reach =  $5\Omega$  (representing the short line)
- Line angle =  $85^\circ$
- Earth Fault compensation:  $k = 0.85 @0^\circ$

The following assumptions were made:

- Load current = 0A, i.e. no pre-fault loading.
- Radial feeder was assumed. Fault inception angle will be set so that no dc offset will be present. For this the inception angle of the current with respect to voltage needs to be equal to the angle of the fault impedance (= line impedance + arc resistance).
- Only single phase faults were investigated
- Only the fault resistance coverage of Zone 1 was tested.

#### **3.3.5.2 Dynamic characteristics testing methodology**

The actual fault resistance reach was determined along the line angle at 10% steps of Z1 reach, i.e. from 0% to 90% of Z1 reach which results in 10 test points.

In order to determine the resistance coverage a test line as shown in figure 3.1 below is drawn and the method used was to search along this line (the reach test), the relay boundary point. The tests were started from the line angle (inside the Mho characteristic) and the points were moved until the point where the relay does not operate, this point then defines the maximum resistance coverage at that specific reactance percentage.

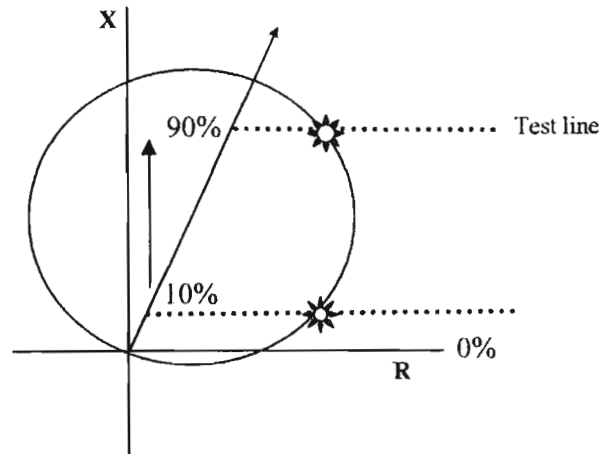


Figure 3.1: Mho characteristic showing the reach test

### 3.3.5.3 Source impedance ratio (SIR)

SIR is the ratio of the source impedance to the line impedance. Source impedance at the point of relay installation has to be selected. Ideally SIR should be specified to the value that reflects the reality. It should, however, be kept in mind that the magnitude of source impedance only influences the amount of movement of the characteristic. Thus if the source impedance is chosen approximately equal to the largest forward reach of the relay under test, the dynamic characteristic will appear double the diameter of the steady state characteristic for forward faults. However when SIR is very high, the relay could be very slow to operate [9]. Following source impedance ratios (SIR) were investigated:

For a 25 ohm line – Long line

- SIR = 0.5;  $Z_s = 12.5\Omega$
- SIR = 1;  $Z_s = 25\Omega$
- SIR = 6;  $Z_s = 150\Omega$

For a 5 ohm line – Short line

- SIR = 0.5;  $Z_s = 2.5\Omega$
- SIR = 6;  $Z_s = 30\Omega$

#### 3.3.5.4 Non homogeneous characteristic testing methodology

In each case, two test points was placed at the fault resistance determined by the reach test minus 10% as well as plus 10%. If the relay still trips instantaneously for the first test (-10%) and in delayed time for the second test (+10%), the relay is considered to be 'not susceptible' to the effect studied. The non-homogeneous tests done at 20%, 50% and 80% of Z1 reach. The main purpose was to determine whether the relay is susceptible or not. If the relay was susceptible for these conditions; further investigation to be performed to determine the causes of this susceptibility, and this investigation is not part of this scope.

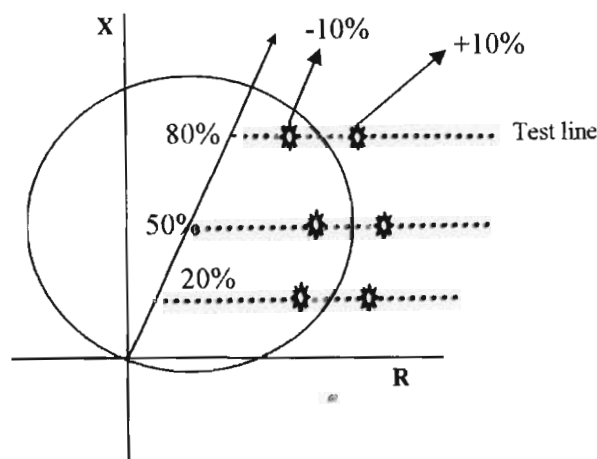


Figure 3.2: Mho characteristic showing the reach test

The following non-homogeneous effects were tested

- DC offset. Tests as described in on the steady state will be done for the following conditions of DC offset:
  - No dc offset: The inception angle of the current with respect to voltage needs to be set to equal to the angle of the fault impedance (= line impedance + arc resistance) to achieve zero dc offset
  - Maximum positive dc offset. The inception angle of the current with respect to voltage needs to be set to the angle of the fault impedance (= line impedance + arc resistance) minus  $90^\circ$  to achieve maximum positive dc offset.
  - Maximum negative dc offset. The inception angle of the current with respect to voltage needs to be set to the angle of the fault impedance (= line impedance + arc resistance) plus  $90^\circ$  to achieve maximum negative dc offset.

### **3.4 LOGIC OF THE RESEARCH**

The method to be used in this research is the deductive method. In a deductive method, a conceptual and theoretical structure is developed and then tested by empirical observation; thus particular instances are deduced from general inferences [3]. Thus for this reason, the deductive method is referred to as moving from the general to the particular.

A theoretical structure is developed through literature survey (presented in Chapter 2 – Literature Review), and used in the collection, analysis and interpretation of data that is to be presented in Chapter 4 – Data/Results.

### **3.5 OUTCOME OF THE RESEARCH**

The outcome of the research refers to whether you are trying to solve a particular problem or make a general contribution to knowledge [3]. This research has been designed to provide recommendations that will allow for improved protection performance.

## 4 CHAPTER 4 : RESULTS

### 4.1 HIGH RESISTANCE FAULT STATISTICS

A histogram of fault resistances measured over four years on the Eskom network is shown in Figure 4.1. 16% of all recorded faults have resistance above 10 primary ohms, which is a significant value.

The dynamic behaviour of a long arc may also result in substantial changes in arc resistance during the fault. For such faults the impedance measured by the relay changes with time during the fault. As a result, a high enough fault resistance may cause the fault impedance locus not to enter the tripping characteristic of the relay or to leave the characteristic during the fault. Such faults are difficult to detect and isolate properly and pose many challenges to protection equipment

The information from the fault recorders also indicated that most faults (about 85% of faults) that occur in the system are faults with small fault resistances of between 0 to 3 ohms. Any type of impedance relay, depending on the length of the line and point of the fault, will easily cover these. Practical value of arc resistance for a 275kV line with a fault current 10kA is around 0.5 ohms [9]. It is important that the characteristic angle of the relay be set less than the line angle in order to cater for arc resistance.

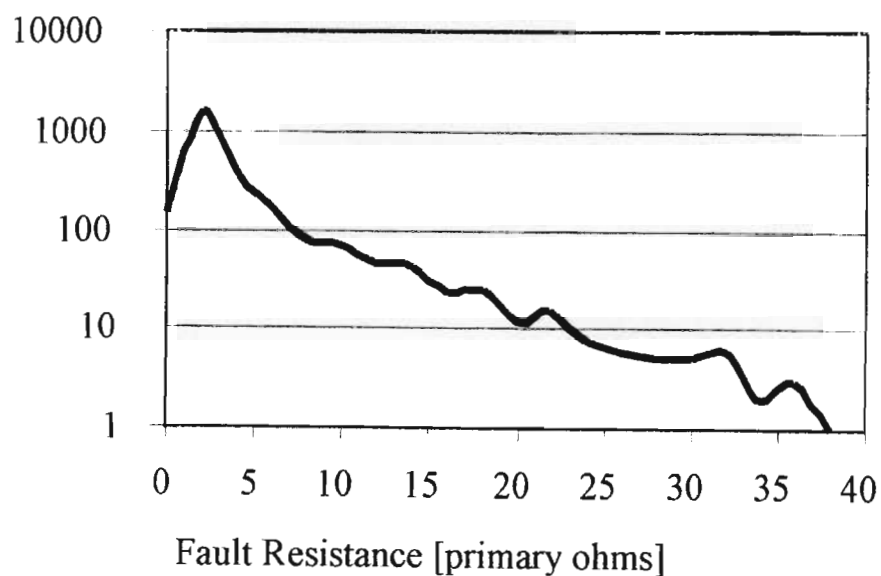


Figure 4.1 Graph of fault resistance [2]

## 4.2 RELAY CHARACTERISTICS TESTS BY SIMULATIONS

### 4.2.1 Plotting the steady state and dynamic characteristics of a Mho relay

For a steady state operation, a mho circle is derived from the equation of a circle using the impedance of a line and relay settings to be plotted on an R-X diagram.

$Z = R + jX$  - Impedance of the line;

$(x - a)^2 + (y - b)^2 = r^2$  - Equation of circle;

$(a, b) = (R/2, X/2)$  - coordinates of a centre of the circle;

$(r = Z/2)$  - Circle radius.

For dynamic characteristic a new impedance named  $Z_p$ , can be computed every sample by dividing the voltage with the fault current. In each and every sample a new centre and the radius is computed which allows a new circle to be plotted at every sample.  $Z_p$  depends on the sampled voltages and currents. With high resistance faults these quantities change as the fault resistance changes. This results in continuously changing mho circles during fault development. For proper evaluation of protection performance during such faults the actually measured fault impedance has to be compared with corresponding, dynamic relay characteristic.

### 4.2.2 Matlab simulation exercise for fault analysis

A high resistance fault occurred on an Eskom transmission 275kV (90km) line. The fault occurred 74km from the end which is being analysed and 16km from the other end.

The Matlab m-file in appendix 1 was created with the modelled installed mho type relay of this 275kV transmission line. A COMTRADE file of an actual recorded fault was played on the Matlab m-file. The voltage and the current signals of the faulted phase (white phase) are shown on the figure 4.7 below with period points P1 to P4.



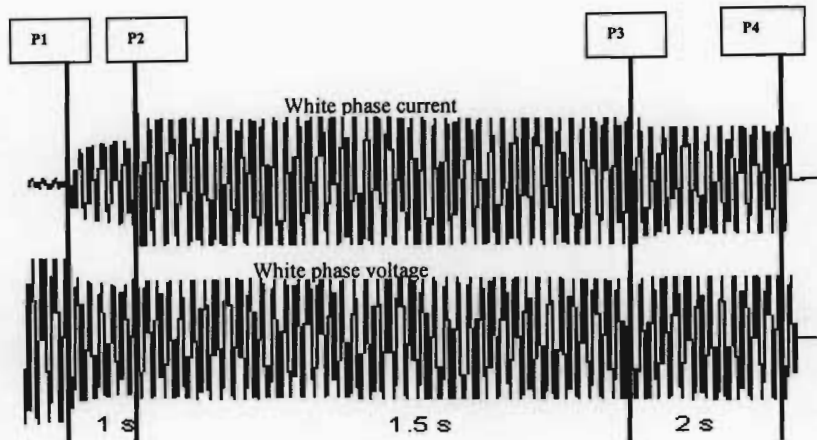


Figure 4.2: White phase voltage and current signals for a high resistance fault

White phase fault developed from point P1 as shown in the figure above. At point P2 the protection at the other end of the line tripped single phase and this caused white phase fault current contribution to increase as seen between points P2 and P3. At point P3 the fault developed into a white to blue phase fault and the white phase fault current reduced. At point P4 back up earth fault protection operated after 1.2 seconds from fault occurrence and finally cleared the fault. This resulted in a long fault duration impacting quality of supply.

The impedance protection applied on this feeder is a mho type impedance protection. The protection relay uses a full cross polarization technique with a polarizing voltage shifted by 12 degrees for phase to earth faults and 30 degrees for three phase faults.

Plots of measured fault impedance, steady state and dynamic relay characteristics during fault development done with a Matlab program are shown on the figures below:

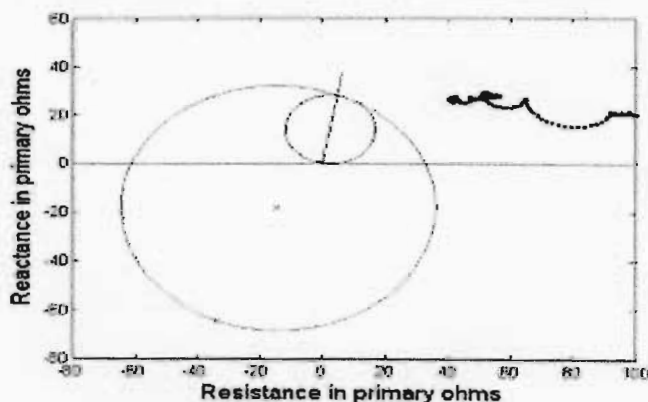


Figure 4.3: Impedance plane for fault impedance locus

The above figure displays the impedance locus with a fault starting with a very high resistance and stayed outside the impedance characteristics until the fault was cleared by the back up E/F protection.

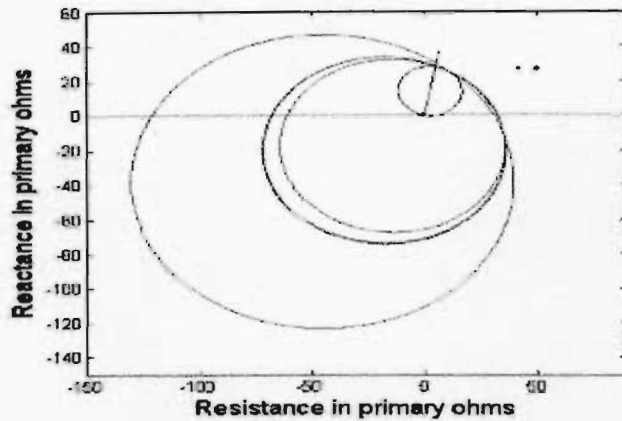


Figure 4.4: Dynamic Impedance plot

In all Eskom's transmission network incidents, failure of protection relays to operate correctly need to be evaluated. A correct overall protection operation occurs when for a primary system fault the minimum amount of breakers are rapidly tripped. If necessary mobilize testing crew to re-test the relay and prove its operational condition. The above analysis proved that the relay did not have a chance to operate as the fault resistance moved fault impedance beyond relay characteristic even when actual polarization of the relay was considered. In this particular condition testing of the relay was not necessary, which save company time and money otherwise required to prove integrity of the protection scheme. Such theoretical evaluation of the relay performance is not an easy task, as many details have to be known about the relay design, which is often not easily available. The initial effort to model all relays installed in the transmission company is substantial.

### 4.3 OMICRON RELAY TEST

#### 4.3.1 SEL 321 dynamic relay tests

##### 4.3.1.1 Long line 25 ohms

For the homogenous system, in order to determine the resistance coverage a test line as shown in figure 3.1, in chapter 3 is drawn and the reach test was done to search along this line, the relay boundary point. The actual fault resistance reach was determined in 10% steps of Z1 reach, from 0% to 90% of Z1 reach. The results are shown in Table 4.1 and graphically represented in figure 4.5.

Table 4.1: SEL321 Long line homogeneous test points

Position of test line		Actual Results from Advanced Distance							
		Constant I		SIR 0.5		SIR 1		SIR 6	
in %	in ohm	R	X	R	X	R	X	R	X
90	22.5	6.61 Ω	22.41 Ω	9.72 Ω	22.41 Ω	10.75 Ω	22.41 Ω	14.05 Ω	22.41 Ω
80	20	11.06 Ω	19.92 Ω	13.13 Ω	19.92 Ω	14.54 Ω	19.92 Ω	22.56 Ω	19.92 Ω
70	17.5	12.51 Ω	17.43 Ω	15.02 Ω	17.43 Ω	17.51 Ω	17.43 Ω	23.75 Ω	17.43 Ω
60	15	13.22 Ω	14.94 Ω	16.65 Ω	14.94 Ω	19.49 Ω	14.94 Ω	34.06 Ω	14.94 Ω
50	12.5	13.55 Ω	12.45 Ω	17.65 Ω	12.45 Ω	23.65 Ω	12.45 Ω	33.37 Ω	12.45 Ω
40	10	13.22 Ω	9.96 Ω	18.04 Ω	9.96 Ω	21.61 Ω	9.96 Ω	42.09 Ω	9.96 Ω
30	7.5	12.60 Ω	7.47 Ω	18.55 Ω	7.47 Ω	22.95 Ω	7.47 Ω	45.15 Ω	7.47 Ω
20	5	11.06 Ω	4.96 Ω	18.68 Ω	4.96 Ω	23.62 Ω	4.96 Ω	43.79 Ω	4.96 Ω
10	2.5	6.61 Ω	2.49 Ω	18.04 Ω	2.49 Ω	24.55 Ω	2.49 Ω	50.30 Ω	2.49 Ω
0	0			17.48 Ω	0.00 Ω	23.67 Ω	0.00 Ω	52.64 Ω	0.00 Ω

For the non-homogeneous system, the two test points were placed at the fault resistance determined by the reach test minus 10% as well as plus 10%. If the relay still trips instantaneously for the first test (-10%) and in delayed time for the second test (+10%), the relay is considered to be 'not susceptible' to the effect studied. The non-homogeneous tests done at 20%, 50% and 80% of Z1 reach. These test points are calculated in the tables 4.2 below for long line reaches and injected into the relay with the Omicron Net sim Software, these points are represented by the red dot (-10%) and the blue dot (+10%). The results are shown in Table 4.2 and graphically represented in figure 4.5.

Table 4.2: SEL Long line non-homogeneous test points

% of Z reach	Long Line (25 ohm reach) Test Point: for +10% & -10% of Actual Pick Up for SIR = 1							
	+10%				-10%			
	Z	Fth	R	X	Z	Fth	R	X
20	28.41 Ω	10.67°	25.93 Ω	4.38 Ω	21.97 Ω	13.16°	21.50 Ω	4.38 Ω
50	29.20 Ω	23.61°	22.63 Ω	12.45 Ω	22.61 Ω	33.42°	13.67 Ω	12.45 Ω
80	25.31 Ω	51.93°	15.60 Ω	19.92 Ω	22.94 Ω	55.71°	13.08 Ω	19.92 Ω

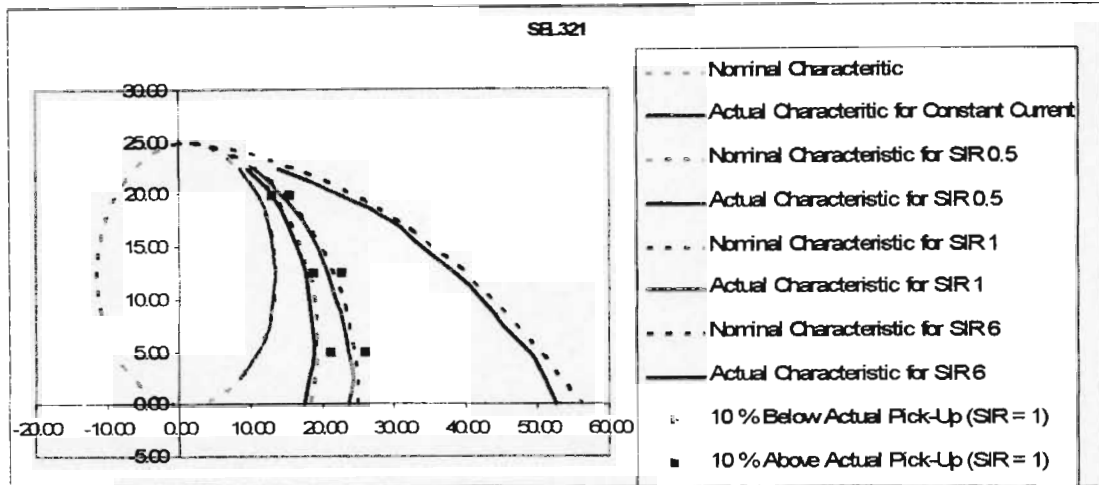


Figure 4.5: SEL Long line characteristics

#### 4.3.1.2 Short line 5 ohms

The results are shown in Table 4.3 and 4.4 and graphically represented in figure 4.6.

Table 4.3: SEL321 Short line homogeneous test point

Position of test line		Actual Results from Advanced Distance							
		Constant I		SIR 0.5		SIR 1		SIR 6	
in %	in ohm	R	X	R	X	R	X	R	X
90	4.5	1.75 Ω	4.48 Ω	1.94 Ω	4.48 Ω	2.14 Ω	4.48 Ω	3.25 Ω	4.48 Ω
80	4	2.24 Ω	3.99 Ω	2.83 Ω	3.99 Ω	2.92 Ω	3.99 Ω	4.75 Ω	3.99 Ω
70	3.5	2.53 Ω	3.49 Ω	3.01 Ω	3.49 Ω	3.51 Ω	3.49 Ω	6.05 Ω	3.49 Ω
60	3	2.86 Ω	2.99 Ω	3.34 Ω	2.99 Ω	3.83 Ω	2.99 Ω	7.18 Ω	2.99 Ω
50	2.5	2.73 Ω	2.49 Ω	3.56 Ω	2.49 Ω	4.21 Ω	2.49 Ω	7.80 Ω	2.49 Ω
40	2	2.65 Ω	1.99 Ω	3.64 Ω	1.99 Ω	4.40 Ω	1.99 Ω	8.42 Ω	1.99 Ω
30	1.5	2.53 Ω	1.49 Ω	3.74 Ω	1.49 Ω	4.59 Ω	1.49 Ω	9.08 Ω	1.49 Ω
20	1	2.20 Ω	1.00 Ω	3.74 Ω	1.00 Ω	4.63 Ω	1.00 Ω	9.66 Ω	1.00 Ω
10	0.5	1.67 Ω	0.50 Ω	3.64 Ω	0.50 Ω	4.77 Ω	0.50 Ω	10.54 Ω	0.50 Ω
0	0			3.36 Ω	0.00 Ω	4.77 Ω	0.00 Ω	10.62 Ω	0.00 Ω

Table 4.4: SEL321 Short line non-homogeneous test point

% of Z reach	Short Line (5 ohm reach) Test Point for +10% & -10% of Actual Pick Up for SIR = 1							
	+10%				-10%			
	Z	Phi	R	X	Z	Phi	R	X
20	5.18 Ω	11.09°	5.08 Ω	1.00 Ω	4.29 Ω	13.42°	4.17 Ω	1.00 Ω
50	5.24 Ω	28.40°	4.61 Ω	2.49 Ω	4.55 Ω	33.19°	3.81 Ω	2.49 Ω
80	5.10 Ω	51.45°	3.18 Ω	3.98 Ω	4.79 Ω	56.26°	2.66 Ω	3.98 Ω

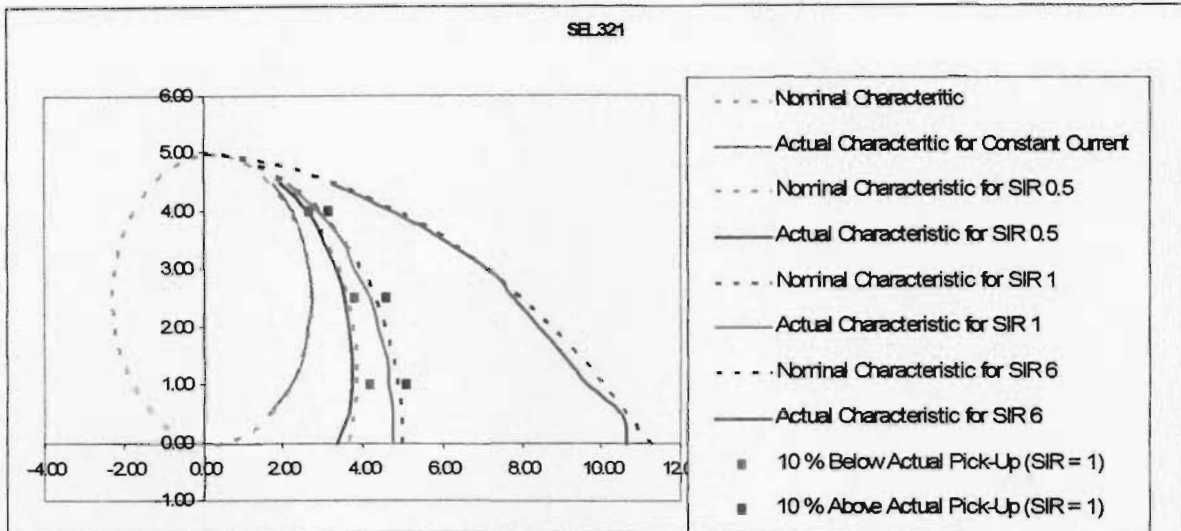


Figure 4.6: SEL321 Short line characteristics

### 4.3.2 GEC YTG Relay tests

#### 4.3.2.1 Relay tests for long line (25 ohms)

The results are shown in Table 4.5 and 4.6 and graphically represented in figure 4.7.

Table 4.5: YTG Long homogeneous test points

Position of test line		Actual Results from Advanced Distance					
		Constant I		SIR 0.5		SIR 1	
in %	in ohm	R	X	R	X	R	X
0	0						
10	2.5	12.170	2.415	12.482	2.415	12.230	2.415
20	5	14.280	4.830	14.742	4.830	14.750	4.830
30	7.5	15.540	7.244	15.852	7.244	15.920	7.244
40	10	16.630	9.659	16.662	9.659	16.620	9.659
50	12.5	16.840	12.070	16.662	12.070	17.100	12.070
60	15	16.470	14.480	16.652	14.490	16.690	14.490
70	17.5	14.120	16.900	16.172	16.900	15.980	16.900
80	20	12.490	19.320	14.882	19.320	14.920	19.320
90	22.5	9.570	21.730	11.882	21.730		

Table 4.6: YTG Long line non homogeneous test points

% of Z reach	Long Line (25 ohm reach) Test Point: for +10% & -10% of Actual Pick Up for SIR = 1							
	-10%				+10%			
	Z	Phi	R	X	Z	Phi	R	X
20	16.81 Ω	16.70°	15.10 Ω	4.83 Ω	14.25 Ω	19.31°	13.41 Ω	4.83 Ω
50	22.08 Ω	33.14°	19.49 Ω	12.07 Ω	19.82 Ω	37.53°	15.72 Ω	12.07 Ω
80	25.02 Ω	50.56°	15.89 Ω	19.32 Ω	23.63 Ω	54.18°	13.94 Ω	19.32 Ω

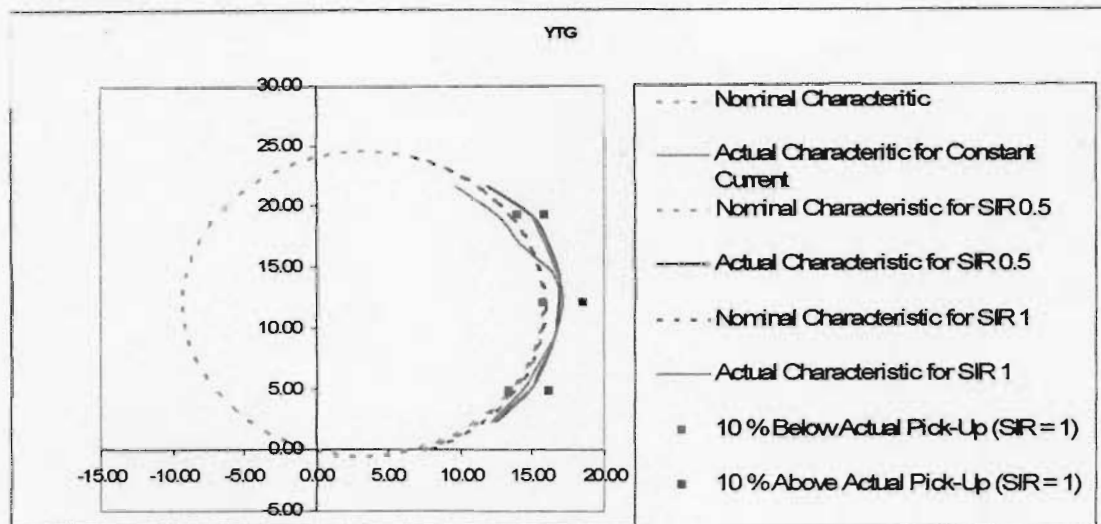


Figure 4.7: YTG Long line characteristics

#### 4.3.2.2 Relay tests for short line (5 ohms) – YTG relay

The results are shown in Table 4.7 and 4.8 and graphically represented in figure 4.8.

Table 4.7: YTG Short line homogeneous test points

Position of test line		Actual Results from Advanced Distance							
		Constant I		SIR 0.5		SIR 1		SIR 6	
in %	in ohm	R	X	R	X	R	X	R	X
0	0							2.322	0.000
10	0.5	2.343	0.483	2.281	0.483	2.340	0.483	2.617	0.483
20	1	2.703	0.966	2.616	0.966	2.734	0.966	2.932	0.966
30	1.5	2.937	1.449	3.001	1.449	2.993	1.449	3.145	1.449
40	2	3.054	1.932	3.109	1.932	3.132	1.932	3.256	1.932
50	2.5	3.072	2.415	3.121	2.415	3.139	2.415	3.166	2.415
60	3	3.023	2.898	3.037	2.898	3.051	2.898	3.065	2.898
70	3.5	2.936	3.381	2.860	3.361	2.890	3.391	2.860	3.381
80	4	2.546	3.864	2.592	3.864	2.599	3.864	2.577	3.864
90	4.5	2.199	4.347	2.192	4.347			2.127	4.347

Table 4.8: YTG Short line non homogeneous test points

% of Z reach	Short Line (5 ohm reach) Test Point: for -10% & -10% of Actual Pick Up for SIR = 1									
	-10%					-10%				
	Z	Phi	R	X		Z	Phi	R	X	
20	3.19 Ω	17.65°	3.04 Ω	0.97 Ω		2.71 Ω	20.89°	2.53 Ω	0.97 Ω	
50	4.16 Ω	35.48°	3.39 Ω	2.41 Ω		3.77 Ω	39.88°	2.89 Ω	2.41 Ω	
90	4.75 Ω	54.50°	2.76 Ω	3.86 Ω		4.57 Ω	57.70°	2.44 Ω	3.86 Ω	

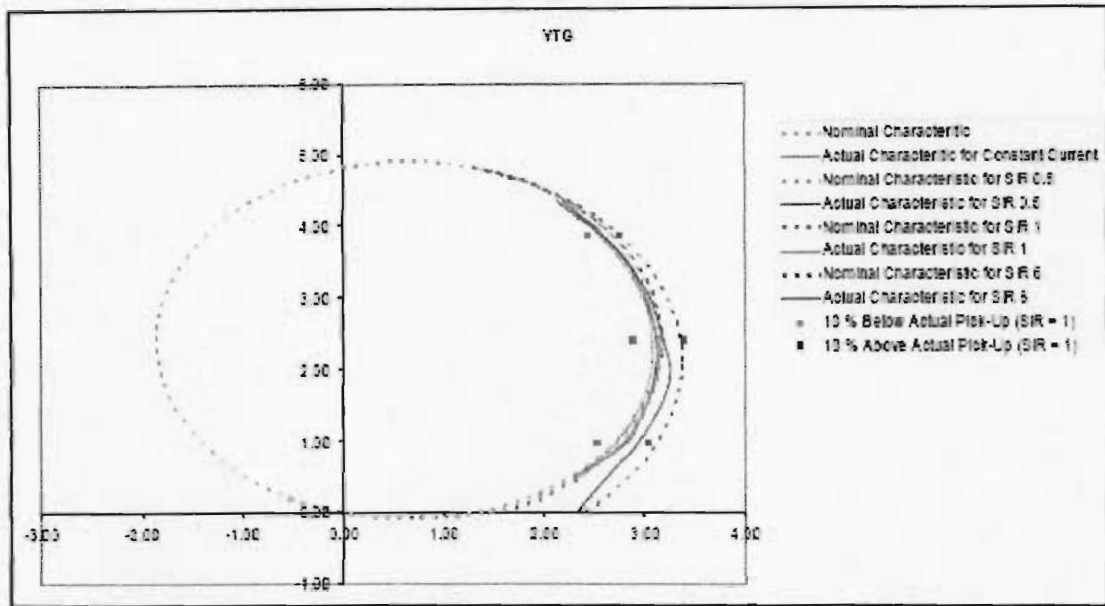


Figure 4.8 YTG Short line characteristics

### 4.3.3 Siemens R3Z27 Relay tests

#### 4.3.3.1 Relay tests for long line (25 ohms) – Plain impedance

The actual arc resistance reach was determined in 10% steps of Z1 reach, from 0% to 90% of Z1 reach, i.e. 10 test points. The results are shown in Table 4.9 and graphically represented in Figure 4.9

Table 4.9: R3Z27 Long line homogeneous test points – Plain impedance

Position of test line		Actual Results from Advanced Distance					
		Constant I		SIR 0.5		SIR 1	
in %	in ohm	R	X	R	X	R	X
0	0	26.000	0.000	25.840	0.000	25.230	0.000
10	2.5	25.880	2.462	25.720	2.462	25.260	2.462
20	5	25.660	4.924	25.520	4.924	24.740	4.924
30	7.5	25.240	7.386	24.920	7.386	23.000	7.386
40	10	24.220	9.848	24.220	9.848	23.720	9.848
50	12.5	22.540	12.310	22.710	12.310	22.370	12.310
60	15	20.120	14.770	21.700	14.770	20.400	14.770
70	17.5	17.720	17.230	19.690	17.230	19.260	17.230
80	20	13.980	19.700	17.320	19.700	14.530	19.700
90	22.5	9.065	22.160	13.350	22.160	9.776	22.160
100	25	4.142	23.490	4.727	26.810	4.009	22.740

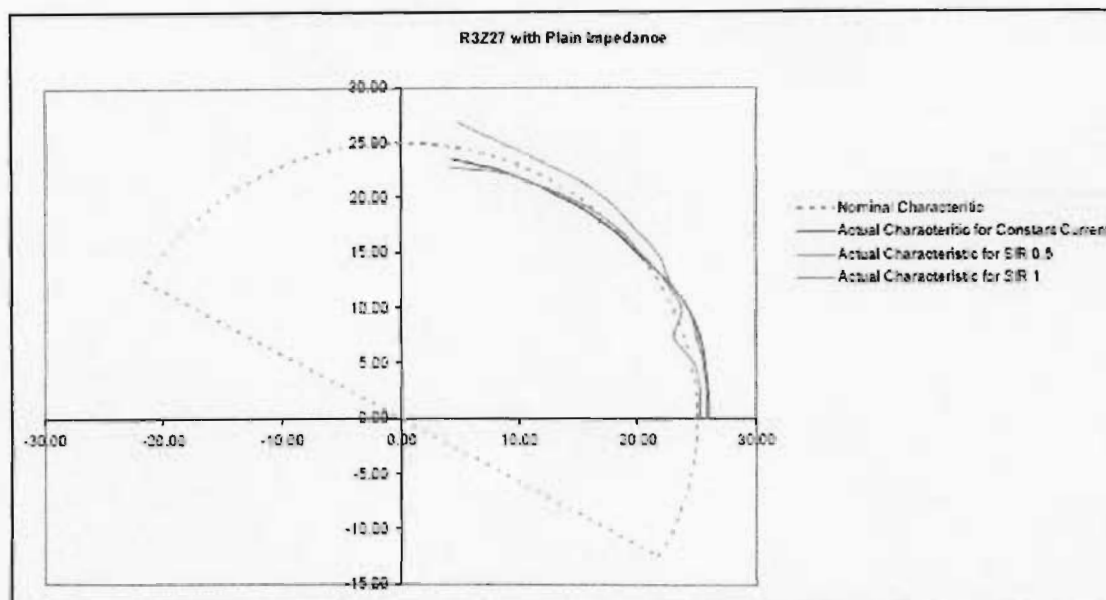


Figure 4.9: R3Z27 Long line homogeneous characteristics, plain impedance

#### 4.3.3.2 Relay tests for long line (25 ohms), modified $k=1.05$

The actual arc resistance reach was determined in 10% steps of  $Z_1$  reach, from 0% to 90% of  $Z_1$  reach, i.e. 10 test points. The results are shown in Table 4.10 and graphically represented in Figure 4.10

Table 4.10: R3Z27 Long line homogeneous test points,  $k=1.05$

Position of test line		Actual Results from Advanced Distance					
		Constant I		SIR 0.5		SIR 1	
in %	in ohm	R	X	R	X	R	X
0	0.0	33.730	0.000	36.830	0.000	36.830	0.000
10	2.5	33.590	2.462	37.020	2.462	36.400	2.462
20	5.0	33.480	4.924	36.960	4.924	36.640	4.924
30	7.5	33.080	7.386	36.330	7.386	36.000	7.386
40	10.0	32.380	9.848	35.750	9.848	35.080	9.848
50	12.5	31.420	12.310	34.630	12.310	34.090	12.310
60	15.0	30.360	14.770	32.860	14.770	32.470	14.770
70	17.5	29.080	17.230	31.440	17.230	30.360	17.230
80	20.0	26.540	19.700	29.070	19.700	28.310	19.700
90	22.5	20.940	22.160	25.900	22.160	24.880	22.160
100	25.0	4.009	22.740	4.381	24.850	4.381	24.850



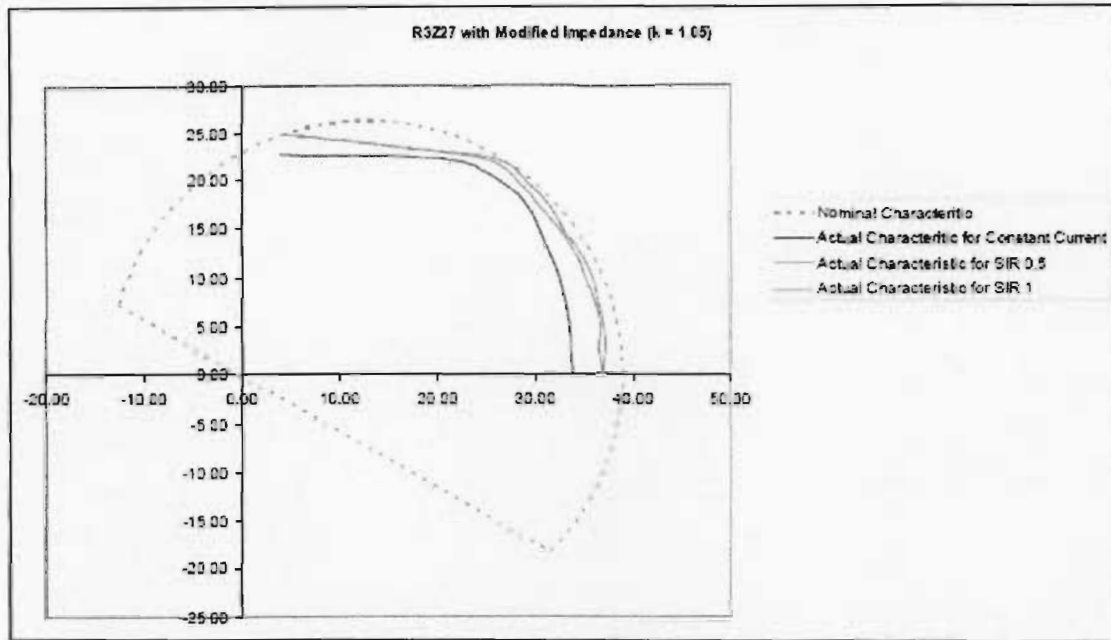


Figure 4.10: R3Z27 Long line homogeneous characteristics,  $k=1.05$

#### 4.3.3.3 Relay tests for long line (25 ohms), $k=2.1$

The actual arc resistance reach was determined in 10% steps of  $Z_1$  reach, from 0% to 90% of  $Z_1$  reach, i.e. 10 test points. The results are shown in Table 4.11 and graphically represented in Figure 4.11

Table 4.11: R3Z27 Long line homogeneous test points,  $k=2.1$

Position of test line		Actual Results from Advanced Distance					
		Constant I		SIR 0.5		SIR 1	
in %	in ohm	R	X	R	X	R	X
0	0	33.770	0.000	37.660	0.000	36.600	0.000
10	2.5	33.780	2.462	37.070	2.462	36.330	2.462
20	5	33.550	4.924	38.110	4.924	36.970	4.924
30	7.5	33.070	7.386	38.240	7.386	37.840	7.386
40	10	32.290	9.848	38.600	9.848	34.810	9.848
50	12.5	31.610	12.310	37.010	12.310	39.260	12.310
60	15	30.560	14.770	36.430	14.770	33.980	14.770
70	17.5	30.560	14.770	36.510	17.230	32.140	17.230
80	20	30.560	14.770	34.470	19.700	30.050	19.700
90	22.5	30.560	14.770	29.570	22.160	30.050	19.700
100	25	2.853	16.180	3.897	22.100	3.559	20.190

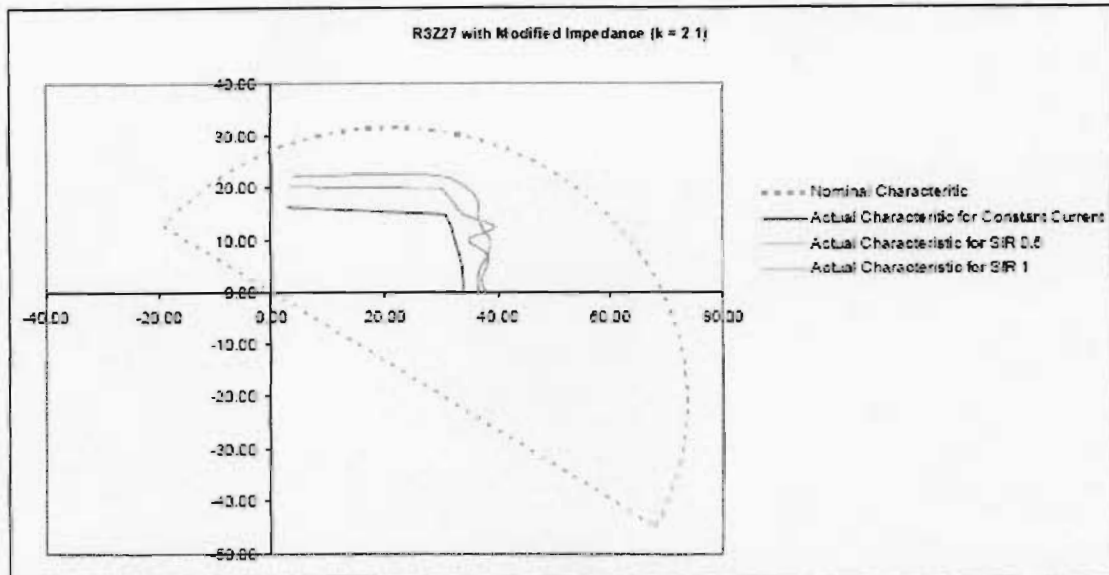


Figure 4.11: R3Z27 Long line homogeneous characteristics,  $k = 2.1$

#### 4.3.3.4 Relay tests for short line (5 ohms) – Plain impedance

The actual arc resistance reach was determined in 10% steps of  $Z_1$  reach, from 0% to 90% of  $Z_1$  reach, i.e. 10 test points. The results are shown in Table 4.12 and graphically represented in Figure 4.12

Table 4.12: R3Z27 Short line homogeneous test points – Plain impedance

Position of test line		Actual Results from Advanced Distance							
		Constant I		SIR 0.5		SIR 1		SIR 6	
in %	in ohm	R	X	R	X	R	X	R	X
0.000	0.000	5.168	0.000	5.322	0.000	5.291	0.000	5.015	0.000
10.000	0.500	5.176	0.492	5.329	0.492	5.268	0.492	4.930	0.492
20.000	1.000	5.105	0.985	5.229	0.985	5.229	0.985	4.918	0.985
30.000	1.500	4.984	1.477	5.048	1.477	5.048	1.477	4.696	1.477
40.000	2.000	4.811	1.970	4.744	1.970	4.777	1.970	4.512	1.970
50.000	2.500	4.543	2.462	4.369	2.462	4.439	2.462	4.369	2.462
60.000	3.000	4.164	2.954	3.975	2.954	3.975	2.954	4.014	2.954
70.000	3.500	3.683	3.447	3.466	3.447	3.466	3.447	3.555	3.447
80.000	4.000	2.900	3.939	2.624	3.939	2.845	3.939	3.010	3.939
90.000	4.500	1.969	4.432	1.738	4.432	1.692	4.432	2.154	4.432
100.000	5.000	0.884	4.728	0.839	4.758	0.823	4.668	0.866	4.909

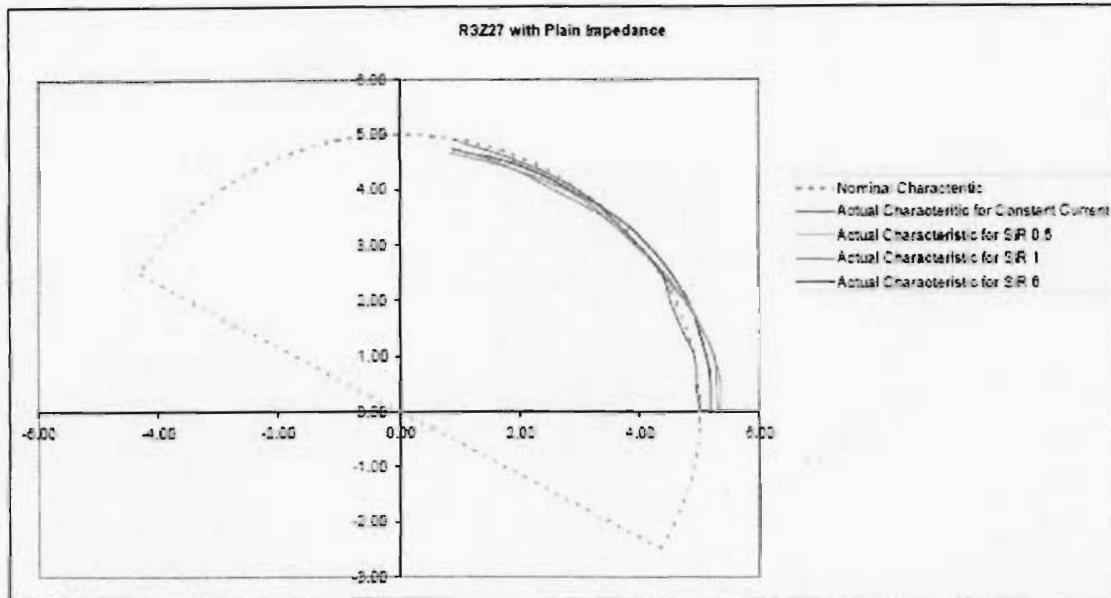


Figure 4.12: R3Z27 Short line homogeneous characteristics, plain impedance

#### 4.3.3.5 Relay tests for short line (5 ohms), $k=1.05$

The actual arc resistance reach was determined in 10% steps of Z1 reach, from 0% to 90% of Z1 reach, i.e. 10 test points. The results are shown in Table 4.13 and graphically represented in Figure 4.13.

Table 4.13: R3Z27 Short line homogeneous test points,  $k=1.05$

Position of test line		Actual Results from Advanced Distance							
		Constant I		SIR 0.5		SIR 1		SIR 6	
in %	in ohm	R	X	R	X	R	X	R	X
0	0	7.739	0	7.863	0	7.801	0	7.491	0
10	0.5	7.716	0.4924	7.778	0.4924	7.84	0.4924	7.466	0.4924
20	1	7.708	0.9848	7.771	0.9848	7.771	0.9848	7.455	0.9848
30	1.5	7.59	1.477	7.655	1.477	7.655	1.477	7.331	1.477
40	2	7.353	1.97	7.353	1.97	7.42	1.97	7.15	1.97
50	2.5	7.068	2.462	6.996	2.462	6.996	2.462	6.925	2.462
60	3	6.687	2.954	6.571	2.954	6.571	2.954	6.494	2.954
70	3.5	6.158	3.447	6.03	3.447	6.03	3.447	5.987	3.447
80	4	5.51	3.939	5.307	3.939	5.206	3.939	5.611	3.939
90	4.5	4.462	4.432	4.086	4.432	4.326	4.432	4.77	4.432
100	5	0.8142	4.617	0.808	4.582	0.8018	4.547	0.8266	4.688

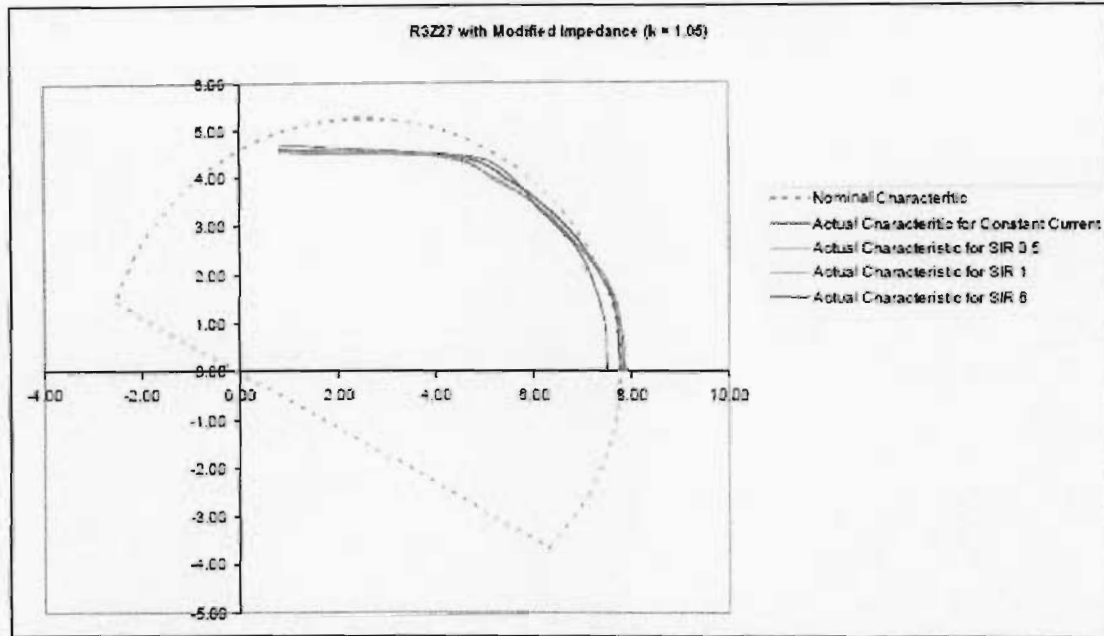


Figure 4.13: R3Z27 Short line homogeneous characteristics,  $k=1.05$

#### 4.3.3.6 Relay tests for short line (5 ohms), $k= 2.1$

The actual arc resistance reach was determined in 10% steps of Z1 reach, from 0% to 90% of Z1 reach, i.e. 10 test points. The results are shown in Table 4.14 and graphically represented in Figure 4.14

Table 4.14: R3Z27 Short line homogeneous test points,  $k=2.1$

Position of test line		Actual Results from Advanced Distance							
		Constant I		SIR 0.5		SIR 1		SIR 6	
in %	in ohm	R	X	R	X	R	X	R	X
0	0.0	11.560	0.000	11.490	0.000	11.490	0.000	12.060	0.000
10	0.5	11.070	0.492	10.990	0.492	10.990	0.492	11.870	0.492
20	1.0	10.590	0.985	10.360	0.985	10.430	0.985	11.420	0.985
30	1.5	9.957	1.477	9.877	1.477	9.797	1.477	10.830	1.477
40	2.0	9.150	1.970	9.150	1.970	9.066	1.970	10.330	1.970
50	2.5	7.941	2.462	8.392	2.462	8.392	2.462	9.742	2.462
60	3.0	7.090	2.954	7.384	2.954	7.481	2.954	8.852	2.954
70	3.5	7.090	2.954	7.384	2.954	7.481	2.954	8.720	3.447
80	4.0	7.090	2.954	7.384	2.954	7.481	2.954	7.401	3.939
90	4.5	7.090	2.954	7.384	2.954	7.481	2.954	7.401	3.939
100	5.0	0.589	3.341	0.608	3.445	0.571	3.326	0.724	4.107

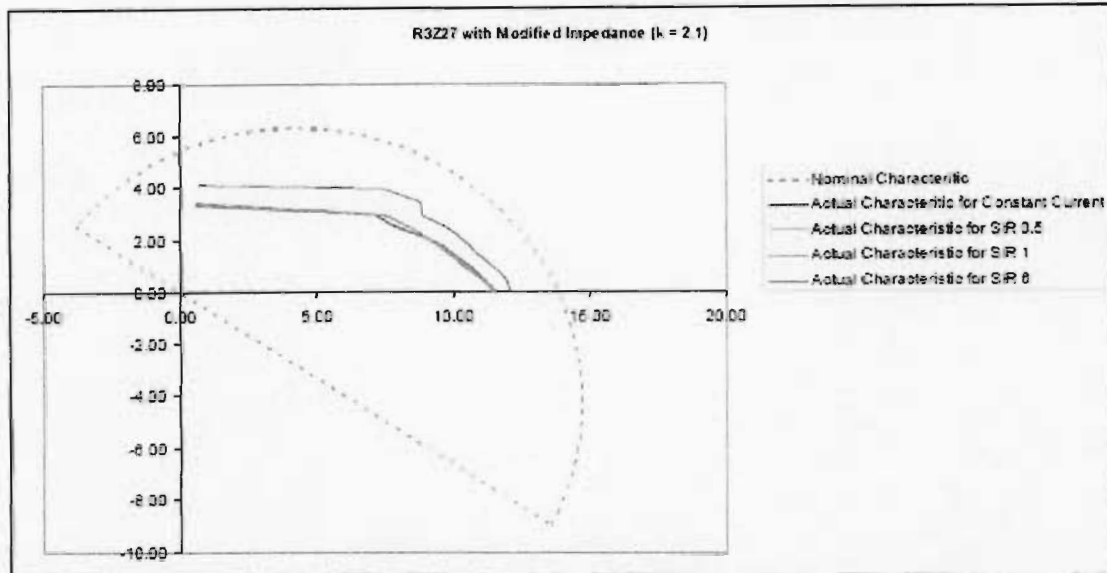


Figure 4.14: R3Z27 Short line homogeneous characteristics,  $k = 2.1$

#### 4.3.4 Siemens R3Z27 relay tests – NON HOMOGENEOUS

##### 4.3.4.1 Relay tests for long line (25 ohms) – Plain impedance

The actual arc resistance reach was tested at 20%, 50% and 80% of Z1 reach. The results are shown in Table 4.15 and graphically represented in Figure 4.15

Table 4.15: R3Z27 Long line non-homogeneous test points, plain impedance

% of Z reach	Long Line (25 ohm reach, Plain impedance): Test Point for +10% & -10% of Actual Pick Up for SIR = 1							
	+10%				-10%			
	Z	Phi	R	X	Z	Phi	R	X
20	27.58 $\Omega$	10.28°	27.14 $\Omega$	4.92 $\Omega$	22.90 $\Omega$	12.42°	22.36 $\Omega$	4.92 $\Omega$
50	27.32 $\Omega$	26.76°	24.39 $\Omega$	12.31 $\Omega$	22.78 $\Omega$	31.17°	20.55 $\Omega$	12.21 $\Omega$
80	25.15 $\Omega$	51.55°	15.64 $\Omega$	19.70 $\Omega$	23.84 $\Omega$	55.72°	13.43 $\Omega$	19.70 $\Omega$

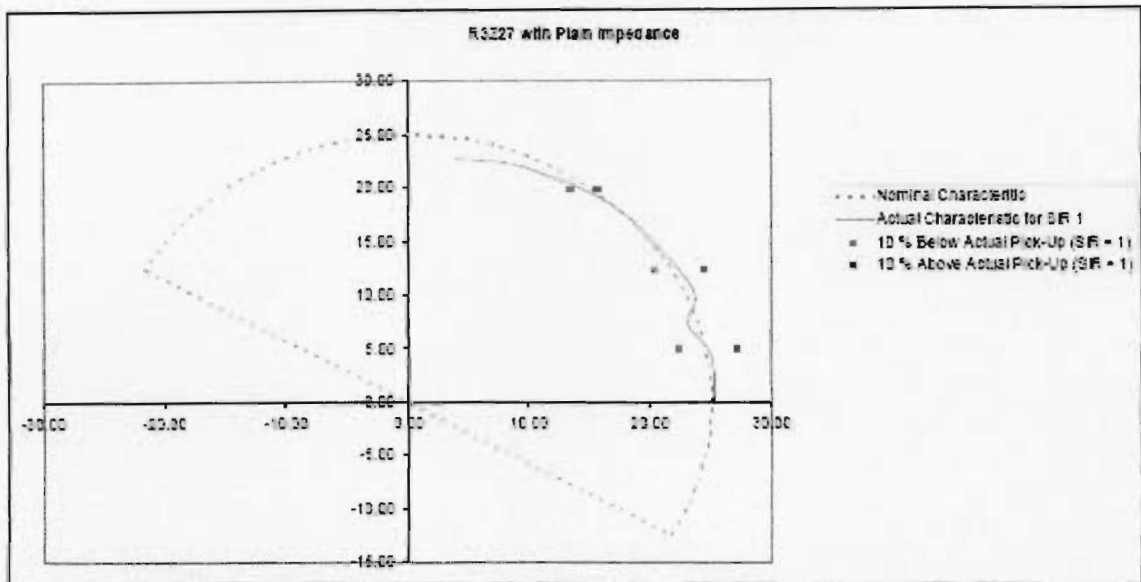


Figure 4.15: R3Z27 Long line Non-homogeneous characteristics, plain impedance

#### 4.3.4.2 Relay tests for long line (25 ohms) – modified, $k=1.05$

The actual arc resistance reach was tested at 20%, 50% and 80% of  $Z_1$  reach. The results are shown in Table 4.16 and graphically represented in Figure 4.16

Table 4.16: R3Z27 Long line non-homogeneous test points,  $k=1.05$ .

% of Z reach	Long Line (25 ohm reach, Modified impedance, $k=1.05$ ): Test Point for +10% & -10% of Actual Pick Up for $S/R = 1$							
	+10%				-10%			
	Z	Phi	R	X	Z	Phi	R	X
20	40.53 $\Omega$	8.98°	40.23 $\Omega$	4.92 $\Omega$	33.43 $\Omega$	8.47°	33.07 $\Omega$	4.92 $\Omega$
50	38.26 $\Omega$	18.27°	37.28 $\Omega$	12.31 $\Omega$	33.26 $\Omega$	21.72°	30.90 $\Omega$	12.31 $\Omega$
80	36.56 $\Omega$	32.60°	30.80 $\Omega$	19.70 $\Omega$	32.48 $\Omega$	37.33°	25.83 $\Omega$	19.70 $\Omega$

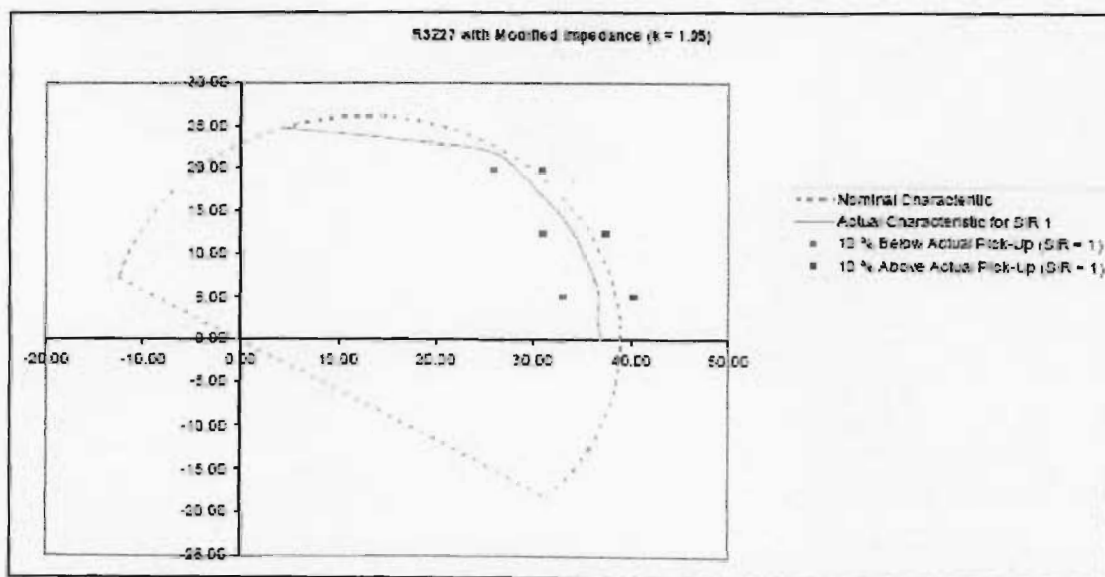


Figure 4.16: R3Z27 Long line Non-homogeneous characteristics,  $k=1.05$

#### 4.3.4.3 Relay tests for long line (25 ohms), modified k =2.1

The actual arc resistance reach was tested at 20%, 50% and 80% of Z1 reach. The results are shown in Table 4.17 and graphically represented in Figure 4.17

Table 4.17: R3Z27 Long line non-homogeneous test points, k =2.1

% of Z reach	Long Line (25 ohm reach, Mod. Impedance, k=2.1) Test Point for +10 % & -10% of Actual Pick Up for SIR = 1							
	+10%				-10%			
	Z	Phi	R	X	Z	Phi	R	X
20	40.88 $\Omega$	8.92°	40.58 $\Omega$	4.92 $\Omega$	33.72 $\Omega$	8.40°	33.36 $\Omega$	4.92 $\Omega$
50	44.79 $\Omega$	15.99°	42.97 $\Omega$	12.31 $\Omega$	37.62 $\Omega$	19.10°	35.55 $\Omega$	12.31 $\Omega$
80	38.18 $\Omega$	31.05°	32.71 $\Omega$	19.70 $\Omega$	33.74 $\Omega$	35.71°	27.39 $\Omega$	19.70 $\Omega$

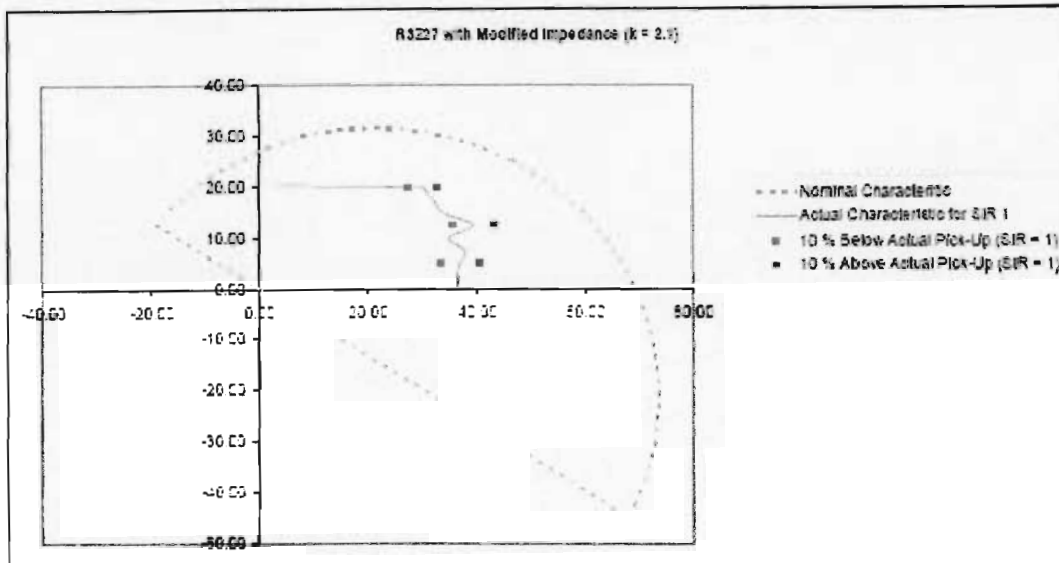


Figure 4.17: R3Z27 Long line Non-homogeneous characteristics, k =2.1

#### 4.3.4.4 Relay tests for short line (5 ohms) – Plain impedance

The actual arc resistance reach was tested at 20%, 50% and 80% of Z1 reach. The results are shown in Table 4.18 and graphically represented in Figure 4.18

Table 4.18: R3Z27 Short line non-homogeneous test points, plain impedance

% of Z reach	Short Line (5 ohm reach, Plain Impedance) Test Point: for +10 % & -10% of Actual Pick Up for SIR = 1							
	+10%				-10%			
	Z	Phi	R	X	Z	Phi	R	X
20	5.82 $\Omega$	9.74°	5.74 $\Omega$	0.98 $\Omega$	4.93 $\Omega$	11.76°	4.72 $\Omega$	0.98 $\Omega$
50	5.43 $\Omega$	26.97°	4.94 $\Omega$	2.46 $\Omega$	4.73 $\Omega$	31.57°	4.04 $\Omega$	2.46 $\Omega$
80	4.99 $\Omega$	52.16°	3.06 $\Omega$	3.94 $\Omega$	4.74 $\Omega$	56.26°	2.63 $\Omega$	3.94 $\Omega$

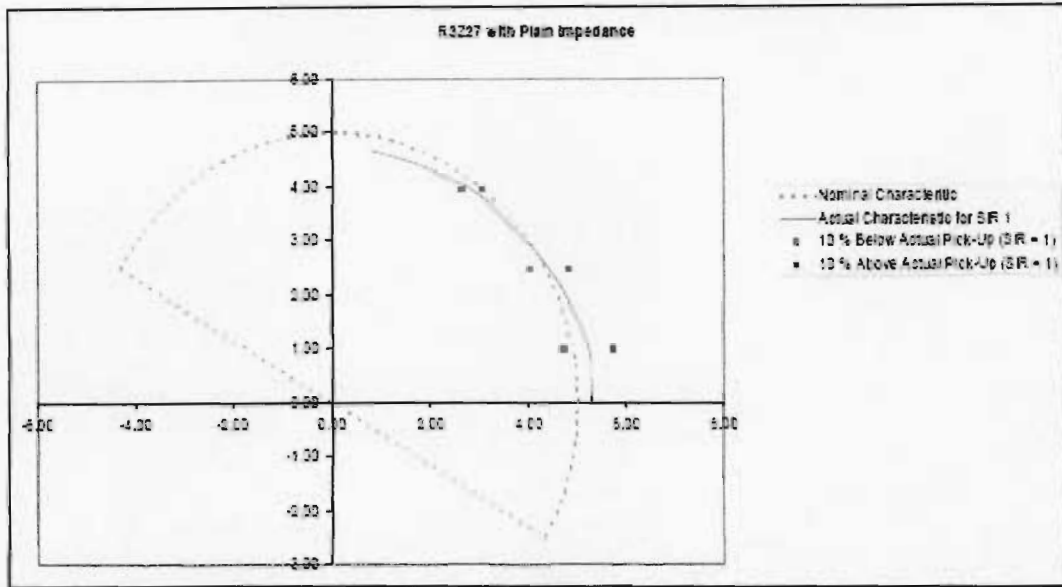


Figure 4.18: R3Z27 Short line Non-homogeneous characteristic, plain impedance

#### 4.3.4.5 Relay tests for short line (5 ohms) – modified $k=1.05$

The actual arc resistance reach was tested at 20%, 50% and 80% of  $Z_1$  reach. The results are shown in Table 4.19 and graphically represented in Figure 4.19

Table 4.19: R3Z27 Short line non-homogeneous test points,  $k = 1.05$

% of $Z$ reach	Short Line (5 ohm) reach, Mod. Impedance $k=1.05$ ; Test Point for -10% & -10% of Actual Pick Up for SIR = 1							
	-10%				-10%			
	Z	Phi	R	X	Z	Phi	R	X
20	8.58 $\Omega$	6.58°	8.53 $\Omega$	0.98 $\Omega$	7.08 $\Omega$	7.99°	7.01 $\Omega$	0.96 $\Omega$
50	8.64 $\Omega$	17.63°	7.65 $\Omega$	2.45 $\Omega$	6.82 $\Omega$	21.22°	6.34 $\Omega$	2.46 $\Omega$
80	6.99 $\Omega$	34.65°	5.66 $\Omega$	3.94 $\Omega$	6.18 $\Omega$	39.64°	4.76 $\Omega$	3.94 $\Omega$



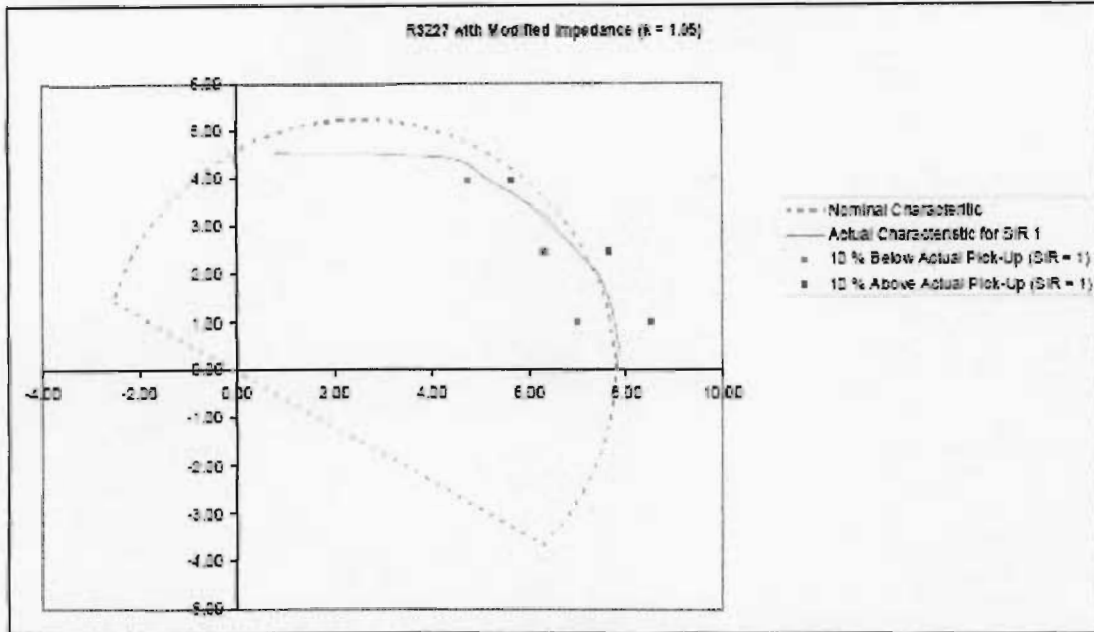


Figure 4.19: R3Z27 Short line Non-homogeneous characteristics,  $k = 1.05$

#### 4.3.4.6 Relay tests for short line (5 ohms) – modified $k=2.1$

The actual arc resistance reach was tested at 20%, 50% and 80% of  $Z_1$  reach. The results are shown in Table 4.20 and graphically represented in Figure 4.20

Table 4.20: R3Z27 Short line non-homogeneous test points,  $k = 2.1$

% of $Z$ reach	Short Line (5 ohm reach, Mod. Impedance, $k=2.1$ ) Test Point for -10 % & -10% of Actual Pick Up for SIR = 1							
	+10%				-10%			
	Z	Phi	R	X	Z	Phi	R	X
20	11.50 $\Omega$	4.91°	11.46 $\Omega$	0.98 $\Omega$	9.46 $\Omega$	5.96°	9.41 $\Omega$	0.98 $\Omega$
50	9.51 $\Omega$	15.00°	9.19 $\Omega$	2.46 $\Omega$	7.96 $\Omega$	17.96°	7.60 $\Omega$	2.46 $\Omega$
80	8.70 $\Omega$	19.86°	8.18 $\Omega$	2.95 $\Omega$	7.40 $\Omega$	23.53°	6.79 $\Omega$	2.95 $\Omega$

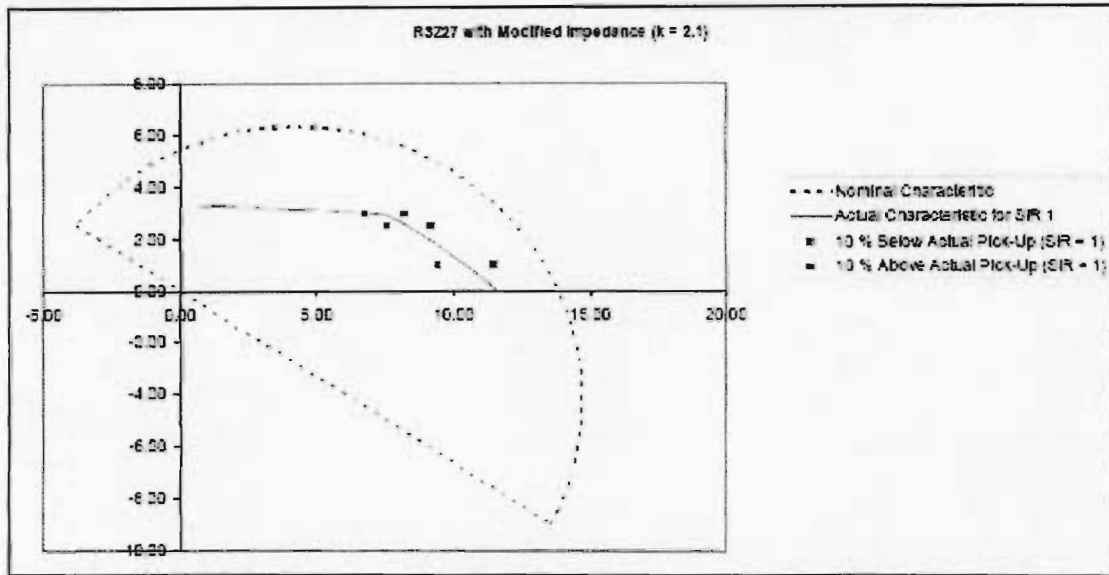


Figure 4.20: R3Z27 Short line Non-homogeneous characteristics,  $k = 2.1$

## 4.4 PROTECTION PERFORMANCE HISTORY

### 4.4.1 Protection performance – 2005 to 2006

Data was collected for Transmission protection performance report for a period of a year, April 2005 until April 2006. This data reveals that more than 50% of incorrect operations encountered on the transmission system are slow clearing of faults due to high resistance faults. All the incorrect operations due to high resistance faults and the related dips due to the faults are listed in table 4.21 below:

Table 4.21: 2005 protection performances

DATE	NAME	RELAY TYPE	DIP TYPE
18/04/2005	Bacchus - Muldersvlei No1 400kV	TLS	Y
18/04/2005	Bacchus - Muldersvlei No1 400kV	TLS	Y
18/04/2005	Bacchus - Muldersvlei No1 400kV	TLS	Y
20/04/2005	Arnot - Prairie No2 275kV	H type	Y
31/05/2005	Apollo - Esselen No1 275kV	Micromho	S
01/06/2005	Bernina - Glockner No1 275kV	H type	X
03/06/2005	Normandie - Umfolozi No1 400kV	TLS	X
05/06/2005	Impala - Invubu No1 275kV	LZ32	T
08/06/2005	Pluto - Watershed No1 275kV	LZ32	Y
25/06/2005	Matimba - Midas No1 400kV	TLS	Y
29/06/2005	Brenner - Lethabo No1 275kV	Micromho	X
29/06/2005	Eiger - Lethabo No1 275kV	YTG	Y
04/07/2005	Aurora - Juno No1 400kV	7sa513	Y
25/07/2005	Hector - Illovo No1 275kV	PXLN	X
25/07/2005	Hector - Illovo No1 275kV	PXLN	Y
25/07/2005	Hector - Illovo No1 275kV	PXLN	X
25/07/2005	Esselen - Jupiter No1 275kV	H type	X
27/07/2005	Arnot - Merensky No1 400kV	REL531	S
08/08/2005	Tutuka - Pegasus No1 400kV	PXLN	Y
14/08/2005	Nevis - Snowdon No2 275kV	YTG	Y
20/08/2005	Minerva - Duvha No1 400kV	R3Z27	Y
21/08/2005	Glockner - Lethabo No2 400kV	YTG	S
24/08/2005	Pluto - Hermes No1 400kV	TLS	Z2
25/08/2005	Avon - Impala No1 275kV	YTG	S
26/08/2005	Bighorn - Pluto No1 275kV	TLS	X

09/09/2005	Hendrina - Vulcan No1 400kV	Micromho	Y
09/09/2005	Line Tripped and L/O	Micromho	Y
10/09/2005	Duvha - Vulcan No1 400kV	Micromho	Y
11/09/2005	Matimba - Pluto No1 400kV	TLS	X
15/09/2005	Arnot - Merensky No1 400kV	REL531	Y
24/09/2005	Majuba - Venus N2 400kV	TLS	Y
25/09/2005	Acornhoek - Marathon No2 275kV	H type	Z
26/09/2005	Matla - Atlas No1 400kV	H type	Y
26/09/2005	Warmbad - Witkop No1 275kV	YTG	X
28/09/2005	Esselen - Pelly No1 275kV	YTG	S
10/10/2005	Ferrum - Olien No1 275kV	YTG	S
10/10/2005	Ferrum - Olien No1 275kV	YTG	S
12/10/2005	Ferrum - Olien No1 275 kV	YTG	S
12/10/2005	Matla - Glockner No1 400kV	YTG	Y
12/10/2005	Matla - Glockner No2 400kV	YTG	Y
18/10/2005	Komatipoort - Infuleni No1 275kV	SEL-321	Z
18/10/2005	Tutuka - Pegasus No1 400kV	PXLN	Y
27/10/2005	Droerivier - Proteus No1 400kV	TLS	Y
01/11/2005	Ferrum - Olien No2 275kV	YTG	T
02/11/2005	Droerivier - Proteus No1 400kV	TLS	S
02/11/2005	Droerivier - Proteus No1 400kV	TLS	S
02/11/2005	Droerivier - Proteus No1 400kV	TLS	Z
02/11/2005	Droerivier - Proteus No1 400kV	TLS	Z
03/11/2005	Matimba - Spitskop No2 400kV	TLS	Y
19/11/2005	Hera - Watershed No1 275kV	YTG	S
05/12/2005	Normandie - Umfolozi No1 400kV	TLS	Z
15/12/2005	Athene - Pegasus No1 400kV	PXLN	X
16/12/2005	Athene - Pegasus No1 400kV	PXLN	X
18/12/2005	Atlas - Snowdon No2 275kV	Micromho	S
18/12/2005	Atlas - Snowdon No2 275kV	Micromho	S
19/02/2006	Acacia - Philippi No1 400kV	YTG	S
19/02/2006	Acacia - Philippi No2 400kV	YTG	S
19/02/2006	Acacia Muldersvlei No1 400kV	YTG	T
28/02/2006	Bacchus - Droerivier No1 400kV	TLS	Z

06/03/2006	Bacchus - Droerivier No1 400kV	TLS	S
06/03/2006	Bacchus - Droerivier No1 400kV	TLS	X
30/03/2006	Boundary - Olien No2 275kV	YTG	T

#### 4.4.2 Protection performance – 2006

Data was collected for transmission report for a period of a year, April 2006 until December 2006. This data reveals that more than 50% of incorrect operations encountered on the transmission system are slow clearing of faults due to high resistance faults. All the incorrect operations due to high resistance faults are listed in table 4.22 below

Table 4.22: 2006 protection performances

10/04/2006	Hydra - Ruigtevallei No1 220kV	SEL321	T
13/04/2006	Droerivier - Hydra No1 400kV	7sa513	X
26/05/2006	Benburg - Esselen No1 275kV	YTG	X
31/05/2006	Apollo - Pluto No1 400kV	YTG	X
05/06/2006	Georgedale - Venus No1 275kV	TLS	Y
06/06/2006	Normandie - Umfolozi No1 400kV	THS	X
14/06/2006	Camden - Normandie No1 400kV	TLS	S
14/06/2006	Duvha - Matla No1 400kV	YTG	Y
21/06/2006	Duvha - Kendal No1 400kV	Micromho	X
22/06/2006	Alpha - Beta No2 765kV		
26/06/2006	Pluto - Watershed No1 275kV	YTG & LZ32	S
28/06/2006	Chivelston - Incandu No1 400kV	TLS	T
12/07/2006	Apollo - Pluto No1 400kV	YTG	X
24/07/2006	Marathon - Prairie No2 275kV	SEL321	S
31/07/2006	Drakensberg - Pegasus No1 400kV	YTG	Y
01/08/2006	Apollo - Kendal No2 400kV	Micromho	Y
01/08/2006	Kendal - Minerva No1 400kV	Micromho	X
21/08/2006	Tutuka - Pegasus No1 400kV	PXLN	Y
21/08/2006	Tutuka - Pegasus No1 400kV	PXLN	Y
21/08/2006	Apollo - Croydon No1 275kV	PYTS	Y
06/10/2006	Majuba - Venus No1 400kV	TLS	S
07/10/2006	Tutuka - Pegasus No1 400kV	YTG	Y
09/10/2006	Invubu - Umfolozi No1 400kV	YTG	Z

12/10/2006	Minerva - Vulcan No1 400kV	YTG	Y
25/10/2006	Esselen - Jupiter No1 275kV	PYTS	Y
11/11/2006	Everest - Makalu No1 275kV	YTG	Y
15/11/2006	Mersey - Venus No1 400kV	7sa513	X

## 4.5 VOLTAGE DIPS

### 4.5.1 S type dips - 2005

Table 4.23: Dips related to Apollo Esselen fault 31/05/05

NAME	DEPTH	DURATION	CLASS
Apollo 400/275kV	37.2	340	S
Benburg 275/132kV	31.3	340	S
Croydon 275/132kV	24.4	340	S
Eiger 275/88kV	18.6	260	Y
Esselen 275/132/88kV	38.2	350	S
Esselen 275/132kV	35.3	340	S
Etna 275/88 kV	16.7	240	Y
Fordsburg 275/275kV	22.3	320	S
Prospect 275/275kV	28	320	S

Table 4.24: Dips related to Arnot Merensky fault 27/07/05

NAME	DEPTH	DURATION	CLASS
Merensky 275/132kV	31	230	S

Table 4.25: Dips related to Glockner Lethabo fault 21/08/05

NAME	DEPTH	DURATION	CLASS
Glockner 400/275	44.9	240	S

Table 4.26: Dips related to Avon Impala fault 25/08/05

NAME	DEPTH	DURATION	CLASS
Athene 400/132kV	12.5	160	Y
Avon 275/132kV	47.4	60	X
Avon 275/132kV	23.9	260	S
Georgedale 275/132kV	12.9	50	Y
Impala 275/132kV	14.8	220	Y
Mersey 400/132kV	14.2	110	Y

Rabbit 1 275/275kV	14.3	40	Y
Rabbit 1 275/275kV	14.1	140	Y
Rabbit 2 275/275kV	12.7	90	Y

Table 4.27: Dips related to Acornhoek Marathon fault 25/09/05

NAME	DEPTH	DURATION	CLASS
Acornhoek 275/132kV	12.1	60	Y
Acornhoek 275/132kV	100	70	T
Acornhoek 275/132kV	100	90	T
Acornhoek 275/132kV	38.8	270	S
Acornhoek 275/132kV	42.2	90	X

Table 4.28: Dips related to Apollo Esselen fault, 10/10/05

NAME	DEPTH	DURATION	CLASS
Olien 275/132kV	43.4	180	S
Olien 275/132kV	37.9	80	X
Olien 275/132kV	41.1	340	S
Olien 275/132kV	21.7	400	S
Olien 275/132kV	46.2	90	X
Olien 275/132kV	42.1	170	S
Olien 275/132kV	41.1	370	S
Olien 275/132kV	34.4	440	S

Table 4.29: Dips related to Hera Watershed fault, 19/11/05

NAME	DEPTH	DURATION	CLASS
Watershed 275/88kV	32.5	50	X
Watershed 275/88kV	74.6	90	T
Watershed 275/88kV	74	100	T

Table 4.30: Dips related to Normandie Unfolozi fault, 05/12/06

NAME	DEPTH	DURATION	CLASS
Normandie 400/88kV	31.9	60	X
Normandie 400/88kV	50.2	70	X
Normandie 400/88kV	25.6	530	S

Table 4.31: Dips related to Bacchus Droerivier fault, 06/03/06

NAME	DEPTH	DURATION	CLASS
Bacchus 400/132kV	43.1	60	X
Bacchus 400/132kV	36.4	60	X
Bacchus 400/132kV	59.5	440	S
Bacchus 400/132kV	27.1	80	Y

#### 4.5.2 Z type dips - 2005

Table 4.32: Z-Dips related to Komatipoort Infuleni fault 18/10/05

NAME	DEPTH	DURATION	CLASS
Komatipoort 275/132kV	55.1	730	Z

Table 4.33: Z-Dips related to Droerivier Proteous fault 02/11/05

NAME	DEPTH	DURATION	CLASS
Droerivier 400/132kV	66	60	T
Droerivier 400/132kV	20.4	160	S
Droerivier 400/132kV	20.2	160	S
Droerivier 400/132kV	20.9	1070	Z
Droerivier 400/132kV	25.5	1490	Z
Droerivier 400/132kV	25.2	70	Y
Droerivier 400/132kV	25.4	70	Y

Table 4.34: Z-Dips related to Aurora Juno fault 19/02/06

NAME	DEPTH	DURATION	CLASS
Aurora 400/132kV	25.7	30	Y
Aurora 400/132kV	55	90	X

4.35: Z-Dips related to Bacchus Droerivier fault 28/02/06

NAME	DEPTH	DURATION	CLASS
Bacchus 400/132kV	88.3	1080	Z
Bacchus 400/132kV	67.5	930	Z
Bacchus 400/132kV	31.8	700	Z
Bacchus 400/132kV	71.6	150	T
Bacchus 400/132kV	50.7	50	X



### 4.5.3 S-type -2006

Table 4.36: Dips related to Camden Normandie fault 14/06/06

NAME	DEPTH	DURATION	CLASS
Camden 400/400kV	15.5	60	Y
Camden 400/400kV	18.4	80	Y
Camden 400/400kV	26.6	350	S

Table 4.37: Dips related to Pluto Watershed fault 26/06/06

NAME	DEPTH	DURATION	CLASS
Watershed 275/88kV	32.5	450	S
Watershed 275/88kV	34.5	150	X
Watershed 275/88kV	34.8	150	X

Table 4.38: Dips related to Marathon Praire fault 24/07/06

NAME	DEPTH	DURATION	CLASS
Marathon 275/132kV	29	240	S
Marathon 275/132kV	28	240	S

### 4.5.4 Z-type – 2006

Table 4.39: Dips related to Invubu Umfolozi fault 09/10/06

NAME	DEPTH	DURATION	CLASS
Komatipoort 400kV	30	930	Z

## **5 CHAPTER 5: ANALYSIS AND DISCUSSION**

### **5.1 INTRODUCTION**

The data presented in Chapter 4 is analysed in this chapter from the following perspectives, namely:

- Analysis of the Omicron test results
- Performance analysis of transmission protection for the period 2005 to 2006 with respect to PEPI incidents that are related to high resistance faults.
- Voltage dips suffered as a result of the high resistance faults that occurred on the lines.
- Comparison of literature survey information to the data collected.

#### **5.1.1 High Resistance fault statistics**

It was shown through the data that was presented in chapter 4 that 16% of all recorded faults have resistance above 10 primary ohms, which is a significant value. There is a need to look at other alternatives to improve the high resistance faults protection performance in Eskom Transmission Lines.

#### **5.1.2 Analysis of distance relay performance**

It was shown that the steady state Mho characteristic caters for very low fault resistance. Faults with high resistance easily fall outside of the characteristics.

Dynamic and variable mho characteristics give a better fault resistance coverage than the steady state mho characteristics. The expanded Mho characteristics provide very little improvement at the end of the specific zone reach coverage. Also the dynamic characteristics depend on the system source impedance. Relays that utilise these characteristics are YTG relays, LZ32 relays, Micromho relays and Type H relays. The R3Z27 relays give the largest resistance coverage independent of source impedance. TLS relays can perform better in the case of high resistance faults provided they are set in the correct mode.

#### **5.1.3 Relay characteristics tests using Matlab simulations;**

The Matlab analysis that was done proved that the relay did not have a chance to operate as the fault resistance moved fault impedance beyond relay characteristic even when actual polarization of the relay was considered. In these particular conditions testing of the relay is not necessary, which can save Eskom time and money otherwise required to prove integrity of the protection scheme. Such theoretical evaluation of the relay performance is not an easy

task, as many details have to be known about the relay design, which is often not easily available. The initial effort to model all relays installed in the Transmission Company is substantial. Once the relay is modelled, however, any subsequent faults can easily be "injected" for theoretical evaluation before expensive testing is undertaken.

## 5.2 OMICRON TEST RESULTS

### 5.2.1.1 Long line (25 ohms)

The fault resistance reach was determined along the line angle at 10% steps of Z1 reach, i.e. from 0% to 90% of Z1 reach which results in 10 test points.

In order to determine the resistance coverage a test line is drawn and the method used was to search along this line (the reach test), the relay boundary point. The tests were started from the line angle (inside the Mho characteristic) and the points were moved until the point where the relay does not operate, this point then defines the maximum resistance coverage at that specific reactance percentage. The comparison of different relays for the maximum resistance coverage is shown in table 5.1, on a long line (25 ohm line) at an SIR of 1.

POSITION OF THE TESTLINE	SEL RELAY	YTG RELAY	R3Z27 Plain	R3Z27 Double offset
0%	23.67Ω		25.230Ω	36.600Ω
10%	24.33Ω	12.230Ω	25.260Ω	36.330Ω
20%	23.62Ω	14.750Ω	24.740Ω	36.970Ω
30%	22.95Ω	15.920Ω	23.000Ω	37.840Ω
40%	21.81Ω	16.620Ω	23.720Ω	34.810Ω
50%	20.85Ω	17.100Ω	22.370Ω	39.260Ω
60%	19.49Ω	16.690Ω	20.400Ω	33.980Ω
70%	17.51Ω	15.980Ω	18.260Ω	32.140Ω
80%	14.34Ω	14.920Ω	14.530Ω	30.050 Ω
90%	10.75Ω		8.776Ω	3.559Ω

Table 5.1: Omicron results for long line

### 5.2.1.2 Short line (5 ohms)

Table 5.2 below shows the comparison of the capability of fault resistance coverage of the three relays which were tested, on a short line (5 ohm line) at an SIR of 1.

POSITION OF THE TEST LINE	SEL RELAY	YTG RELAY	R3Z27 Plain	R3Z27 Double offset
0%	4.77Ω		5.291Ω	11.490Ω
10%	4.77Ω	2.34Ω	5.268Ω	10.990Ω
20%	4.63Ω	2.784Ω	5.229Ω	10.430Ω
30%	4.59Ω	2.998Ω	5.048Ω	9.797Ω
40%	4.40Ω	3.132Ω	4.777Ω	9.066Ω
50%	4.21Ω	3.139Ω	4.439Ω	8.392Ω
60%	3.83Ω	3.051Ω	3.975Ω	7.481Ω
70%	3.51Ω	2.890Ω	3.466Ω	7.481Ω
80%	2.92Ω	2.599Ω	2.845Ω	7.481Ω
90%	2.14Ω		1.692Ω	7.481Ω

Table 5.2: Omicron results for a short line

The above analysis correlates with the literature survey that was done, R3Z27 being the relay that gives more fault resistance coverage and YTG has the least coverage of fault resistance.

### 5.3 TRANSMISSION PROTECTION PERFORMANCE ANALYSIS

The Transmission systems protection has different relays which are summarised in figure 5.1 below:

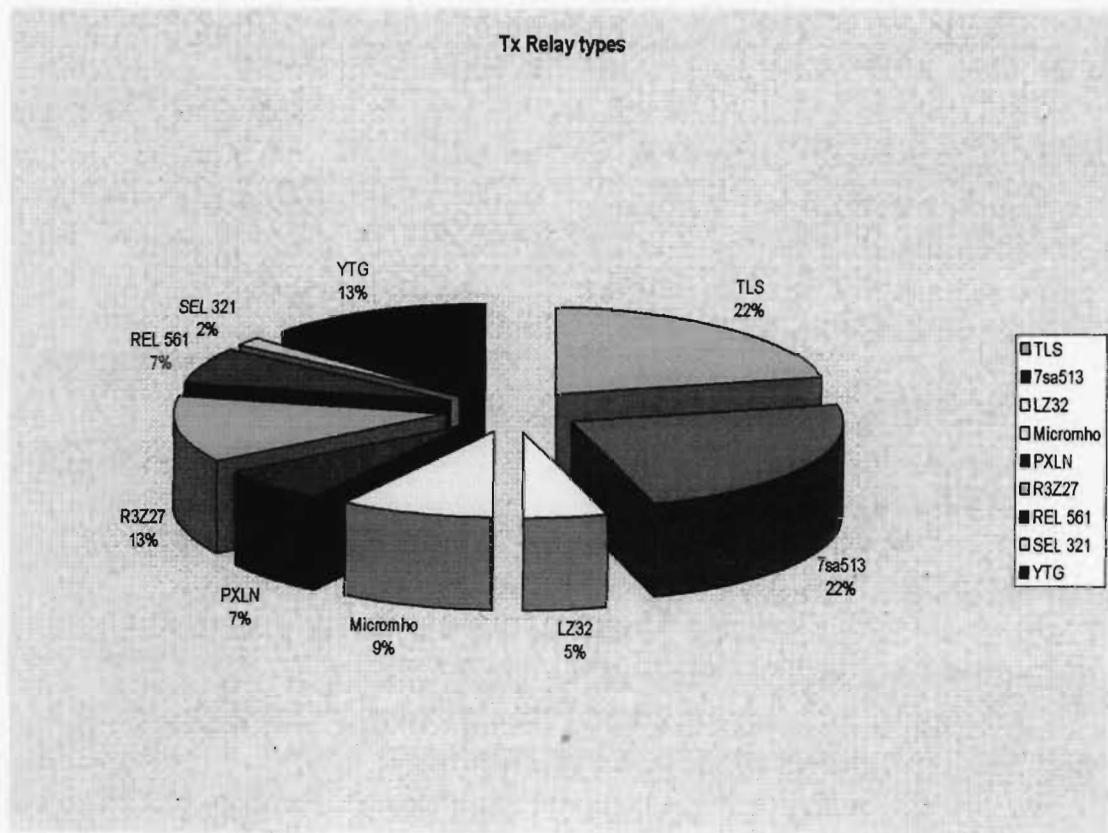


Figure 5.1: Relay types in Eskom Transmission

Table 4.21 shows the summary of the data was collected for Transmission protection performance report for a period of a year, April 2005 until April 2006. This data reveals that more than 50% of incorrect operations encountered on the transmission system are slow clearing of faults due to high resistance faults. This data was collected from Transmission system operation and performance department. Figure 5.2 below gives an analysis in terms of the percentage of HR faults performance per relay.

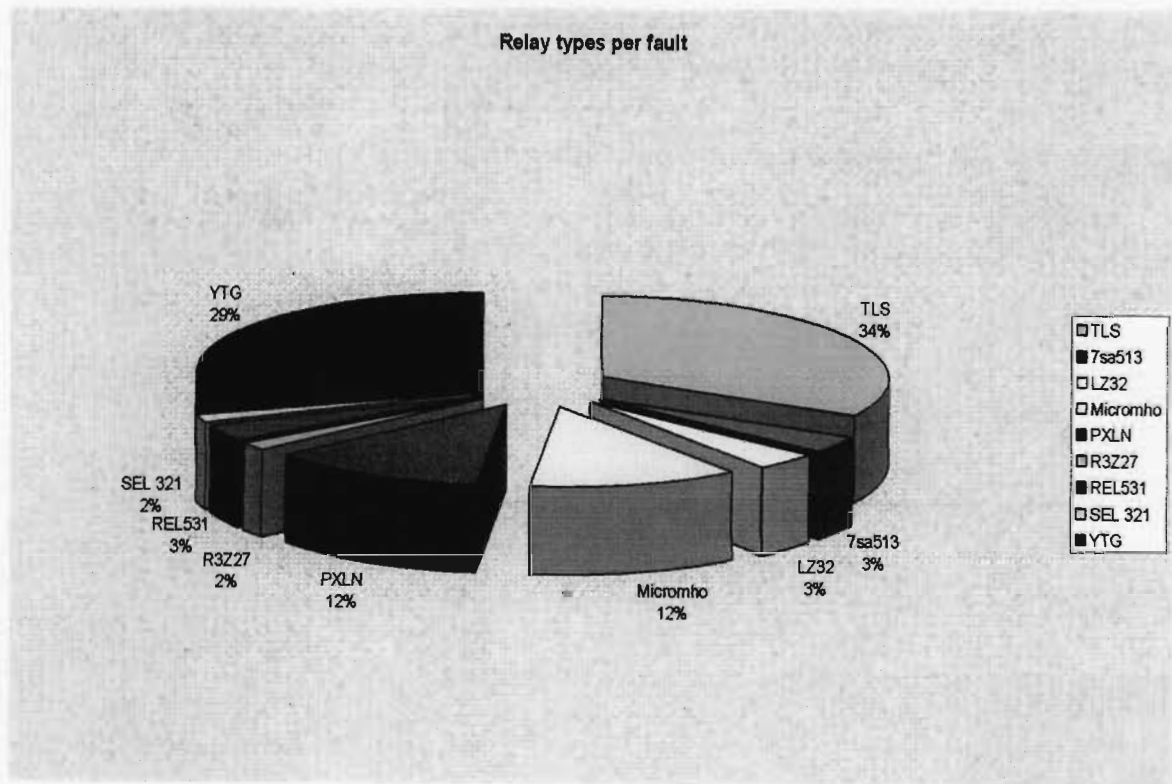


Figure 5.2: Protection performance for 2005

Same analysis as above was done for year 2006 April to December; the results are shown in Table 4.27. The results shows 51% of all PEPI faults were caused by slow clearances due to high resistance faults. The figure 5.3 below gives an analysis in terms of the percentage of HR faults per relay.

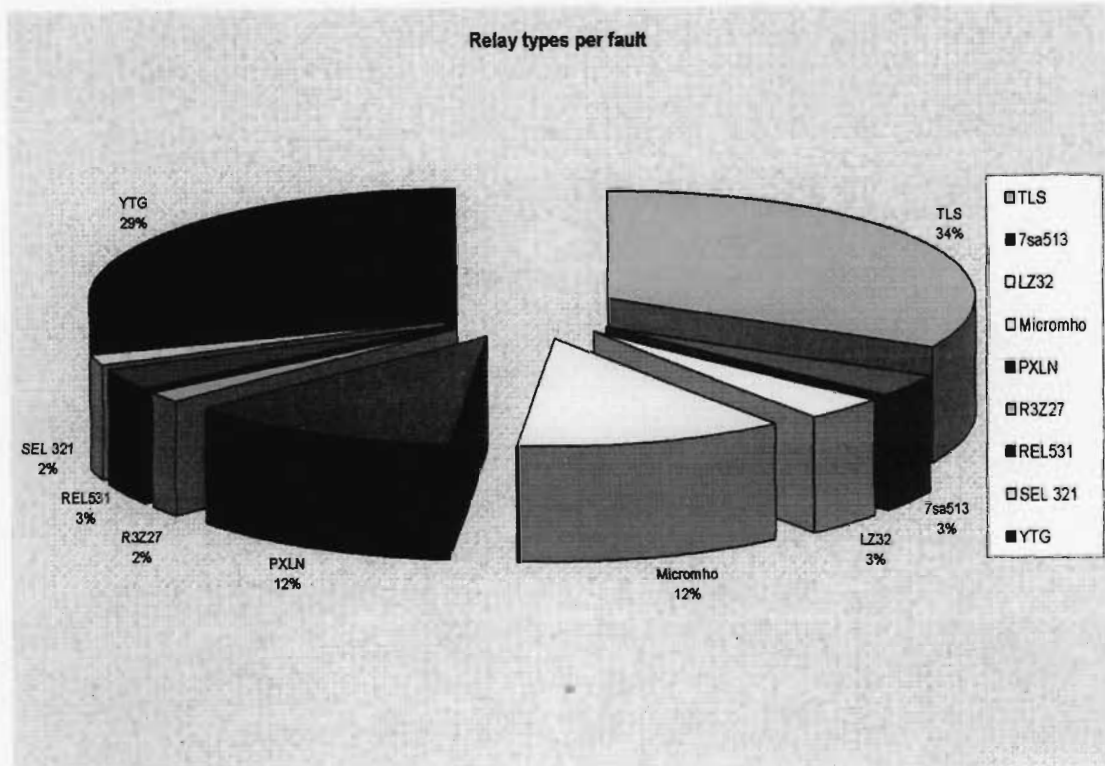


Figure 5.3: Protection performance for 2006

## 5.4 SUMMARY

From this analysis the YTG relay showed the worst performance on high resistance faults coverage, Eskom Transmission system has the installed base of 13%. In all the slow clearances of faults incidents that occurred in 2005 listed in table 4.21, YTG contributed 29% of these incidents. In 2006, the protection performance results also showed the same pattern, the incidents are listed in table 4.22. R3Z27 relays have the same installed base as the YTG relays, but this relays have only contributed 2% of the PEPI incidents from the data that was collected in 2005 and 2006. The TLS performed much better as compared to the YTG relay, the installed base for the TLS relays was 22% and contributed 34% of the PEPI incidents due to high resistance faults.

Siemens 7SA513 and the ABB REL 561 relays showed a better performance for high resistance faults. These relay uses a quadrilateral characterises for the earth faults. The quadrilateral characteristic gives a better fault resistance coverage as compared to the Mho type characteristics.

## 5.5 VOLTAGE DIPS PERFORMANCE

Comparing the dips that occurred due to high resistance faults with the compatibility levels given by the NRS048 standard. See the table 5.3 below:

CLASS OF DIP	2005 (12 months)	2006 (9 months)	NRS 048 LIMIT
	April - March	April to Dec	
Z	8	1	5
T	4	2	6
S	16	4	11
X	12	8	45
Y	15	11	88

Table 5.3 : Number of dips per year for each category of dip window

From the results in table 5.3 above, high resistance faults contribute Z dips which are more than the limit set by NRS048 standard. When analysing the results, it should be noted that the 2006 results is the history for 9 months only compared to 12 months for 2005. Therefore it does not mean that there is an improvement on the voltage dip performance between 2005 and 2006. High resistance faults are mostly characterized by Z, T and S type of dips due to the long durations and these are the type of dips that pose high risks in most of the plants with motors and drives.



## **6 CHAPTER 6: RECOMMENDATIONS**

### **6.1 YTG - R3Z27 PROTECTION SCHEME**

The R3Z27 relay offers high fault resistance coverage, whilst the YTG gives less fault resistance coverage even when the expansion dynamic characteristic is considered. In many cases the R3Z27 relay operates for high resistance faults where the YTG relay fails. As both are impedance relays, the coverage of any fault resistance is limited by the load.

These relays have almost reached their end of the manufacturer recommended life and they are due for replacement by 2012. The author recommends replacement of such schemes with the latest Technology that has the directional earth fault comparison capability.

There are no further setting and or philosophy recommendations different to the current applied in Eskom Transmission that can be implemented in order to improve performance immediately.

### **6.2 YTG - LZ32 PROTECTION SCHEME**

Both the relays offer very limited fault resistance coverage and the current applied philosophy allows for setting for maximum high resistance faults coverage that the relays can handle.

This relays have reached their end of the manufacturer recommended life and they are due for replacement by 2012. The author recommends replacement of such schemes with the latest Technology that has the directional earth fault comparison capability.

There are no further setting and or philosophy recommendations different to the current applied in Eskom Transmission that can be implemented in order to improve performance immediately.

### **6.3 H-TYPE - MHO PROTECTION SCHEME**

These relays use a cross-polarized mho with a memory action for zone 1. Very few of these schemes are still available in Eskom Transmission systems and the few remaining are due for replacement by 2008.

The author recommends replacement of such schemes with the latest Technology that has the directional earth fault comparison capability.

## **6.4 TLS – TLS PROTECTION SCHEME**

TLS relay has different type of characteristics; it can be set as a reactance relay or a Mho relay. The author recommends main 1 and main 2 to be set differently. The author recommends main 1 to use the mho type characteristics and main 2 the reactance type until such time that they are replaced with the latest Technology that has the directional earth fault comparison capability. The mho type can be set as Lens or tomato depending on the length of the line. TLS relays are due for replacement by 2014.

## **6.5 MICROMHO MICROMHO PROTECTION SCHEME**

The relay uses a 16% partially cross-polarised mho characteristic. There are no further setting and or philosophy recommendations different to the current applied in Eskom Transmission that can be implemented in order to improve performance immediately. Micromho relays are due for replacement by 2014.

## **6.6 SLYP/SCLN – SLYP/SLCN PROTECTION SCHEME**

SLYP/SLCN relay has different type of characteristics; it can be set as a reactance relay or a Mho relay. The author recommends main 1 and main 2 to be set differently. The author recommends main 1 to use the mho type characteristics and main 2 the reactance type until such time that they are replaced with the latest Technology that has the directional earth fault comparison capability. The mho type can be set as Lens or tomato depending on the length of the line. SLYP/SCLN relays are due for replacement by 2009.

## **6.7 REL 531 - REL 531 PROTECTION SCHEME**

The following features are optionally available for high resistance fault protection

- Instantaneous over current

The instantaneous residual over current function is suitable as back-up protection for phase to earth faults close to the terminal. This enables a short back-up fault clearance time for the phase to earth faults with high fault current. The instantaneous, non-directional, earth-fault over current protection (IOC), which can operate in 15 ms (50 Hz nominal system frequency) for faults characterized by very high currents, is included in some of the REL 531 terminals

- Time delay over current protection

The time delayed residual over current protection (TOC) which is an earth-fault protection, serves as a built-in local back-up function to the distance protection function. The time delay makes it possible to set the relay to detect high resistance faults and still perform selective trip.

- Definite and inverse time delayed residual over current protection (TEF)

Earth-faults with high fault resistances can be detected by measuring the residual current ( $3I_0$ ). Directional earth-fault protection is obtained by measuring the residual current and the angle between this current and the zero-sequence voltage ( $3V_0$ ).

The earth-fault over current protection is provided with second harmonic restraint, which blocks the operation if the residual current ( $3I_0$ ) contains 20% or more of the second harmonic component to avoid tripping for inrush current.

It is not possible to measure the distance to the fault by using the zero-sequence components of the current and voltage, because the zero-sequence voltage is a product of the zero-sequence components of current and source impedance. It is possible to obtain selectivity by the use of a directional comparison scheme, which uses communication between the line ends.

- Directional comparison

In the directional comparison scheme, information of the fault current direction is transmitted to the other line end. A short operate time enables auto-reclosing after the fault. During a single-phase reclosing cycle, the auto-reclosing device must block the directional comparison earth-fault scheme.

The author recommends the implementation of Directional Earth fault comparison. The function is optionally available as part of the scheme

## **6.8 7SA513 – 7SA513 PROTECTION SCHEME**

The following features are optionally available for high resistance fault protection

- Directional earth fault with non directional back up

Directional earth fault can be used as a definite time or inverse time over current protection. Definite time provides adjustable pick up stage and adjustable time delay. For inverse time an over current value and a time multiplier can be set.

- Directional inverse time zero sequence voltage

This function operates with an inverse time characteristics whose trip time is dependent on the magnitude of the zero sequence voltage

- Directional comparison earth fault comparison

It is a directional protection function that has been extended to form a directional comparison. This can be achieved with the aid of telecommunication systems. Carrier channel is essential for each direction, which transmits signals of the directional earth fault protection to the other end of the line. Tripping is only allowed if the relay has picked up and the signal was received from the other end. This function has an advantage that it can be used as a primary protection, allows for accelerated tripping.

The author recommends the implementation of directional earth fault comparison.

## **6.9 SEL 321- SEL 321 PROTECTION SCHEME**

SEL-321 has a Mho characteristic for phase faults, and quadrilateral characteristic for earth faults.

There are no further setting and or philosophy recommendations different to the current applied in Eskom Transmission that can be implemented in order to improve performance immediately.

## **7 CHAPTER 7: CONCLUSIONS**

### **7.1 FULFILMENT OF THE OBJECTIVES**

The main objective of this research was to gain clear understanding of the capability of the existing relays used in Eskom Transmission network and to give recommendations on the refinements to the EHV transmission line protection philosophy required to improve future protection performance.

This was achieved by analysing the specific relay's manufacturer documentation, and the protection performance for two years with respect to the specific dips that were caused by high resistance faults.

Digital simulations using Matlab and Omicron relay tests was carried out to determine the capability most relays used in Eskom Transmission to detect high resistance faults.

### **7.2 HIGHLIGHTS OF THE RESEARCH**

Recommendations were made to the current Eskom's protection philosophy to include directional earth fault comparison function on all Eskom Transmission feeder protection schemes.

### **7.3 FURTHER RESERACH**

#### **7.3.1 Creating models for all the relays to do the theoretical evaluation to improve fault investigation**

Theoretical evaluation of the relay performance using Matlab or any other software is not an easy task, as many details have to be known about the relay design, which is often not easily available. The initial effort to model all relays installed in the transmission company is substantial. Once the relay is modelled, however, any subsequent faults can easily be "injected" for theoretical evaluation before expensive testing is undertaken

#### **7.3.2 Determining the optimum setting for the directional earth fault relays to ensure maximum security.**

## LIST OF REFERENCES

- [1] '*Eskom Annual Report*', Eskom visual media, South Africa, 2001.
- [2] Adam Bartylak "*Evaluation of weak infeed tripping technique on the Eskom transmission network*", 3rd International Conference on Power System Protection and Automation, New Delhi, India, Nov 2004
- [3] Dugan, R. C. McGranaghan, M. F., & Beaty, H. W. "*Electrical Power Systems Quality*", McGraw-Hill Companies, New York.1996
- [4] P.E. Arendse '*Principles of distance protection*' Eskom Distribution, February 1998
- [5] J .G. Andrichak, G.E. Alexander "*Ground distance relaying: Problems and Principles*" General Electric Co, Malvern, PA. Presented to the Nineteenth Annual Western Protective Relay Conference Spokane, Washington October 20, 1991
- [6] John Berdy and Keneth Winick "*Application Guide for the Use of Distance Relays*" GE Webpage Publication, GER3199,
- [7] J. G. Andrichak and G. E. Alexander, General Electric Co., "*Distance Relays fundamentals*", GE Webpage Publication, GER-3966
- [8] P.M Marot, G H Topham; "*Testing and evaluation of the TLS relay characteristics*" Protection Engineering Eskom, 1996
- [9] GEC "*Protective Relays Application Guide*", 1995
- [10] Joe Mooney, P.E, Jackie Peer, "*Application Guidelines for Ground Fault Protection*" Schweitzer Engineering laboratories website, 1997
- [11] Adam Bartylak, Anita Oommem. Comfort Masike, Gift Moima, Harry Troskie, Malcolm Govender, Sheldon Klein, Simon Pomeroy, Thokozani Mthethwa."*Protection settings philosophy for Transmission and sub-transmission grid*, Eskom operation philosophy document, 10 November 2003

- [12] G.H Topham. "***Transmission System High Resistance Faults: Protection Requirements and Capability***", Research proposal, Resources and Strategy Research Division, June 2002
- [13] GEC, '***YTG relay instruction manual***', 1965
- [14] GE, '***TLS relay instruction manual***', 1990
- [15] Siemens, '***R3Z23 relay instruction manual***', 1965
- [16] Brown Boveri, '***LZ32 relay instruction manual***', 1963
- [17] Reyrolle, '***Type H relay instruction manual***', 1960
- [18] GE, '***Slyp Slcn relay instruction manual***', 1965
- [19] GEC, '***Micromho relay manual***', 1990
- [20] Siemens, '***Numerical distance protection for EHV system, 7SA513 instruction manual V3.2/3.3***', Order number C53000-G1176-C103-6, 1998
- [21] Schweitzer, '***SEL-321-5 Phase and ground distance relay instruction manual***', 1996
- [22] ABB, '***Application manual REL 531\*2.3, High speed line distance protection terminal***', Document No: IMRK 506 107-UEN, Issued: June 2003
- [23] Wilkinson S.B., Matthews C.A., Keeney M.F., "***Design Considerations in the Development of a New Ground Distance Relay***," IEEE Transactions on Power Apparatus and Systems, Vol. PAS-98, Sept./Oct. 1979, pp 1566-1575, Reprinted in GER-3089.
- [24] R. Zivanovic, '***Part4 notes for Protection Systems Design and Application***' Msc lecture notes for the University of Kwazulu Natal, 2004
- [25] Adam Bartylak "***Definition and terminology used in the evaluation of Transmission protection performance***", Eskom document number trmamaah5, May 2006
- [26] NRS-048-1: (1<sup>st</sup> edition) Part 2: Minimum Standards, 1996

[27] Vajeth Riaz, Mtolo Dumsani, Dama Dipeen “*Cost of a Network fault Affecting a Transmission Supply Point*”, Eskom research report, Eskom, South Africa, 2003



## BIBLIOGRAPHY

- [1] Rhulani Matshidza *“Transmission system high resistance faults: protection requirements and capability -- WG progress report”* Eskom protection workshop, Nov 2003
- [2] R. Matshidza, A Bartylak, Prof. Zivanovic, Prof. N.M Ijumba *“Analysis of the dynamic behaviour of distance protection systems on Eskom transmission networks”* SAUPEC conference, JHB Wits university, 26-28 January 2005.
- [3] Rhulani Matshidza, Adam Bartylak, Rastko Zivanovic, *“Impact of high resistance faults on impedance protection performance”* Presented to 18th International Conference on Electricity Distribution, CIRED, Turin, 6-9 June 2005
- [4] J. Roberts, A. Guzman, E.O. Schweitzer, III Pullman, Washington, *“V/I does not make a distance relay* , Schweitzer Engineering Laboratories, Inc
- [5] Edmund O. Schweitzer, III Schweitzer Engineering Laboratories, Inc. Pullman, Washington *“New developments in distance relay polarization and fault type selection”* Presented before the 16th annual western protective relay conference Spokane, Washington, October 24-26, 1989
- [6] Edmund Stokes-Waller and Paul Keller, *“Power network and protection performance analysis on the Eskom Transmission system based on Digital Fault records”* Presented before South African Power System Protection Conference, 2000.
- [7] M. Kezunovic, Texas A&M University USA *“An advanced simulation and testing environment for testing, application and performance assessment of protection equipment”* Bibliography of relay literature, 1996 IEEE committee report
- [8] *“IEEE Standard Common Format for Transient Data Exchange (COMTRADE) for Power Systems”*. IEEE Std C37.111-1999 (Revision of IEEE Std C37.111-1991)
- [9] G.E. Alexander, J.G. Andrichak, W.Z. Tyska, S.B. Wilkinson *“Effects of load flow on relay performance”* Presented to the Thirty-Ninth Annual, Texas A&M relay conference College Station, Texas April 14 - 16, 1986

[10] M Pöller, B Maier DigSILENT GmbH, Germany. A Dierks, Alectrix, South Africa  
*“Simulating the steady state and transient response of protective relay’s* ,2001

[11] Tyska W. Z., *“Polarization of Ground Distance Relays”* A Paper Presented at the Texas  
A&M Relay Conference, April 16-18, 1984.

[12] S.B. Wilkinson and C.A. Mathews *“Dynamic characteristics of Mho Distance relays”*  
Western Protective Relay Conference, October 16-18, 1978

92

## LIST OF APPENDIXES

### APPENDIX 1: Matlab m-file,

The following matlab m-file was created for a steady state and dynamic relay model.

```
clear all;
% 1.signal input
load olien.txt           % loads data from the open file pointed by user
signals = olien (:,1:length(olien(1,:)));
vr = signals(1:1000,3); %red phase voltage           % one signal selected for analysis
vs = signals(1:1000,4); %white phase voltage         % one signal selected for analysis
vb = signals(1:1000,5); %blue phase voltage          % one signal selected for analysis
id = signals(1:1000,7); %red phase current
is = signals(1:1000,8); %white phase current         % one signal selected for analysis
ib = signals(1:1000,9); %blue phase current
ir = signals(1:1000,10); %residual current
ts = signals(1:1000,2)/1000000;
w0 = 2*pi*50;
Ts = ts(2)-ts(1);
R = 0.00878;
L = 0.04953; %
k0 = 0.86;
warning off

% 2. Differential equation based technique
M = length(vs);
for k = 2:M-2
    den = (is(k)*(is(k+2)-is(k))-is(k+1)*(is(k+1)-is(k-1)));
    Re(k) = (vs(k)*(is(k+2)-is(k))-vs(k+1)*(is(k+1)-is(k-1)))/den;
    Xe(k) = w0*2*Ts*(is(k)*vs(k+1)-is(k+1)*vs(k))/den;
end
% figure(1)
%subplot (211), plot(ts(2:end-1),Xe) %ylabel('X [pu]')
%subplot(212), plot(ts(2:end-1),Re) %ylabel('R [pu]', xlabel('time [s]'))

% 3. Recursive DFT
```

```

% Current phasor estimation, Red phase current
s = id;          % with replica impedance
N = 1/50/Ts;    % number of samples per one 50Hz cycle
theta = 2*pi/N; % sampling angle (digital frequency)
Idm = zeros(N,1); psi = zeros(N,1); Id = zeros(N,1);
for q = N : M-1
    if q == N      % starting with the full-cycle DFT
        Yc = 0; Ys = 0; y = s(q-N+1:q);
        for k = 1 : N
            n = k-1;
            Yc = Yc + y(k)*cos(n*theta); Ys = Ys + y(k)*sin(n*theta);
        end
        Yc = (2/N)*Yc; Ys = (2/N)*Ys;
        Idm = sqrt(Yc^2+Ys^2); psi = atan(Yc/Ys);
        Id(q) = Idm*exp(j*psi); % initial phasor with the correction for
            % the replica impedance angle (phir)
    else
        % recursive DFT formula for phasor calculation
        Id(q) = Id(q-1) + (2/N)*(s(q)-s(q-N))*exp(-j*theta*(q-1));
    end
end
Idm = abs(Id); psi = angle(Id);
%figure(2)
%plot(ts(1:end-1),id(1:end-1),ts(1:end-1),Idm,ts(1:end-1),Id(q))
%ylabel('Red phase current [pu]', xlabel('time [s]')

% 3. recursive DFT
% Current phasor estimation, white phase current
s = is;          % with replica impedance
N = 1/50/Ts;    % number of samples per one 50Hz cycle
theta = 2*pi/N; % sampling angle (digital frequency)
Im = zeros(N,1); psi = zeros(N,1); I = zeros(N,1);
for q = N : M-1
    if q == N      % starting with the full-cycle DFT
        Yc = 0; Ys = 0; y = s(q-N+1:q);
        for k = 1 : N
            n = k-1;

```

```

        Yc = Yc + y(k)*cos(n*theta); Ys = Ys + y(k)*sin(n*theta);
    end
    Yc = (2/N)*Yc; Ys = (2/N)*Ys;

    Im = sqrt(Yc^2+Ys^2); psi = atan(Yc/Ys);
    I(q) = Im*exp(j*psi); % initial phasor with the correction for
        % the replica impedance angle (phir)
else
    % recursive DFT formula for phasor calculation
    I(q) = I(q-1) + (2/N)*(s(q)-s(q-N))*exp(-j*theta*(q-1));
end
end
Im = abs(I); psi = angle(I);
%figure(3)
%plot(ts(1:end-1),is(1:end-1),ts(1:end-1),Im,ts(1:end-1),I(q))
%ylabel('White phase current [pu]', xlabel('time [s]')

% 3. Recursive DFT
% Current phasor estimation, Blue phase current
s = ib; % with replica impedance
N = 1/50/Ts; % number of samples per one 50Hz cycle
theta = 2*pi/N; % sampling angle (digital frequency)
Ibm = zeros(N,1); psi = zeros(N,1); Ib = zeros(N,1);
for q = N : M-1
    if q == N % starting with the full-cycle DFT
        Yc = 0; Ys = 0; y = s(q-N+1:q);
        for k = 1 : N
            n = k-1;
            Yc = Yc + y(k)*cos(n*theta); Ys = Ys + y(k)*sin(n*theta);
        end
        Yc = (2/N)*Yc; Ys = (2/N)*Ys;

        Ibm = sqrt(Yc^2+Ys^2); psi = atan(Yc/Ys);
        Ib(q) = Ibm*exp(j*psi); % initial phasor with the correction for
            % the replica impedance angle (phir)
    else
        % recursive DFT formula for phasor calculation

```

```

    Ib(q) = Ib(q-1) + (2/N)*(s(q)-s(q-N))*exp(-j*theta*(q-1));
end
end
Ibm = abs(Ib); psi = angle(Ib);
%figure(4)
%plot(ts(1:end-1),ib(1:end-1),ts(1:end-1),Ibm,ts(1:end-1),Ib(q))
%ylabel('Blue phase current [pu]', xlabel('time [s]')

% 4. Recursive DFT neutral current
% Current phasor estimation
s = ir;          % with replica impedance
N = 1/50/Ts;     % number of samples per one 50Hz cycle
theta = 2*pi/N;  % sampling angle (digital frequency)
Im = zeros(N,1); psi = zeros(N,1); Ir = zeros(N,1);
for q = N : M-1
    if q == N      % starting with the full-cycle DFT
        Yc = 0; Ys = 0; y = s(q-N+1:q);
        for k = 1 : N
            n = k-1;
            Yc = Yc + y(k)*cos(n*theta); Ys = Ys + y(k)*sin(n*theta);
        end
        Yc = (2/N)*Yc; Ys = (2/N)*Ys;

        Irm = sqrt(Yc^2+Ys^2); psi = atan(Yc/Ys);
        Ir(q) = Irm*exp(j*psi); % initial phasor with the correction for
            % the replica impedance angle (phir)
    else
        % recursive DFT formula for phasor calculation
        Ir(q) = Ir(q-1) + (2/N)*(s(q)-s(q-N))*exp(-j*theta*(q-1));
    end
end
end
Im = abs(Ir); psi = angle(Ir);
%figure(5)
%plot(ts(1:end-1),ir(1:end-1),ts(1:end-2),Irm)
%ylabel('Residual current [pu]', xlabel('time [s]')

% Voltage phasor estimation, white voltage

```

```

% 5. recursive DFT
s1 = vs;          % with replica impedance
N = 1/50/Ts;     % number of samples per one 50Hz cycle
theta = 2*pi/N;  % sampling angle (digital frequency)
Vm = zeros(N,1); psiv = zeros(N,1); V = zeros(N,1);
for q = N : M-1
    if q == N      % starting with the full-cycle DFT
        Yc = 0; Ys = 0; y = s1(q-N+1:q);
        for k = 1 : N
            n = k-1;
            Yc = Yc + y(k)*cos(n*theta); Ys = Ys + y(k)*sin(n*theta);
        end
        Yc = (2/N)*Yc; Ys = (2/N)*Ys;

        Vm = sqrt(Yc^2+Ys^2); psiv = atan(Ys/Yc);
        V(q) = Vm*exp(j*psiv); % initial phasor with the correction for
            % the replica impedance angle (phir)
    else
        % recursive DFT formula for phasor calculation
        V(q) = V(q-1) + (2/N)*(s1(q)-s1(q-N))*exp(-j*theta*(q-1));
    end
end
Vm = abs(V); psi = angle(V);
%figure(6)
%plot(ts(1:end-1),vs(1:end-1),ts(1:end-1),Vm)
%ylabel('White phase voltage [pu]', xlabel('time [s]')

% Voltage phasor estimation, red phase
% 6. recursive DFT
s1 = vr;          % with replica impedance
N = 1/50/Ts;     % number of samples per one 50Hz cycle
theta = 2*pi/N;  % sampling angle (digital frequency)
Vrm = zeros(N,1); psiv = zeros(N,1); Vr = zeros(N,1);
for q = N : M-1
    if q == N      % starting with the full-cycle DFT
        Yc = 0; Ys = 0; y = s1(q-N+1:q);
        for k = 1 : N

```

```

    n = k-1;
    Yc = Yc + y(k)*cos(n*theta); Ys = Ys + y(k)*sin(n*theta);
end
Yc = (2/N)*Yc; Ys = (2/N)*Ys;

Vrm = sqrt(Yc^2+Ys^2); psiv = atan(Ys/Yc);
Vr(q) = Vrm*exp(j*psiv); % initial phasor with the correction for
    % the replica impedance angle (phir)
else
    % recursive DFT formula for phasor calculation
    Vr(q) = Vr(q-1) + (2/N)*(s1(q)-s1(q-N))*exp(-j*theta*(q-1));
end
end
Vrm = abs(Vr); psi = angle(Vr);
%figure(7)
%plot(ts(1:end-1),vr(1:end-1),ts(1:end-1),Vrm)
%ylabel('Red phase voltage [pu]', xlabel('time [s]')

% Voltage phasor estimation, blue phase
% 7. recursive DFT
s1 = vb; % with replica impedance
N = 1/50/Ts; % number of samples per one 50Hz cycle
theta = 2*pi/N; % sampling angle (digital frequency)
Vbm = zeros(N,1); psiv = zeros(N,1); Vb = zeros(N,1);
for q = N : M-1
    if q == N % starting with the full-cycle DFT
        Yc = 0; Ys = 0; y = s1(q-N+1:q);
        for k = 1 : N
            n = k-1;
            Yc = Yc + y(k)*cos(n*theta); Ys = Ys + y(k)*sin(n*theta);
        end
        Yc = (2/N)*Yc; Ys = (2/N)*Ys;

        Vbm = sqrt(Yc^2+Ys^2); psiv = atan(Ys/Yc);
        Vb(q) = Vbm*exp(j*psiv); % initial phasor with the correction for
            % the replica impedance angle (phir)
    else

```



```

% recursive DFT formula for phasor calculation
Vb(q) = Vb(q-1) + (2/N)*(s1(q)-s1(q-N))*exp(-j*theta*(q-1));
end
end
Vbm = abs(Vb); psi = angle(Vb);
%figure(8)
%plot(ts(1:end-1),vb(1:end-1),ts(1:end-1),Vbm)
%ylabel('Blue phase voltage [pu]', xlabel('time [s]')

Zc = R+j*w0*L;          % line impedance
Z = abs(Zc); phi = angle(Zc);
r = 0.75;                % reach (%)

% 8. Polarising quantities
Zd = (V/(I(q)+ k0*Ir(q))); % measured impedance
Zda = abs(Zd);
phid = angle(Zd); % 1.11352;
%x = (Zd/2)*cos(phid)
%y = (Zd/2)*sin(phid)

Zd1 =V(q)/(I(q)+ k0*Ir(q));
%Rd = Zda*cos(phid);
%Xd = Zda*sin(phid);
Ip = I(q)+ k0*(Ir(q)); %faulted current
Vop = Z*Ip-V(q); % operating quantity
Op = r*Zc-Zd;
Vpol = V; % polarising quantity
Pol = Zd;

%figure(7)
%plot(ts(1:end-2),Vop),
%hold
%plot(ts(1:end-2),Vpol)

% 9. mho function
Zc = R+j*w0*L;          % line impedance
Z = abs(Zc); phi = angle(Zc);

```

```

r = 0.75;          % reach (%)
a = (r*Z/2)*cos(phi); % circle centre
b = (r*Z/2)*sin(phi);
c = r*Z/2;        % radius
Rc1 = (a-c):0.0001:(c+a);
Xc1 = b + sqrt(c^2-(Rc1-a).^2);
Rc2 = (c+a):-0.0001:(-c+a);
Xc2 = b - sqrt(c^2-(Rc2-a).^2);
Rc = [Rc1 Rc2];
Xc = [Xc1 Xc2];

figure(8)
plot(Rc,Xc)% ,Rd(:,1),Xd(:,1))
hold
plot([0,2*a(1:end-1)],([0 2*b(1:end-1)])

% 10. Polarised mho function
Zd = (V/(I(q)+ k0*Ir(q))); % line impedance
Zp = abs(Zd); phid = 1.11352;
r = 0.75;          % reach (%)
ap = abs((r*Zd/2)*cos(phid)); % circle centre
bp = abs((r*Zd/2)*sin(phid));
cp = abs(r*Zd/2); % radius
f=0;
while f<=(length(Zd))
    f = f+1
    %for j = 0:j<=500
    %j = j+1;
end
Rc3 = (ap-cp):0.0001:(cp+ap);
Xc3 = bp + sqrt(cp^2-(Rc3-ap).^2);
Rc4 = (cp+ap):-0.0001:(-cp+ap);
Xc4 = bp - sqrt(cp^2-(Rc4-ap).^2);
Rcp = [Rc3 Rc4];
Xcp = [Xc3 Xc4];
%f=f+1; end

```

## APPENDIX 2: YTG RELAY SETTINGS

# SETTING OF THE GEC DISTANCE PROTECTION RELAY YTG

VOLTAGE: 400 kV  
 SCHEME : HFZ3200  
 CT RATIO: 2400 / 1  
 VT RATIO: 400 kV / 110V

Z ratio = 0.66  
 Z base = 1600

### LINE PARAMETERS:

Line length	Conductor Type		50 ° Temp	Plant lim.	
[km]			[MVA]	[MVA]	
80	TWIN BEAR		581	1191	
R80	Ro	X1	Xo	B1	Bo
[p.u.]	[p.u.]	[p.u.]	[p.u.]	[p.u.]	[p.u.]
0.00181	0.01616	0.01568	0.05736	0.47696	0.33224

	Z Line 1		Z Line o		Zload min	
	□	angle °	□	angle °	□	angle °
Primary	25.26	83.31	95.35	74.27	234.95	36.87
Secondary	16.67	83.31	62.93	74.27	155.07	36.87
ZE/ZL	0.925					

## CALCULATIONS OF YTG RELAY SETTINGS

### Type of Scheme Mode

Use P.U.R (Permissive Underreach) mode

### Residual Compensation Factor For Earth Fault, Kr

Earth fault impedance :  $Z_e = (Z_o - Z_1)/3$

$$\begin{aligned} K_r &= (Z_o/Z_1 - 1)/3 \\ &= (62.93/16.67 - 1)/3 \\ &= 0.925 \end{aligned}$$

### Phase Fault Settings (YTG)

#### Relay Characteristic Angle

Set = 85 ° for Zone 1, Zone 2 and Zone 3  
 Thus q1 & q2 = 85 °

This is the maximum setting closest to the line angle, since the line angle is 83.31

q1 =	85	°
q2 =	85	°

Difference between line characteristic angle and maximum setting is :

$$83.31 - 85 = -1.69$$

Correction factor is equal  $1 / \cos ( 8.31 ) = 1.011$

**Zone 1 Reach**

**Philosophy:**

Zone 1 reach must be set to 80% of the line impedance

$$\begin{aligned} \text{Zone 1 reach} &= 80\% * 1.011 * Z_{\text{line}} \\ &= 80\% * 1.011 * 16.67 \\ &= 13.4827 \quad \square \text{ secondary} \\ &= 80.88 \quad \% \text{ of line impedance} \end{aligned}$$

**Zone 1 Settings**

Actual Zone 1 reach = $k1 * k4 * k5 * k6 * k8$
--

k8 plug setting : If Zone 1 required < 36 sec ; k8 = 1  
 If Zone 1 required > 36 sec ; k8 = 2  
 (Check if relay has k8 = 2 available)

Zone 1 required = 13.4827  secondary

Therefore select k8 =

**Range adjusting CT (Coarse Adjustment) k5 plug setting :**

Range available . 32/16/8/4/2/1/0.5

Choose k5 > Zone 1 required (13.4827) ohms sec

Therefore select k5 =

**k6 : Determined from relay characteristic angle setting :**

q1 = 85 °

From the nomogram on relay k6 =

**Range adjusting CT (Medium Adjustment) k4 plug setting :**

Range available : 1/0.91/0.82/0.74/0.67/0.61/0.55

For k1 calibrated 0.90 - 1.00, Select k4 > Zone 1 required/(k5\*k6\*k8)

For k1 calibrated 1.00 - 1.12, Select k4 < Zone 1 required/(k5\*k6\*k8)

Relay has k1 calibrated : 0.9-1.00

$$\begin{aligned} k4 &< \text{Zone 1 required ( sec)/(k5*k6*k8)} \\ &< 13.4827 / (K5*K6*K8) \\ &< 0.42 \end{aligned}$$

Select k4 =

**Fine adjustment k1 potentiometer :**

Range available : 0.9-1.00 (Continuously variable)

$$\begin{aligned} k1 &= \text{Zone 1 required (ohms sec)/(k4*k5*k6*k8)} \\ &= 13.4827 / (k4*k5*k6*k8) \\ &= 0.77 \end{aligned}$$

Select k1 =

**Actual Zone 1 Reach**

Not required

**Neutral Impedance Replica (NIR)**

**Relay characteristic angle :**

q1 & q2 on the NIR relay are set to the same value as the impedance relay.

SET :	q1 =	85	°
	q2 =	85	°

**Required earth fault current compensation :**

$$\begin{aligned} \text{Actual \% compensation} &= (Z_0/Z_1 - 1)/3 * 100\% \\ &= 92.5 \quad \% \end{aligned}$$

$$k_r \text{ required} = 92.5 \quad \%$$

$$(k_4 * k_5)_{nir} = k_r * (k_4 * k_5)_{ytg}$$

**Range adjusting CT (Coarse Adjustment) k5(NIR) plug setting :**

Range available : 32/16/8/4/2/1/0.5

$$\begin{aligned} k_5(nir) &> k_r(k_4 * k_5)_{ytg} \\ &> 0.925 * (0.55 * 32) \\ &> 16.28 \end{aligned}$$

$$\text{Select } k_5(nir) = \boxed{32}$$

**Range adjusting CT (Medium Adjustment) k4nir plug setting**

Range available : 0.55/0.61/0.67/0.74/0.82/0.91/1.0

$$\begin{aligned} k_4(nir) &> k_r(k_4 * k_5)_{ytg} / k_5nir \\ &> 0.925 * (0.55 * 32) / 32 \\ &> 0.51 \end{aligned}$$

$$\text{Select } k_4(nir) = \boxed{0.55}$$

**Actual earth fault current compensation :**

$$\begin{aligned} \text{Actual } k_r &= (k_4 * k_5)_{nir} / (k_4 * k_5)_{ytg} \\ &= 100 \quad \text{(Over compensated)} \end{aligned}$$

Limits : Actual kr to be within +/- 5% of required kr value.

$$\begin{aligned} \text{Actual } k_r &= (100 - 92.5) / 92.5 \\ &= 8.11 \quad \% \end{aligned}$$

SET :	k4nir =	0.55	
	k5nir =	32	
	q1 =	85	°
	q2 =	85	°

## SUMMARY OF THE SETTINGS FOR THE GEC DISTANCE PROTECTION RELAY YTG

STATION : 0 0

CT ratio :	2400 / 1	VT ratio :	400 kV/110V
Z ratio:	0.66		

LINE PARAMETERS :		Length :	80 km
	Primary ohms	Secondary ohms	Angle deg
Z <sub>0</sub>	95.35 <input type="checkbox"/>	62.93 <input type="checkbox"/>	74.27 °
Z <sub>1</sub>	25.26 <input type="checkbox"/>	16.67 <input type="checkbox"/>	83.31 °

**YTG RELAY SETTINGS SUMMARY**

	K1	K4	K5	
New	0.96	0.55	32	

	K8	$\cos \theta$	$\cos \theta$
New	1	85°	85°
			K6 = 1    K6 = 1

**YTG & YTO REACHES**

	sec <input type="checkbox"/>	%
Zone 1 = K1*K4*K5*K6*K8 =	16.9	101.38

**NIR SETTINGS**

	K4	K5	$\cos \theta$	$\cos \theta$
New	0.55	32	85°	85°

## APPENDIX 3: SEL 321 RELAY SETTINGS

### SEL 321 data sheet

<u>Line Terminal settings</u>		<u>Description</u>	<u>Range</u>
RELID	SEL-321	Relay Identifier	17 Characters
TRMID		Terminal Identifier	39 Characters
Z1MAG	25.26	Positive-Seq Line Impedance magnitude	0.25 - 1275 ohms
Z1ANG	83.31	Positive-Seq Line Impedance angle	40 deg to 90 deg
Z0MAG	95.35	Zero-Seq Line Impedance Magnitude	0.25 - 1275 ohms
Z0ANG	74.27	Zero-Seq Line Impedance Angle	40 deg to 90 deg
LOCAT	Y	Fault location Enable	Y,R,N
LL	80.00	Line Length	0.1 - 999 unitless
CTR	2400.00	Current transformer ratio	1 - 6000
PTR	3636.36	Voltage transformer ratio	1 - 10 000

<u>Enable zones of distance settings</u>			
PMHOZ	4	Number of mho phase distance zones	N,1,2,3,4
GMHOZ	N	Number of mho ground distance zones	N,1,2,3,4
QUADZ	4	Number of quadrilateral ground distance zones	N,1,2,3,4

<u>Distance zones and overcurrent levels direction settings</u>			
DIR1	F	Distance Zone 1 / Overcurrent Level 1 Direction:	F/R
DIR2	F	Distance Zone 2 / Overcurrent Level 2 Direction:	F/R
DIR3	R	Distance Zone 3 / Overcurrent Level 3 Direction:	F/R
DIR4	F	Distance Zone 4 / Overcurrent Level 4 Direction:	F/R

<u>Zone reaches</u>			
Z1P	20.21	Impedance reach: Zone 1:	0.25 to 320 ohms secondary
Z2P	30.31	Impedance reach: Zone 2:	0.25 to 320 ohms secondary
Z3P	37.89	Impedance reach: Zone 3:	0.25 to 320 ohms secondary
Z4P	75.78	Impedance reach: Zone 4:	0.25 to 320 ohms secondary

<u>Mho phase distance overcurrent supervision settings</u>			
50PP1	0.20	Phase-Phase overcurrent: Zone 1:	(0.2 - 34 amps sec.)
50PP2	0.20	Phase-Phase overcurrent: Zone 2:	(0.2 - 34 amps sec.)
50PP3	0.20	Phase-Phase overcurrent: Zone 3:	(0.2 - 34 amps sec.)
50PP4	0.20	Phase-Phase overcurrent: Zone 4:	(0.2 - 34 amps sec.)

<u>MHO ground distance settings</u>			
Z1MG	*	Impedance reach: Zone 1:	(0.25 - 320 OHMS SEC)
Z2MG	*	Impedance reach: Zone 2:	(0.25 - 320 OHMS SEC)
Z3MG	*	Impedance reach: Zone 3:	(0.25 - 320 OHMS SEC)
Z4MG	*	Impedance reach: Zone 4:	(0.25 - 320 OHMS SEC)

<u>Quadrilateral ground distance settings</u>			
XG1	20.07	Reactive reach: Zone 1:	(0.25 - 320 OHMS SEC)
XG2	30.11	Reactive reach: Zone 2:	(0.25 - 320 OHMS SEC)
XG3	37.63	Reactive reach: Zone 3:	(0.25 - 320 OHMS SEC)
XG4		Reactive reach: Zone 4:	(0.25 - 320 OHMS SEC)
RG1	100.35	Resistive reach: Zone 1:	(0.25 - 320 OHMS SEC)
RG2	150.53	Resistive reach: Zone 2:	(0.25 - 320 OHMS SEC)
RG3	188.16	Resistive reach: Zone 3:	(0.25 - 320 OHMS SEC)
RG4		Resistive reach: Zone 4:	(0.25 - 320 OHMS SEC)

**Ground distance overcurrent supervision settings**

<b>50L1</b>	<b>0.10</b>	Phase overcurrent supervision: Zone 1:	(0.1-20 AMPS SEC)
<b>50L2</b>	<b>0.10</b>	Phase overcurrent supervision: Zone 2:	(0.1-20 AMPS SEC)
<b>50L3</b>	<b>0.10</b>	Phase overcurrent supervision: Zone 3:	(0.1-20 AMPS SEC)
<b>50L4</b>	<b>0.10</b>	Phase overcurrent supervision: Zone 4:	(0.1-20 AMPS SEC)
<b>50G1</b>	<b>0.10</b>	Residual overcurrent supervision: Zone 1	(0.1-20 AMPS SEC)
<b>50G2</b>	<b>0.10</b>	Residual overcurrent supervision: Zone 2:	(0.1-20 AMPS SEC)
<b>50G3</b>	<b>0.10</b>	Residual overcurrent supervision: Zone 3:	(0.1-20 AMPS SEC)
<b>50G4</b>	<b>0.10</b>	Residual overcurrent supervision: Zone 4:	(0.1-20 AMPS SEC)

**Zero-sequence compensation factor settings**

<b>k01M</b>	<b>0.93</b>	Zone 1 Zero-Seq compensation factor 1 magnitude:	(0-4)
<b>k01A</b>	<b>-12.27</b>	Zone 1 Zero-Seq compensation factor 1 Angle:	(+/-45 degrees)
<b>k0M</b>	<b>0.93</b>	Zones 2, 3 & 4 Zero-Seq compensation factor 2 magnitude:	(0-4)
<b>k0A</b>	<b>-12.27</b>	Zones 2, 3 & 4 Zero-Seq compensation factor 2 angle:	(+/-45 degrees)
<b>T</b>	<b>-7.00</b>	Non-homogeneous correction angle:	(+/-120 degrees)



## APPENDIX 3:R3Z27 RELAY SETTINGS

# SETTING OF THE SIEMENS DISTANCE PROTECTION RELAY R3Z27

STATION: KENDAL  
CIRCUIT : TUTUKA  
VOLTAGE: 400 kV

FDR : 3

DONE BY : R.D. MATSHIDZA  
CHECKED: K.C. MASIKE  
DATE : 05-Aug-05

SCHEME : 1 FZ 5501  
CT RATIO: 2400 / 1  
VT RATIO: 400 kV / 110V

Z ratio = 0.66  
Z base = 1600  $\Omega$

### LINE PARAMETERS:

Line length [km]	Conductor Type		50° Th lim. [MVA]	Plant lim [MVA]	
80	▼		1595	1595	
R1 [p.u.]	Ro [p.u.]	X1 [p.u.]	Xo [p.u.]	B1 [p.u.]	Bo [p.u.]
0.0184	0.01616	0.01568	0.0270	0.1760	0.3322

	Z Line 1		Z Line 0		Zload min	
	$\phi$	angle °	$\phi$	angle °	$\phi$	angle °
Primary	25.26	83.31	95.35	74.27	100.31	36.87
Secondary	16.67	83.31	62.93	74.27	66.2	36.87
ZE/ZL	0.925					

### CALCULATIONS OF RELAY SETTINGS

#### PROTECTION MODE AND RELAY CHARACTERISTICS

a) Select PUR mode

Three different characteristics are available with the R3Z27 relay

1. **Impedance:** Normally used on long lines (line impedance > 25 ohms)
2. **Single Offset Impedance:** Normally used for medium length lines (line impedance 10 - 25 ohms)
3. **Double Offset Impedance:** Normally used for short lines (line impedance < 10 ohms)

Select K = 1.05 plug position to obtain single offset impedance characteristic if W = kX.

NB : Since Zone 3 is to be set in the forward direction ; no reverse (red) plug settings are required

SET : K = 1.05  
Insert plug in 

**ZERO SEQUENCE COMPENSATION**

Purpose to match the earth impedance to the line impedance,  $Z_e : Z_l$

$$\begin{aligned} Z_e &= \text{Fictitious earth impedance} \\ &= (Z_0 - Z_1)/3 = (62.93 - 16.67)/3 \\ &= 15.42 \text{ ohms sec} \end{aligned}$$

$$\begin{aligned} \text{Compensation factor : } q &= Z_e/Z_l = f + g \\ &= 15.420 / 16.670 \\ &= 0.925 \quad (92.5 \% \text{ compensation}) \end{aligned}$$

Settings :  $q = f + g$  to prevent overreaching of earth fault measurement

**ZERO SEQUENCE COMPENSATION PLUG SETTINGS (g - Coarse, f - Fine)**

Range available :  $g = 0.0$  to  $2.25$  in steps of  $0.25$   
 $f = 0.0$  to  $0.2$  in steps of  $0.05$

SELECT  $f = 0.15$   
 $g = 0.75$

Actual compensation = 90 % *Undercompensated*

$$\begin{aligned} \text{Earth fault reach factor} &= (1 + q(\text{set})) / (1 + q(\text{reqd})) \\ &= (1 + 0.9) / (1 + 0.925) \\ &= 0.99 \quad * \text{Phase fault reach} \end{aligned}$$

SET :	$g = 0.75$
	$f = 0.15$

**FAULT IMPEDANCE ANGLES (Relay Characteristic Angles)**

Range available :  $k = 60^\circ, 67^\circ, 73^\circ, 80^\circ$

Actual positive sequence impedance angle =  $83.31^\circ$   
 Actual zero sequence impedance angle =  $74.27^\circ$

SELECT :  $k$  (f - f) =  $85^\circ$  (Forward - green direction)  
 (f - E) =  $75^\circ$  (Forward - green direction)

SET :	(f - f) = $85^\circ$
	(f - E) = $75^\circ$
Both in forward - green direction	

**DIRECTIONAL SPECIFICATIONS**

All Zones are to " look " in the forward direction i.e. towards  
 There will be no reverse reach due to the directional element whose  
 characteristic passes through the origin of the impedance characteristic.

R3Z27 relays have five Zones, Zones 1 to 3 are derived from the measuring  
 unit, under directional control. Zones 4 and 5 are derived from the starter  
 units, Zone 4 being under directional control, Zone 5 being under non-directional.

Eskom scheme 1 FZ 5501 does not have the Zone 4 facility - Timer t4 is used to block autoreclosure  
 before the Zone 3 timer times out.

**a) Line CT's earthed on line side :**

SET : R,S,T plugs (2 pin) 111 position (Panel A)

**b) t3 and t4 directional plugs :**

SET : t3 & t4 (3 pin) in forward direction (Panel A)

**c) Angle of restraint :**

The directional unit can be set for 60° or 90°. Normally the 60° setting  
 is used. The 90° setting is used only if the line section to be protected  
 is followed by a power transformer (star-star auto connection) used for  
 phase angle control.

SET : Angle of restraint 60 ° (1 pin plug) (Panel B)

**d) Zone 3 directional specification :**

SET : r3 in forward direction (2 pin),green section (Panel B)

**ZONE SETTINGS**

Relay reach = r = (CT Ratio \* W)/(5C \* VT Ratio)

For impedance characteristic, W = Z

For modified impedance characteristic, W = kX

- where : Z is the reach required for the Zone (impedance)
- X is the reach required for the Zone (reactance)
- k = 1.05 for the single offset characteristic
- k = 2.1 for the double offset characteristic

In this case the single offset characteristic is chosen.

!

SET : W = kX  
 k = 1.05

**ZONE 1 SETTINGS**

Zone 1 required reach = 80% of X1 (X1= 25.088 ohms prim)

$$X1 = 0.8 * 25.088$$

$$= 20.0704 \text{ ohms prim}$$

$$\text{Relay reach} = 1/(5C) * \text{CT/VT Ratio} * 1.05 * 20.0704$$

$$= 1/5C * 0.66 * 1.05 * 20.0704$$

$$r = 2.7818 / C$$

Select C as low as possible to minimise power consumption in the voltage circuit taking into account that r (max) = 19.9 + 1 and that there is adequate range to achieve the Zone 3 setting  
Range available: C = 0.1/0.2/0.5/1.0 forward

*The setting 'C' can be optimised when the Zone reaches have been determined.*

SELECT C = 0.2

SET :	C =	0.2
-------	-----	-----

$$r = 2.7818 / 0.2$$

$$= 13.909 \cong (\text{Relay})$$

$$\cong 1 \geq r - 1$$

$$\geq 13.909 - 1$$

$$\geq 12.909$$

r1 is the setting on the resistor chain corresponding to Zone 1 reach.

SELECT r1 = 13.0

$$\text{Zone 1 reach X1} = (5 * r * C) / (k * \text{CT/VT Ratio})$$

$$20.2 \cong \text{prim}$$

$$80.52 \quad \%$$

SET :	r1 =	13	
		3	+ 0 (+10)

# SUMMARY OF SETTING FOR THE SIEMENS DISTANCE PROTECTION RELAY R3Z27

VOLTAGE: 400 kV

DRAWING No.: 0

SCHEME : 1 FZ 5501

CT RATIO: 2400 / 1

Z ratio = 0.66

VT RATIO: 400 kV / 110V

Z base = 1600  $\cong$

### LINE PARAMETERS

	Z Line 1		Z Line o		Zload min	
	$\cong$	angle °	$\cong$	angle °	$\cong$	angle °
Primary	25.26	83.31	95.35	74.27	100.31	36.87
Secondary	16.67	83.31	62.93	74.27	66.2	36.87
ZE/ZL	0.925	Length	80	km		

### R3 Z27 Measuring Unit

R,S,T	K	$\cong$ Ph	$\cong$ $\angle$
LHS	1.05	85°	75°
rI	C	OFFSET	
13	0.2	SINGLE	

### R3Z27 Zone Reaches

	Primary ( $\cong$ )	% of the line
Zone 1 = $(5*rI*C)/(K*Zratio)$	20.20 $\cong$	80.52 %

➔

➔➔